CHEMISTRY
A European Journal

Supporting Information

A Multicolor Large Stokes Shift Fluorogen-Activating RNA Aptamer with Cationic Chromophores

Christian Steinmetzger,[a] Navaneethan Palanisamy,[b, d] Kiran R. Gore,[c, e] and Claudia Höbartner*[a, b, c]

chem_201805882_sm_miscellaneous_information.pdf

SUPPORTING INFORMATION

Supporting Information

69451 Weinheim, Germany

A multicolor large Stokes shift fluorogen-activating RNA aptamer with cationic chromophores

Christian Steinmetzger,[a] Navaneethan Palanisamy,[b]# Kiran R. Gore[c]§ and Claudia Höbartner*[a,b,c]

Abstract: *Large Stokes shift (LSS) fluorescent proteins (FPs) exploit excited state proton transfer pathways to enable fluorescence emission from the phenolate intermediate of their internal 4-hydroxybenzylidene imidazolone (HBI) chromophore. An RNA aptamer named Chili mimics LSS FPs by inducing highly Stokes-shifted emission from several new green and red HBI analogs that are non-fluorescent when free in solution. The ligands are bound by the RNA in their protonated phenol form and feature a cationic aromatic side chain for increased RNA affinity and reduced magnesium dependence. In combination with oxidative functionalization at the C2 position of the imidazolone, this strategy yielded DMHBO$^+$, which binds to the Chili aptamer with a low-nanomolar K_D. Because of its highly red-shifted fluorescence emission at 592 nm, the Chili–DMHBO$^+$ complex is an ideal fluorescence donor for Förster resonance energy transfer (FRET) to the rhodamine dye Atto 590 and will therefore find applications in FRET-based analytical RNA systems.*

DOI: 10.1002/anie.2018XXXXX

SUPPORTING INFORMATION

Table of Contents

Experimental Procedures

1. General Information

1.1. Materials

All standard chemicals and solvents were purchased from commercial suppliers and were used without further purification. Organic solvents for optical spectroscopy were purchased from Acros Organics. Aluminum-backed plates coated with silica gel and a fluorescent indicator were used for thin layer chromatography (TLC). The plates were visualized with UV light. Additionally, exposing the plates to ammonia vapor rendered HBI compounds orange or violet. Silica gel 60, 0.032-0.063 mm (230-450 mesh) was used for column chromatography.

DNA templates for in vitro transcription were purchased from Microsynth and purified by denaturing PAGE (15–20% polyacrylamide). 3'-Amino-modified RNA oligonucleotide was prepared by solid-phase synthesis using 5'-*O*-DMT-2'-*O*-TOM-protected 3'-β-cyanoethyl phosphoramidites of N^6-acetyladenosine, N^4-acetylcytidine, N^2-acetylguanosine, uridine (purchased from Chemgenes) and amino-on solid support (purchased from Link technologies) as described previously.[1] Ribonucleotide triphosphates (NTPs) were purchased from Jena Bioscience. RNase T1, Antarctic phosphatase, T4 Polynucleotide kinase (PNK), and T4 RNA Ligase were purchased from New England Biolabs. T7 RNA polymerase was prepared in house following a published procedure with minor modifications.[2] Atto 590-NHS was purchased from ATTO-TEC.

1.2. NMR spectroscopy

NMR spectra were acquired on Bruker Avance III and Avance III HD spectrometers between 300 and 600 MHz as well as Varian Mercury Plus and Inova spectrometers between 300 and 600 MHz.

Chemical shifts (δ) in ppm are referenced to the solvent residual signals (^{1}H and ^{13}C) or on the unified scale (other nuclei).[3] Coupling constants (J) are reported in Hz with the following multiplet designations: s (singlet), d (doublet), t (triplet), q (quartet), m (multiplet), br (broad).

All spectral assignments were verified by additional 2D experiments. Occasionally, carbon atoms adjacent to nitrogen did not give an observable signal in the 1D ^{13}C spectra. Their chemical shifts were obtained from the respective 2D experiments instead and are indicated by an asterisk.

1.3. Mass spectrometry

High resolution ESI mass spectra in positive or negative ion mode were acquired on Bruker micrOTOF, micrOTOF-Q III and maXis instruments.

2. Synthetic procedures for chromophores

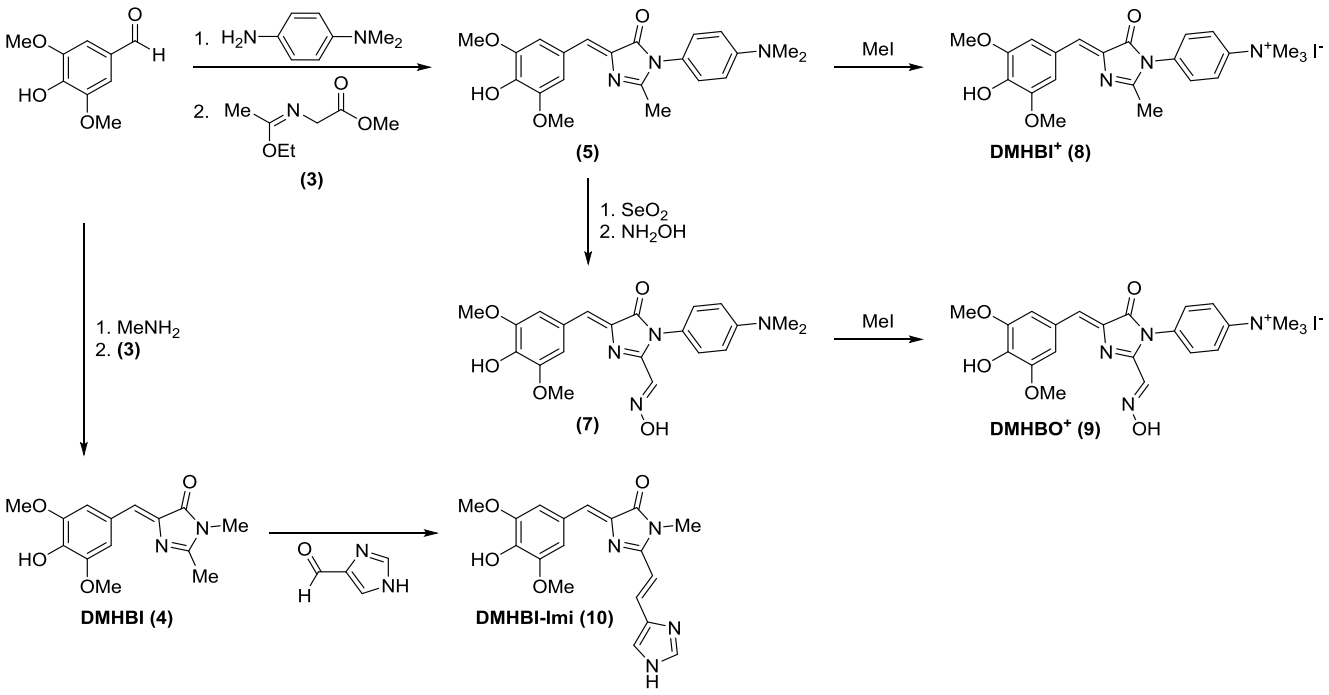

Scheme S1. Overview of DMHBI chromophore syntheses.

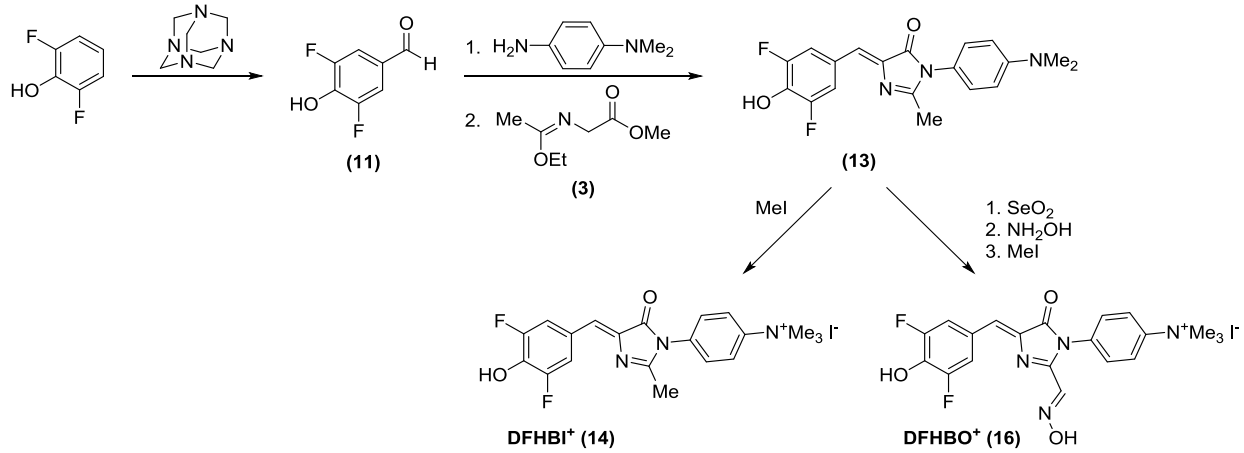

Scheme S2. Overview of DFHBI chromophore syntheses.

2.1. 4-Hydroxy-3,5-dimethoxy-*N*-methylbenzaldimine (1)

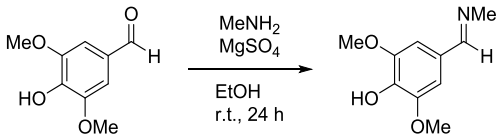

(1)

A suspension of 4-hydroxy-3,5-dimethoxybenzaldehyde (4.55 g, 25.0 mmol, 1.00 eq.) and $MgSO_4$ (3.61 g, 30.0 mmol, 1.20 eq.) in methylamine (33% in EtOH, 31.1 mL, 250 mmol, 10.0 eq.) was stirred at ambient temperature for 24 h. Afterwards, the solution was filtered over a Celite plug. The solids were rinsed with CH_2Cl_2 (3×20 mL) and the filtrate was evaporated under reduced pressure. The imine **1** was obtained as a pale yellow solid (4.05 g, 20.8 mmol, 83%) that was sufficiently pure for all further reactions. For analysis, the crude product was recrystallized from EtOH.

^{1}H NMR (300 MHz, $CDCl_3$): δ (ppm) = 8.16 (q, *J* = 1.6 Hz, 1 H, CHN), 6.97 (s, 2 H, Ph-2,6-H), 3.92 (s, 6 H, OCH_3), 3.49 (d, *J* = 1.6 Hz, 3 H, NCH_3);

^{13}C{^{1}H} NMR (125 MHz, $CDCl_3$): δ (ppm) = 162.2 (CHN), 147.6 (Ph-C3,5), 137.9 (Ph-C4), 127.5 (Ph-C1), 104.9 (Ph-C2,6), 56.5 (OCH_3), 48.1 (NCH_3);

HR-MS (ESI+): *m*/*z* calc. ($C_{10}H_{14}NO_3$, $[M+H]^+$): 196.0968, found: 196.0973.

2.2 4-Hydroxy-3,5-dimethoxy-*N*-(4-(dimethylamino)phenyl)benzaldimine (2)

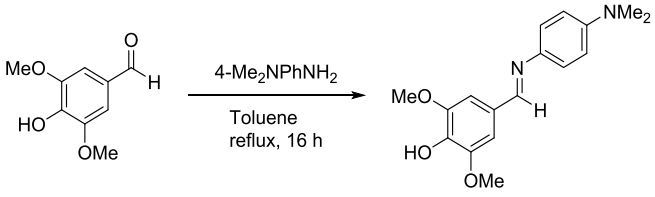

(2)

A solution of 4-hydroxy-3,5-dimethoxybenzaldehyde (1.82 g, 10.0 mmol, 1.00 eq.) and 4-(dimethylamino)aniline (1.36 g, 10.0 mmol, 1.00 eq.) in toluene (40 mL) was heated to reflux with a Dean-Stark trap for 16 h. Afterwards, the solvent was completely removed under reduced pressure and the resulting dark oil was taken up in hot toluene (30 mL). Addition of pentane (30 mL) resulted in the formation of a yellow suspension from which a dark solid separated. The solid was removed by decantation and the supernatant was treated again with pentane (60 mL). Decantation and addition of pentane (60 mL) were repeated once more, resulting in the formation of yellow needles, which were collected by filtration and washed with a small amount of pentane to obtain compound **2** in a pure form (2.03 g, 6.77 mmol, 68%). A second batch of the product was obtained from the dark solid by dissolving it in hot toluene (30 mL), cooling to ambient temperature and slowly adding the solution to hexane (150 mL) while stirring. This resulted in a dark yellow precipitate that was collected and washed with a small amount of hexane.

^{1}H NMR (300 MHz, $CDCl_3$): δ (ppm) = 8.38 (s, 1 H, CHN), 7.30–7.11 (m, 4 H, NAr-2,6-H, Ph-2,6-H), 6.81–6.71 (m, 2 H, NAr-3,5-H), 5.80 (s_{br}, 1 H, OH), 3.98 (s, 6 H, OCH_3), 2.98 (s, 6 H, NCH_3);

^{13}C{^{1}H} NMR (75 MHz, $CDCl_3$): δ (ppm) = 155.6 (CHN), 149.6* (NAr-C4), 147.4 (Ph-C3,5), 141.2* (NAr-C1), 138.3* (Ph-C4), 128.6* (Ph-C1), 122.3 (NAr-C2,6), 113.1 (NAr-C3,5), 105.4 (Ph-C2,6), 56.6 (OCH_3), 40.9 (NCH_3);

HR-MS (ESI+): *m*/*z* calc. ($C_{17}H_{21}N_2O_3$, $[M+H]^+$): 301.1547, found: 301.1551.

2.3. Methyl (*Z*)-2-((1-ethoxyethylidene)amino)acetate (3)[4]

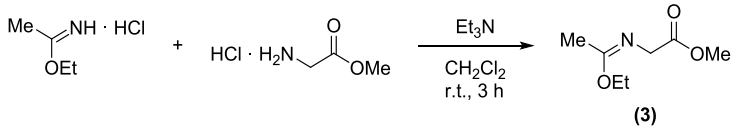

(3)

To a suspension of ethyl acetimidate hydrochloride (4.63 g, 37.5 mmol, 1.00 eq.) and methyl glycinate hydrochloride (4.71 g, 37.5 mmol, 1.00 eq.) in dry CH_2Cl_2 (150 mL) was added Et_3N (5.2 mL, 37.5 mmol, 1.00 eq.). The resulting mixture was stirred at ambient temperature for 3 h. Afterwards, it was washed with H_2O (2×150 mL) and brine (150 mL) and the organic phase was dried over $MgSO_4$. Evaporation of the solvent under reduced pressure afforded compound **3** as a colorless liquid (5.08 g, 31.9 mmol, 85%). Spectral data

matched those reported previously.[4] The product can be stored under an inert atmosphere at –20 °C for several weeks without decomposition.

^{1}H NMR (300 MHz, $CDCl_3$): δ (ppm) = 4.10 (q, J = 7.1 Hz, 2 H, OCH_2), 4.05 (s, 2 H, NCH_2), 3.73 (s, 3 H, OCH_3), 1.87 (s, 3 H, CCH_3), 1.26 (t, J = 7.1 Hz, 3 H, OCH_2CH_3);

HR-MS (ESI+): *m*/*z* calc. ($C_7H_{13}NNaO_3$, $[M+Na]^+$): 182.0788, found: 182.0788.

2.4. (*Z*)-5-(4-Hydroxy-3,5-dimethoxybenzylidene)-2,3-dimethyl-3,5-dihydro-4*H*-imidazol-4-one (4)

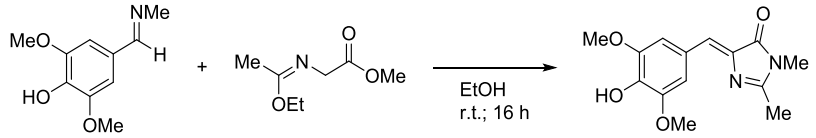

(1) **(3)** **(4)**

Imine **1** (976 mg, 5.00 mmol, 1.00 eq.) was suspended in EtOH (5 mL). Upon addition of imidate **3** (876 mg, 5.50 mmol, 1.10 eq.) a slightly exothermic reaction occurred. The mixture was stirred at ambient temperature for 16 h. Afterwards, the mixture was filtered and the precipitate was washed thoroughly with Et_2O (50 mL) providing compound **4** as an orange solid (1.13 g, 4.09 mmol, 82%).

^{1}H NMR (300 MHz, DMSO-d_6): δ (ppm) = 9.02 (s_{br}, 1 H, OH), 7.62 (s, 2 H, Ph-2,6-H), 6.89 (s, 1 H, benzylidene-H), 3.80 (s, 6 H, OCH_3), 3.09 (s, 3 H, NCH_3), 2.34 (s, 3 H, CCH_3);

^{13}C{^{1}H} NMR (125 MHz, DMSO-d_6): δ (ppm) = 169.4 (Imi-C4), 162.2 (Imi-C2), 147.6 (Ph-C3,5), 138.4 (Ph-C4), 136.2 (Imi-C5), 125.7 (benzylidene-C), 124.3 (Ph-C1), 110.1 (Ph-C2,6), 56.0 (OCH_3), 26.1 (NCH_3), 15.4 (CCH_3);

HR-MS (ESI+): *m*/*z* calc. ($C_{14}H_{16}N_2NaO_4$, $[M+Na]^+$): 299.1002, found: 299.1004;

TLC (toluene/acetone 1:1): R_f = 0.51.

2.5. (*Z*)-3-(4-(Dimethylamino)phenyl)-5-(4-hydroxy-3,5-dimethoxybenzylidene)-2-methyl-3,5-dihydro-4*H*-imidazol-4-one (5)

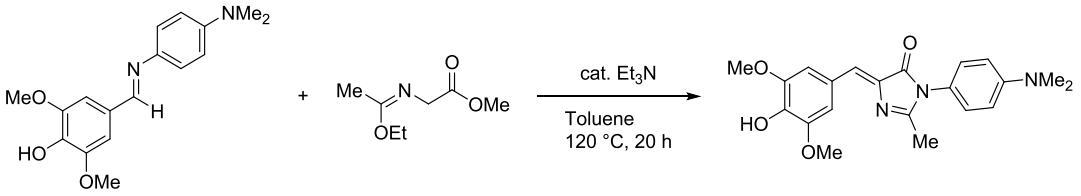

(2) **(3)** **(5)**

A mixture of imine **2** (601 mg, 2.00 mmol, 1.00 eq.), imidate **3** (382 mg, 2.40 mmol, 1.20 eq.) and Et_3N (4 drops) in toluene (2 mL) was stirred at 120 °C for 20 h. Afterwards, the solvent was evaporated under reduced pressure. The crude product was dissolved in hot $CHCl_3$ (50 mL) and precipitated by the addition of hexane (100 mL). The precipitate was washed with hexane (3×15 mL) affording compound **5** as a yellow solid (599 mg, 1.57 mmol, 79%).

^{1}H NMR (300 MHz, $CDCl_3$): δ (ppm) = 7.55 (s, 2 H, Ph-2,6-H), 7.13–7.01 (m, 3 H, benzylidene-H and NAr-2,6-H), 6.82–6.72 (m, 2 H, NAr-3,5-H), 5.90 (s_{br}, 1 H, OH), 3.96 (s, 6 H, OCH_3), 3.00 (s, 6 H, NCH_3), 2.24 (s, 3 H, CCH_3);

^{13}C{^{1}H} NMR (125 MHz, $CDCl_3$): δ (ppm) = 170.5 (Imi-C4), 161.9 (Imi-C2), 150.6 (NAr-C4), 147.1 (Ph-C3,5), 137.4 (Ph-C4), 137.0 (Imi-C5), 128.1 (NAr-C2,6), 127.9 (Ph-C1), 126.1 (benzylidene-C), 122.0 (NAr-C1), 112.8 (NAr-C3,5), 109.5 (Ph-C2,6), 56.5 (OCH_3), 40.7 (NCH_3), 16.7 (CCH_3);

HR-MS (ESI+): *m*/*z* calc. ($C_{21}H_{24}N_3O_4$, $[M+H]^+$): 382.1761.1002, found: 382.1772;

TLC (CH_2Cl_2/MeOH 98:2 + 1% AcOH): R_f = 0.83.

2.6. (*Z*)-1-(4-(Dimethylamino)phenyl)-4-(4-hydroxy-3,5-dimethoxybenzylidene)-5-oxo-4,5-dihydro-1*H*-imidazole-2-carbaldehyde (6)

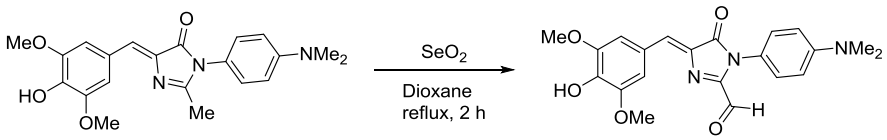

(5) **(6)**

Compound **5** (572 mg, 1.50 mmol, 1.00 eq.) and SeO_2 (200 mg, 1.80 mmol, 1.20 eq.) were suspended in dioxane (25 mL) and heated to reflux for 2 h. While still hot, the supernatant was decanted off from the deposited solids and the solvent was removed under reduced pressure. Purification of the residue by column chromatography ($CHCl_3$/EtOH 99:1–9:1 + 1% AcOH) afforded compound **6** as a black solid (413 mg, 1.04 mmol, 70%).

^{1}H NMR (400 MHz, $CDCl_3$): δ (ppm) = 9.74 (s, 1 H, CHO), 7.66 (s, 2 H, Ph-2,6-H), 7.51 (s, 1 H, benzylidene-H), 7.17–7.07 (m, 2 H, NAr-H), 6.92–6.79 (m, 2H, NAr-H) 6.15 (s_{br}, 1 H, OH), 3.99 (s, 6 H, OCH_3), 3.02 (s, 6 H, NCH_3);

^{13}C{^{1}H} NMR (100 MHz, $CDCl_3$): δ (ppm) = 183.5 (CHO), 170.0* (Imi-C4), 152.9* (Imi-C2), 149.9* (NAr-C4), 147.5 (Ph-C3,5), 139.9 (Ph-C4), 137.9 (benzylidene-C), 136.8, 127.8, 125.6 (Ph-C1), 111.2 (Ph-C2,6), 56.6 (OCH_3), 41.1* (NCH_3), two resonances were not observed;

HR-MS (ESI−): *m*/*z* calc. ($C_{21}H_{20}N_3O_5$, $[M-H]^-$): 394.14084, found: 394.13946;

TLC (Hex/EtOAc 1:1): R_f = 0.21.

2.7. (*Z*)-1-(4-(Dimethylamino)phenyl)-4-(4-hydroxy-3,5-dimethoxybenzylidene)-5-oxo-4,5-dihydro-1*H*-imidazole-2-carbaldehyde oxime (7)

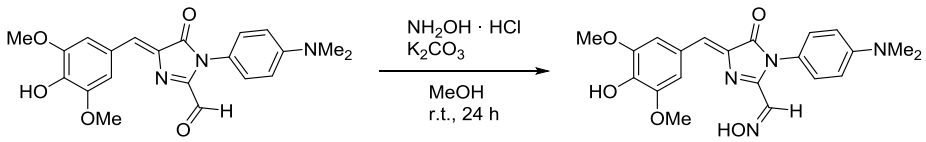

(6) **(7)**

Aldehyde **6** (198 mg, 500 µmol, 1.00 eq.), hydroxylamine hydrochloride (41.7 mg, 600 µmol, 1.20 eq.) and K_2CO_3 (38.0 mg, 275 µmol, 0.55 eq.) were suspended in MeOH (1.25 mL) and stirred at ambient temperature for 24 h. Afterwards, the solvent was removed under reduced pressure. Purification of the residue by column chromatography (CH_2Cl_2–CH_2Cl_2/MeOH 98:2 + 1% AcOH) afforded the oxime **7** (75.1 mg, 183 µmol, 37%).

^{1}H NMR (400 MHz, DMSO-d_6): δ (ppm) = 12.38 (s_{br}, 1 H, NOH), 9.42 (s_{br}, 1 H Ph-4-OH), 7.79 (s, 1 H, CHN), 7.74 (s, 2 H, Ph-2,6-H), 7.17 (s, 1 H, benzylidene-H), 7.13–7.07 (m, 2 H, NAr-3,5-H), 6.77–6.73 (m 2 H, NAr-2,6-H), 3.82 (s, 6 H, OCH_3), 2.94 (s, 6 H, NCH_3);

^{13}C{^{1}H} NMR (100 MHz, DMSO-d_6): δ (ppm) = 169.6 (Imi-C5), 154.0 (Imi-C2), 150.0 (NAr-C4), 147.9 (Ph-C3,5), 140.4 (CHN), 139.6 (Ph-C4), 136.0 (Imi-C4), 129.8 (benzylidene-C), 128.4 (NAr-C2,6), 124.5 (Ph-C1), 122.5 (NAr-C1), 112.1 (NAr-C3,5), 110.7 (Ph-C2,6), 56.0 (OCH_3), 40.1 (NCH_3);

HR-MS (ESI+): *m*/*z* calc. ($C_{21}H_{22}N_4NaO_5$, $[M+H]^+$): 433.14879, found: 43314870;

TLC (Toluene/Acetone 7:3 + 1% AcOH): R_f = 0.28.

2.8. (*Z*)-5-(4-Hydroxy-3,5-dimethoxybenzylidene)-2-methyl-3-(4-(trimethylammonium)phenyl)-3,5-dihydro-4*H*-imidazol-4-one iodide (8)

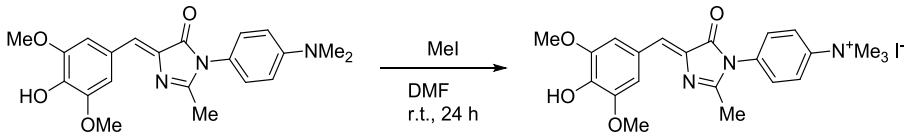

(5) **(8)**

Compound **5** (66.8 mg, 175 µmol, 1.00 eq.) and methyl iodide (109 µL, 1.75 mmol, 10.0 eq.) were dissolved in DMF (3.5 mL) and stirred at ambient temperature for 24 h. Removal of the solvent under reduced pressure afforded the product **8** as a dark solid (92.0 mg, 175 µmol, >99%).

^{1}H NMR (500 MHz, DMSO-d_6): δ (ppm) = 9.28 (s_{br}, 1 H, OH), 8.18–8.11 (m 2 H, NAr-3,5-H), 7.76–7.69 (m, 2 H, NAr-2,6-H), 7.71 (s, 2 H, Ph-2,6-H), 7.06 (s, 1 H, benzylidene-H), 3.81 (s, 6 H, OCH_3), 3.66 (s, 9 H, NCH_3), 2.26 (s, 3 H, CCH_3);

^{13}C{^{1}H} NMR (125 MHz, DMSO-d_6): δ (ppm) = 168.8 (Imi-C4), 159.8 (Imi-C2), 147.9 (Ph-C3,5), 146.5 (NAr-C4), 139.0 (Ph-C4), 135.4 (Imi-C4), 135.0 (NAr-C1), 128.8 (NAr-C2,6), 127.6 (benzylidene-C), 124.3 (Ph-C1), 121.9 (NAr-C3,5), 110.3 (Ph-C2,6), 56.5 (NCH_3), 56.1 (OCH_3), 16.5 (CCH_3);

HR-MS (ESI+): *m*/*z* calc. ($C_{22}H_{26}N_3O_4$, $[M\text{-}I]^+$): 396.1918, found: 396.1926.

2.9. (*Z*)-4-(4-Hydroxy-3,5-dimethoxybenzylidene)-5-oxo-1-(4-(trimethylammonium)phenyl)-4,5-dihydro-1*H*-imidazole-2-carbaldehyde oxime iodide (9)

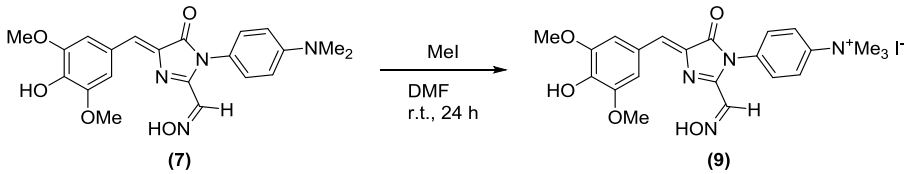

(7) (9)

Compound **7** (51.3 mg, 125 µmol, 1.00 eq.) and methyl iodide (78 µL, 1.25 mmol, 10.0 eq.) were dissolved in DMF (2.5 mL) and stirred at ambient temperature for 24 h. Removal of the solvent under reduced pressure afforded the product **9** (70.0 mg, 125 µmol, >99%).

^{1}H NMR (400 MHz, DMSO-d_6): δ (ppm) = 12.35 (s, 1 H, NOH), 9.50 (s_{br}, 1 H Ph-4-OH), 8.12–8.07 (m 2 H, NAr-2,6-H), 7.91 (s, 1 H, CHN), 7.77 (s, 2 H, Ph-2,6-H), 7.71–7.65 (m, 2 H, NAr-3,5-H), 7.25 (s, 1 H, benzylidene-H), 3.82 (s, 6 H, OCH_3), 3.65 (s, 9 H, NCH_3);

^{13}C{^{1}H} NMR (100 MHz, DMSO-d_6): δ (ppm) = 168.7 (Imi-C5), 152.5 (Imi-C2), 148.0 (Ph-C3,5), 146.4 (NAr-C4), 140.5 (CHN), 139.9 (Ph-C4), 135.8 (NAr-C1), 135.4 (Imi-C4), 130.8 (benzylidene-C), 129.3 (NAr-C2,6), 124.3 (Ph-C1), 121.3 (NAr-C3,5), 110.9 (Ph-C2,6), 56.6 (NCH_3), 56.1 (OCH_3);

HR-MS (ESI+): *m*/*z* calc. ($C_{22}H_{25}N_4O_5$, $[M\text{-}I]^+$): 425.18195, found: 425.18280.

2.10. 2-((*E*)-2-(1*H*-Imidazol-4-yl)vinyl)-((*Z*)-5-(4-Hydroxy-3,5-dimethoxybenzylidene))-3-methyl-3,5-dihydro-4*H*-imidazol-4-one (10)

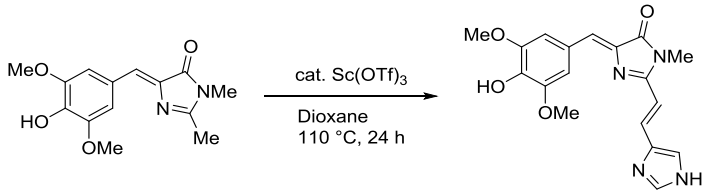

(4) (10)

Compound **4** (55.3 mg, 200 µmol, 1.00 eq.), imidazole-4-carbaldehyde (24.0 mg, 250 µmol, 1.25 eq.) and scandium triflate (14.8 mg, 30.0 µmol, 15.0 mol%) were dissolved in anhydrous dioxane (1 mL) in a closed vial. The mixture was stirred at 110 °C (oil bath temperature) for 24 h. Afterwards, the solvent was removed under reduced pressure. Purification of the residue by column chromatography (toluene/DMF 4:1–1:9) afforded the product as a brown solid (44.7 mg, 126 µmol, 63%).

^{1}H NMR (500 MHz, DMSO-d_6): δ (ppm) = 12.41 (s_{br}, 1 H, NH), 9.11 (s_{br}, 1 H Ph-4-OH), 7.85 (d, J = 15.4 Hz, 1 H, vinyl-2-H), 7.82 (s, 1 H, vinyl-Imi-2-H), 7.71 (s, 2 H, Ph-2,6-H), 7.62 (s, 1 H, vinyl-Imi-5-H), 6.95 (d, J = 15.4 Hz, 1 H, vinyl-1-H), 6.90 (s, 1 H, benzylidene-H), 3.85 (s, 6 H, OCH_3), 3.22 (s, 3 H, NCH_3);

^{13}C{^{1}H} NMR (125 MHz, DMSO-d_6): δ (ppm) = 169.9 (Imi-C4), 159.1 (Imi-C2), 147.8 (Ph-C3,5), 138.5 (Ph-C4), 137.9* (vinyl-Imi-C4), 137.4 (Imi-C5), 132.9* (vinyl-C2), 125.1 (Ph-C1), 124.8 (benzylidene-C), 110.1 (Ph-C2,6), 109.5 (vinyl-C1), 56.0 (OCH_3), 26.2 (NCH_3);

HR-MS (ESI+): *m*/*z* calc. ($C_{18}H_{19}N_4O_4$, $[M+H]^+$): 355.1401, found: 355.1399.

2.11. 3,5-Difluoro-4-hydroxybenzaldehyde (11)

(11)

A solution of 3,5-difluorophenol (4.65 g, 35.7 mmol, 1.00 eq.) and hexamethylene tetramine (5.01 g, 35.7 mmol, 1.00 eq.) in trifluoroacetic acid (36 ml) was heated to reflux for 28 h. Afterwards, the volatiles were removed under reduced pressure, the residue was taken up in CH_2Cl_2 (75 ml) and washed with saturated aqueous $NaHCO_3$ solution (2×50 ml). The aqueous phase was first neutralized with 1 M NaOH, then brought to pH 1 with conc. HCl and back-extracted with CH_2Cl_2 (3×50 ml). The combined organic phases were dried over $MgSO_4$ and the solvent was evaporated under reduced pressure to afford the product as a pale yellow solid (4.37 g, 27.6 mmol, 77%). Spectral data matched those reported previously.[5]

^{1}H NMR (400 MHz, $CDCl_3$): δ (ppm) = 9.81 (t, *J* = 1.9 Hz, 1 H, CHO), 7.54–7.44 (m, 2 H, Ph-2,6-H);

^{19}F{^{1}H} NMR (376 MHz, $CDCl_3$): δ (ppm) = −133.0 (Ph-3,5-F).

2.12 3,5-Difluoro-4-hydroxy-*N*-(4-(dimethylamino)phenyl)benzaldimine (12)

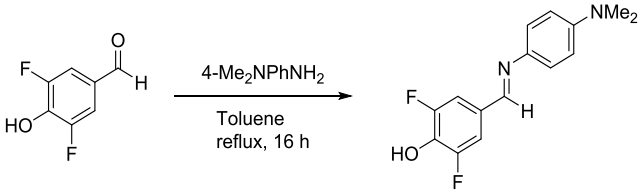

(12)

A solution of 3,5-difluoro-4-hydroxybenzaldehyde (**11**, 3.16 g, 20.0 mmol, 1.00 eq.) and 4-(dimethylamino)aniline (2.72 g, 20.0 mmol, 1.00 eq.) in toluene (80 mL) was heated to reflux with a Dean-Stark trap for 16 h. Afterwards, the solvent was completely removed under reduced pressure. The crude imine was obtained as a dark brown solid (5.48 g, 19.8 mmol, >99%) that was sufficiently pure for further reactions. For analytical purposes, a small sample of the material was purified by recrystallization from toluene. The product is prone to decomposition upon exposure to moisture.

^{1}H NMR (400 MHz, DMSO-d_6): δ (ppm) = 10.59 (s_{br}, 1 H, OH), 8.50 (s, 1 H, CHN), 7.59–7.47 (m, 2 H, Ph-2,6-H), 7.28–7.19 (m, 2 H, NAr-2,6-H), 6.79–6.70 (m, 2 H, NAr-3,5-H), 2.92 (s, 6 H, NCH_3);

^{13}C{^{1}H} NMR (100 MHz, DMSO-d_6): δ (ppm) = 152.9 (CHN), 152.3 (d, *J* = 242.9 Hz, Ph-C3,5),149.4 (NAr-C4), 139.3 (NAr-C1), 135.9 (Ph-C4), 127.8 (Ph-C1), 122.4 (NAr-C2,6), 112.6 (NAr-C3,5), 111.1 (d, *J* = 18.0 Hz, Ph-C2,6), 40.2 (NCH_3);

^{19}F{^{1}H} NMR (376 MHz, DMSO-d_6): δ (ppm) = −131.9 (Ph-3,5-F);

HR-MS (ESI+): *m*/*z* calc. ($C_{15}H_{15}F_2N_2O$, $[M+H]^+$): 277.11524, found: 277.11503.

2.13. (*Z*)-3-(4-(Dimethylamino)phenyl)-5-(3,5-difluoro-4-hydroxybenzylidene)-2-methyl-3,5-dihydro-4*H*-imidazol-4-one (13)

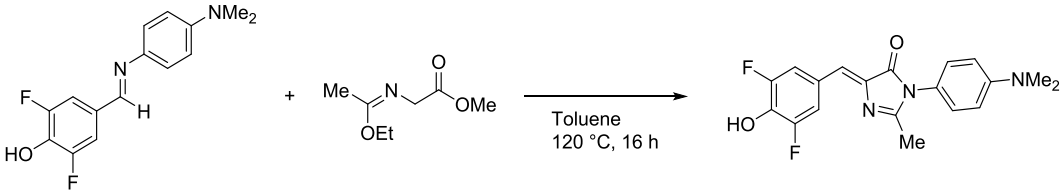

(12) **(3)** **(13)**

A mixture of imine **12** (553 mg, 2.00 mmol, 1.00 eq.) and imidate **3** (382 mg, 2.40 mmol, 1.20 eq.) in toluene (2 mL) was stirred at 120 °C for 16 h. Afterwards, the solvent was evaporated under reduced pressure. The crude product was purified by column chromatography (hexane/EtOAc 6:4–4:6) affording compound **13** as an orange crystalline solid (256 mg, 0.72 mmol, 36%).

^{1}H NMR (400 MHz, DMSO-d_6): δ (ppm) = 10.98 (s_{br}, 1 H, OH), 8.08–7.96 (m, 2 H, Ph-2,6-H), 7.18–7.11 (m, 2 H, NAr-2,6-H), 6.97 (s, 1 H, benzylidene-H), 6.83–6.75 (m, 2 H, NAr-3,5-H), 3.95 (s, 6 H, NCH_3), 2.17 (s, 3 H, CCH_3);

^{13}C{^{1}H} NMR (100 MHz, DMSO-d_6): δ (ppm) = 169.4 (Imi-C4), 163.8 (Imi-C2), 151.8 (d, *J* = 241.8 Hz, Ph-C3,5), 150.3 (NAr-C4), 138.0 (Imi-C5), 135.8 (Ph-C4), 128.2 (NAr-C2,6), 124.7 (Ph-C1), 123.3 (benzylidene-C), 121.4 (NAr-C1), 115.4–115.0 (m, Ph-C2,6), 112.3 (NAr-C3,5), 40.1 (NCH_3), 16.2 (CCH_3);

^{19}F{^{1}H} NMR (376 MHz, DMSO-d_6): δ (ppm) = −132.3 (Ph-3,5-F);

HR-MS (ESI+): *m*/*z* calc. ($C_{19}H_{18}F_2N_3O_2$, $[M+H]^+$): 358.13616, found: 358.13516;

TLC (hexane/EtOAc 4:6): R_f = 0.49.

2.15. (*Z*)-1-(4-(Dimethylamino)phenyl)-4-(3,5-difluoro-4-hydroxybenzylidene)-5-oxo-4,5-dihydro-1*H*-imidazole-2-carbaldehyde (15)

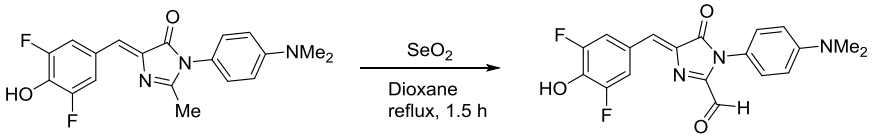

(13) (15)

Compound **13** (190 mg, 532 µmol, 1.00 eq.) and SeO_2 (70.8 mg, 638 µmol, 1.20 eq.) were suspended in dioxane (10 mL) and heated to reflux for 1.5 h. Afterwards, the solvent was removed under reduced pressure. Purification of the residue by column chromatography (hexane/EtOAc 3:7) afforded compound **15** (80.1 mg, 216 µmol, 41%). Some minor impurities were present but did not affect further reactions. The product is prone to decomposition upon exposure to moisture.

^{1}H NMR (400 MHz, DMSO-d_6): δ (ppm) = 9.65 (s, 1 H, CHO), 8.19–8.12 (m, 2 H, Ph-2,6-H), 7.51 (s, 1 H, benzylidene-H), 7.17–7.17 (m, 2 H, NAr-2,6-H), 6.79–6.70 (m, 2H, NAr-3,5-H), 2.95 (s, 6 H, NCH_3);

^{13}C{^{1}H} NMR (100 MHz, DMSO-d_6): δ (ppm) = 184.1 (CHO), 169.1* (Imi-C5), 154.2* (Imi-C2), 151.9* (d, J = 235.0 Hz, Ph-C3,5), 150.1 (NAr-C4), 137.5 (Ph-C4), 132.6 (benzylidene-C), 127.8 (NAr-C2,6), 121.5 (NAr-C1), 117.2–116.3 (m, Ph-C2,6), 111.9 (NAr-C3,5), 40.2 (NCH_3), two resonances were not observed;

^{19}F{^{1}H} NMR (376 MHz, DMSO-d_6): δ (ppm) = −131.7 (Ph-3,5-F);

HR-MS (ESI−): *m*/*z* calc. ($C_{19}H_{14}F_2N_3O_3$, $[M-H]^-$): 370.10087, found: 370.10094;

TLC (Hex/EtOAc 3:7): R_f = 0.31.

2.16. (*Z*)-4-(3,5-Difluoro-4-hydroxy-benzylidene)-5-oxo-1-(4-(trimethylammonium)phenyl)-4,5-dihydro-1*H*-imidazole-2-carbaldehyde oxime iodide (16)

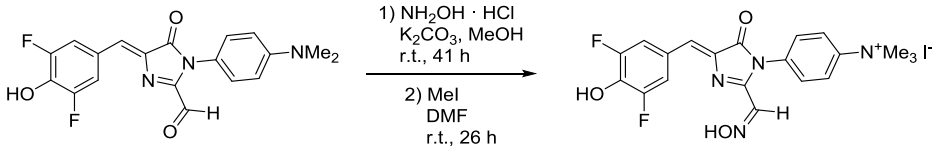

(15) (16)

Aldehyde **15** (62.8 mg, 169 µmol, 1.00 eq.), hydroxylamine hydrochloride (12.9 mg, 186 µmol, 1.10 eq.) and K_2CO_3 (25.7 mg, 186 µmol, 1.10 eq.) were suspended in MeOH (1 mL) and stirred at ambient temperature for 41 h. Afterwards, the solvent was removed under reduced pressure and the residue was purified by column chromatography ($CHCl_3$/EtOH 98:2 + 1% AcOH) to yield the acetate of the intermediate oxime. A part of the material (80.0 mg) and methyl iodide (112 µL) were dissolved in DMF (4 mL) and stirred at ambient temperature for 22 h. Since some starting material was still present, a second portion of methyl iodide (60.0 µl) was added and the reaction was continued for 4 h. Removal of the solvent under reduced pressure afforded the product **16** as an orange solid (122 mg).

^{1}H NMR (400 MHz, DMSO-d_6): δ (ppm) = 12.51 (s, 1 H, NOH), 8.16 (s_{br}, 1 H Ph-4-OH), 8.14–8.04 (m 4 H, NAr-2,6-H, Ph-2,6-H), 7.89 (s, 1 H, CHN), 7.72–7.66 (m, 2 H, NAr-3,5-H), 7.25 (s, 1 H, benzylidene-H), 3.65 (s, 9 H, NCH_3);

^{13}C{^{1}H} NMR (100 MHz, DMSO-d_6): δ (ppm) = 168.6 (Imi-C5), 152.5* (Imi-C2), 152.0* (d, J = 233.8 Hz, Ph-C3,5), 146.5 (NAr-C4), 140.0 (CHN), 137.2 (Ph-C4), 135.5 (NAr-C1), 129.3 (NAr-C2,6), 127.4 (benzylidene-C), 121.5 (NAr-C3,5), 115.9 (Ph-C2,6), 56.6 (NCH_3), two resonances were not observed;

^{19}F{^{1}H} NMR (376 MHz, DMSO-d_6): δ (ppm) = −132.0 (Ph-3,5-F);

HR-MS (ESI+): *m*/*z* calc. ($C_{20}H_{19}F_2N_4O_3$, $[M-I]^+$): 401.14197, found: 401.14156.

3. RNA Synthesis

3.1. In vitro transcription of RNA aptamers

In vitro transcription reactions were performed with T7 RNA polymerase using the corresponding DNA template and T7 promoter strand (1 µM each) in an aqueous solution containing 40 mM Tris-HCl, pH 8.0, 30 mM $MgCl_2$, 10 mM DTT, 4 mM of each NTP and 2 mM spermidine at 37 °C for 5 h. The transcription products were purified by denaturing PAGE (15% acrylamide/bis-acrylamide 19:1, 7 M urea, 0.7 × 200 × 300 mm) with running buffer 1x TBE (89 mM Tris, 89 mM boric acid, 2 mM EDTA, pH 8.3), at 35 W constant power. The products were visualized by UV shadowing on a TLC plate and extracted by crush & soak into TEN buffer (10 mM Tris-HCl, pH

8.0, 1 mM EDTA, 300 mM NaCl) and recovered by precipitation with ethanol. Typical yields were 1–2 nmol RNA from 100 µL transcription reactions as determined by UV absorbance.

3.2. Synthesis of Chili RNA containing a 3'-Atto590-labeled tail

3'-Amino-functionalized RNA was 5'-phosphorylated with PNK (2 nmol RNA in 30 µL aqueous solution containing 50 mM Tris-HCl, 1 mM $MgCl_2$, 5 mM DTT, 0.1 mM spermidine, 1 mM ATP and 5 units PNK) at 37 °C for 3 h and isolated by precipitation with ethanol. The residue was dissolved in sodium bicarbonate buffer (100 mM, 10 µL, pH 9.0) and a solution of Atto 590-NHS ester in DMF (5 mM, 5 µL) was added. The resulting reaction mixture was incubated in the dark at 37 °C for 3 h. Then, TEN buffer was added (150 µL) and the RNA oligonucleotide was recovered by precipitation with ethanol (500 µL). The blue pellet was dissolved in water (5 µL), mixed with aliquots of the Chili RNA (2 nmol) and the DNA splint (2 nmol) in a final volume of 20 µL, heated to 95 °C for 2 min and kept at ambient temperature for 15 min. Then, ligation buffer (3 µL of 10x buffer: 500 mM Tris-HCl, pH 7.5, 100 mM $MgCl_2$, 100 mM DTT), ATP (3 µL of 10 mM) as well as T4 RNA ligase (3 µL of 10 u/µL) were added and the reaction mixture was incubated at 37 °C for 6 hours. The ligation product was isolated by PAGE, extracted into TEN and recovered by precipitation as described above.

4. UV-Vis spectroscopy

Steady-state UV-Vis spectra were measured on a JASCO V-770 spectrophotometer equipped with a PAC-743 cell changer. An Implen NanoPhotometer P 360 was used for RNA quantification. Regular absorption spectra were measured in disposable semi-micro polystyrene cuvettes. Relative quantum yields were measured in a Starna 16.10 sub-micro cuvette (10 mm path length).

Stock solutions of each dye in DMSO were prepared at a concentration of 10 mM. These were further diluted with DMSO to a concentration of 1 mM before being used for the preparation of the samples. The final DMSO concentration in the samples was < 2%.

All measurements were conducted at 25 °C.

UV-VIS pH titration for determination of pK_a values

The following samples were prepared:

- Dye (11 µM) in Britton-Robinson buffer[6] pH 1–12 (30 mM, 20 steps)
- Dye (11 µM) in aqueous HCl pH 0.42 (0.38 M)
- Dye (11 µM) in aqueous HCl pH 0.12 (0.76 M)

Background-corrected UV-Vis spectra of each sample were measured using identical parameter settings:

- Bandwidth: 2.0 nm
- Response: 0.06 s
- Data interval: 0.5 nm
- Scan speed: 1000 nm/min

The absorbance values A at the absorption maximum were fitted to the following model derived from the Henderson-Hasselbalch equation:

$$A = a + \frac{b - a}{(1 + 10^{pK_{a,1} - pH})} + \frac{c - b}{(1 + 10^{pK_{a,2} - pH})} \quad (1)$$

p$K_{a,1}$ describes the equilibrium between the cationic and neutral species, whereas p$K_{a,2}$ d describes the equilibrium between the neutral and anionic species. If fewer or more than two pK_a values are needed, the last term can be omitted or repeated analogously.

5. Fluorescence spectroscopy

Steady-state fluorescence spectra were measured on a JASCO FP-8300 spectrofluorometer equipped with an FCT-817S cell changer. Absolute quantum yields were determined using an ILF-835 integrating sphere with the appropriate spectral correction parameters.

Regular emission and excitation spectra were measured in Hellma ultra-micro quartz cuvettes (1.5×1.5 mm, 3×3 mm or 10×2 mm path lengths). For kinetic assays a JASCO FMM-200 micro quartz cuvette with a magnetic stir bar (5×5 mm path length) was used. Absolute quantum yields were measured in a Jasco 6808-H150A liquid cell (1×10×250 mm side length).

Stock solutions of each dye in DMSO were prepared at a concentration of 10 mM. These were further diluted with DMSO to a concentration of 100 µM before being used in the preparation of the samples. The final DMSO concentration in the samples was < 1%.

All measurements were conducted at 25 °C.

5.1. K^+ binding

The following samples were prepared:

- Chili RNA Aptamer (0.5 µM) and DMHBI (0.5 µM) in buffer containing KCl (0–125 mM, 11 steps), HEPES pH 7.5 (40 mM) and $MgCl_2$ (5 mM). Before addition of $MgCl_2$ and DMHBI, the RNA was annealed at 95 °C for 3 min and then kept at ambient temperature for 20 min. Afterwards, the solution was incubated at 4 °C for 16 h

Fluorescence spectra of each sample were measured using identical parameter settings:

- Ex wavelength: 400 nm
- Em range: 420–750 nm
- Ex bandwidth: 2.5 nm
- Em bandwidth: 10 nm
- Response: 50 ms
- PMT voltage: 740V
- Data interval: 0.2 nm
- Scan speed: 500 nm/min

After background subtraction (buffer), the resulting spectra were integrated. The data points were fitted to the Hill equation to obtain an apparent K_D.

5.2. Dye screening

The following solutions were prepared:

- Buffer containing KCl (125 mM), HEPES pH 7.5 (80 mM) and $MgCl_2$ (5 mM)
- Dye (1 µM) in buffer containing KCl (125 mM), HEPES pH 7.5 (80 mM) and $MgCl_2$ (5 mM)
- Chili RNA aptamer (1 µM) in buffer containing KCl (125 mM), HEPES pH 7.5 (80 mM) and $MgCl_2$ (5 mM). Before addition of $MgCl_2$, the RNA was annealed at 95 °C for 3 min and then kept at ambient temperature for 20 min. Afterwards, the solution was incubated at 4 °C for 16 h
- *E. coli* tRNA (approx. 1 µM or 10 µM) in buffer containing KCl (125 mM), HEPES pH 7.5 (80 mM) and $MgCl_2$ (5 mM). Before addition of $MgCl_2$, the RNA was annealed at 95 °C for 3 min and then kept at ambient temperature for 20 min. Afterwards, the solution was incubated at 4 °C for 16 h
- Quadruplex DNA (10 µM) in buffer containing KCl (125 mM), HEPES pH 7.5 (80 mM) and $MgCl_2$ (5 mM). Before addition of $MgCl_2$, the RNA was annealed at 95 °C for 3 min and then kept at ambient temperature for 20 min. Afterwards, the solution was incubated at 4 °C for 16 h
- Spinach RNA aptamer (10 µM) in buffer containing KCl (125 mM), HEPES pH 7.5 (80 mM) and $MgCl_2$ (5 mM). Before addition of $MgCl_2$, the RNA was annealed at 95 °C for 3 min and then kept at ambient temperature for 20 min. Afterwards, the solution was incubated at 4 °C for 16 h
- Broccoli RNA aptamer (10 µM) in buffer containing KCl (125 mM), HEPES pH 7.5 (80 mM) and $MgCl_2$ (5 mM). Before addition of $MgCl_2$, the RNA was annealed at 95 °C for 3 min and then kept at ambient temperature for 20 min. Afterwards, the solution was incubated at 4 °C for 16 h

The dye solution (7.5 µl) was mixed with either the Chili aptamer or one of the other RNA/DNA solutions (7.5 µl) and kept at ambient temperature for 3 min before starting the measurement. A background spectrum was obtained from the buffer.

Fluorescence spectra of each sample were measured using identical parameter settings:

- Ex wavelength: maximum of the Chili RNA aptamer–dye complex
- Em range: Ex+20–750 nm
- Ex bandwidth: 2.5 nm
- Em bandwidth: 5 nm

- Response: 50 ms
- PMT voltage: 680 V
- Data interval: 0.2 nm
- Scan speed: 500 nm/min

After background subtraction (buffer), the resulting spectrum was integrated.

5.3. Equilibrium binding titration

The following samples were prepared:

- Dye (0.1 µM) in buffer containing KCl (125 mM), HEPES pH 7.5 (40 mM) and $MgCl_2$ (5 mM)
- Chili RNA Aptamer (0.001–8 µM, 15 steps) and dye (0.1 µM) in buffer containing KCl (125 mM), HEPES pH 7.5 (40 mM) and $MgCl_2$ (5 mM). Before addition of $MgCl_2$ and dye, the RNA was annealed at 95 °C for 3 min and then kept at ambient temperature for 20 min. Afterwards, the solution was incubated at 4 °C for 16 h

In case of $DMHBO^+$, the concentrations of the RNA and the dye were 1/10 of those indicated above.

Fluorescence spectra of each sample were measured using identical parameter settings:

- Ex wavelength: maximum of the current RNA-dye combination
- Em range: Ex+20–750 nm
- Ex bandwidth: 2.5 nm
- Em bandwidth: 5 nm
- Response: 1 s
- PMT voltage: adjusted for optimal signal intensity at the highest RNA concentration
- Data interval: 0.2 nm
- Scan speed: 500 nm/min

After background subtraction (dye in buffer), the resulting spectra were integrated. The data points were fitted to the following expression describing one-site binding with ligand depletion:

$$I = \frac{x}{2}\left[\left(c_{\mathrm{dye,\,initial}} + c_{\mathrm{RNA,\,initial}} + K_{\mathrm{d}}\right) - \sqrt{\left(c_{\mathrm{dye,\,initial}} + c_{\mathrm{RNA,\,initial}} + K_{\mathrm{d}}\right)^2 - 4 \cdot c_{\mathrm{dye,\,initial}} \cdot c_{\mathrm{RNA,\,initial}}}\right] \quad (2)$$

5.4. Mg^{2+} dependence

The following samples were prepared:

- Buffer containing KCl (125 mM), HEPES pH 7.5 (80 mM) and $MgCl_2$ (5 mM)
- Aptamer (0.5 µM) and dye (0.5 µM) in buffer containing KCl (125 mM), HEPES pH 7.5 (40 mM) and $MgCl_2$ (0 or 5 mM). Before addition of $MgCl_2$ and dye, the RNA was annealed at 95 °C for 3 min and then kept at ambient temperature for 20 min. Afterwards, the solution was incubated at 4 °C for 16 h

A background spectrum was obtained from the buffer.

Fluorescence spectra of each sample were measured using identical parameter settings:

- Ex wavelength: maximum of the current RNA-dye combination
- Em range: Ex+20–750 nm
- Ex bandwidth: 2.5 nm
- Em bandwidth: 5 nm
- Response: 2 s
- PMT voltage: adjusted for optimal signal intensity at a Mg^{2+} concentration of 5 mM

- Data interval: 0.5 nm
- Scan speed: 500 nm/min

After background subtraction, the resulting spectrum was integrated.

5.5. Association kinetics

The following solutions were prepared:

- Dye in H_2O (15.75, 21, 31.5, 42 and 52.5 μM)
- Chili RNA aptamer (26.25 nM) in buffer containing KCl (131.25 mM), HEPES pH 7.5 (42 mM) and $MgCl_2$ (5.5 mM). Before addition of $MgCl_2$, the RNA was annealed at 95 °C for 3 min and then kept at ambient temperature for 20 min

For each concentration, the dye solution (20 µl) was quickly injected into the Chili RNA aptamer solution (400 µL) and the fluorescence intensity was monitored for 10 min while stirring the mixture.

Fluorescence time courses of each sample were measured using identical parameter settings:

- Ex wavelength: maximum of the current RNA-dye combination
- Em wavelength: maximum of the current RNA-dye combination
- Ex bandwidth: 1 nm
- Em bandwidth: 20 nm
- Response: 50 ms
- PMT voltage: adjusted for optimal signal intensity
- Data interval: 2 s

A part of the RNA solution was kept at 4 °C for 72 h and the measurements were repeated to check for possible slow folding processes.

The data points were fitted to a biexponential association model.

5.6. Absolute quantum yield measurement

The following samples were prepared:

- EtOH
- Coumarin 153 in EtOH (0.1–50 μM, 9 steps)

Fluorescence spectra of each sample were measured using identical parameter settings:

- Ex wavelength: 418 nm
- Em range: 438–750 nm
- Ex bandwidth: 2.5 nm
- Em bandwidth: 2.5 nm
- Response: 1 s
- PMT voltage: 450 V
- Data interval: 0.2 nm
- Scan speed: 100 nm/min

The spectra were integrated between 403 and 433 nm to obtain the scattering intensities s_c (dye solutions) and s_0 (pure EtOH) as well as between 433 and 750 nm to obtain the respective fluorescence intensities f_c and f_0. From these, the absolute quantum yield of Coumarin 153 was calculated according to the following equation:

$$\phi_{\mathrm{std,\,abs}} = \frac{s_0 - s_c}{f_c - f_0} \tag{3}$$

Data are shown in Figure S8; the absolute quantum yield was 0.529 ± 0.006, which compares well with literature values.[7]

5.7. Relative quantum yield measurement

The following samples were prepared:

- EtOH
- Buffer containing KCl (125 mM), HEPES pH 7.5 (40 mM) and $MgCl_2$ (5 mM)
- Coumarin 153 in EtOH (2.5, 5 and 10 µM)
- Dye (2.5, 5 and 10 µM) in buffer containing KCl (125 mM), HEPES pH 7.5 (40 mM) and $MgCl_2$ (5 mM)
- Chili RNA aptamer (10, 12.3 and 17 µM) and dye (2.5, 5 and 10 mM, respectively) in buffer containing KCl (125 mM), HEPES pH 7.5 (40 mM) and $MgCl_2$ (5 mM). Before addition of $MgCl_2$, the RNA was annealed at 95 °C for 3 min and then kept at ambient temperature for 20 min. Afterwards, the solution was incubated at 4 °C for 16 h

Fluorescence spectra of each sample were measured using identical parameter settings:

- Ex wavelength: maximum of the RNA-dye combination that was to be studied
- Em range: Ex+20–750 nm
- Ex bandwidth: 2.5 nm
- Em bandwidth: 2.5 nm
- Response: 1 s
- PMT voltage: adjusted for optimal signal intensity at the highest concentration of Coumarin 153
- Data interval: 0.2 nm
- Scan speed: 100 nm/min

After background subtraction (EtOH or buffer, respectively), the spectra were integrated to obtain the fluorescence intensities *f*.

Next, background-corrected UV-Vis spectra of each sample were measured, again using identical parameter settings:

- Bandwidth: 1.0 nm
- Response: 0.06 s
- Data interval: 0.2 nm
- Scan speed: 400 nm/min

The absorbance *A* at the fluorescence excitation wavelength λ_{Ex} was converted to an absorption factor *a* corrected for the excitation monochromator bandwidth $\Delta\lambda_{Ex}$:

$$a = \int_{\lambda_{Ex}-\Delta\lambda_{Ex}/2}^{\lambda_{Ex}+\Delta\lambda_{Ex}/2} 1 - 10^{-A}\, d\lambda \tag{4}$$

The fluorescence intensities *f*, absorption factors *a* and refractive indices η of the respective solvents were used to calculate the relative quantum yield by linear fitting. Here, x refers to the aptamer-dye complex or dye alone and std refers to Coumarin 153:

$$\phi_{x,\,rel} = \phi_{std,\,abs} \cdot \frac{f_x}{a_x} \cdot \frac{a_{std}}{f_{std}} \cdot \frac{\eta_x^2}{\eta_{std}^2} \tag{5}$$

5.8. Deoxyribozyme kinetics

The following solution was prepared:

- Chili RNA aptamer (0.47 µM) and $DMHBO^+$ (0.47 µM) in buffer containing KCl (125 mM), HEPES pH 7.5 (40 mM) and $MgCl_2$ (5 mM). Before addition of $MgCl_2$, the RNA was annealed at 95 °C for 3 min and then kept at ambient temperature for 20 min. Afterwards, the solution was incubated at 4 °C for 6 h. The total volume of the sample was 14.3 µL

The solution was then quickly mixed with 0.7 µL of the 10-23 DNA enzyme solution (100 µM).

Fluorescence spectra were measured immediately prior to and every 6 s for 40 min after mixing both components using identical parameter settings:

- Ex wavelength: 456 nm
- Em range: 550–700 nm
- Ex bandwidth: 2.5 nm

- Em bandwidth: 5 nm
- Response: 0.1 s
- PMT voltage: 680 V
- Data interval: 1 nm
- Scan speed: 10000 nm/min

6. Gel electrophoresis

6.1. Tb^{3+} probing

RNA structure probing with Tb^{3+} was performed with 5'-^{32}P-labeled RNA. The Chili RNA transcript was first dephosphorylated with Antarctic alkaline phosphatase for 30 min at 37 °C, followed by extraction with phenol/chloroform/isoamyl alcohol. The RNA was recovered by precipitation with ethanol and then 5'-phosphorylated with PNK using gamma-^{32}P-ATP for 1 h at 37 °C, followed by PAGE purification (10% PAGE, 1x TBE, 35 W). For structure probing reactions, 5' ^{32}P-labelled RNA (1 µM) was prepared in buffer containing 50 mM Tris-HCl pH 8.0 and 100 mM KCl, heated at 75 °C for 3 min and kept at room temperature for 15 min. Then, 10 mM $MgCl_2$ and 30 µM DMHBI (or H_2O) were added and the mixture was incubated at room temperature for 10 min. After addition of terbium (III) chloride, the mixture was incubated at 37 °C for the indicated time (5–15 min). The reaction was mixed with stop solution (80% formamide, 89 mM Tris-HCl, 89 mM boric acid, pH 8.3, 50 mM EDTA) and aliquots were analyzed on 15% denaturing PAGE. Reference lanes were prepared by digestion of the RNA with RNase T1 and by alkaline hydrolysis with $NaHCO_3$.

6.2. Native PAGE

The following samples were mixed with 1 µL glycerol loading buffer (6x) and loaded onto a 10% native polyacrylamide gel (1 × 80 × 100 mm):

- 20, 10, 5, 2, 1, 0.5 pmol Chili RNA in 5 µL H_2O
- 5 µL H_2O
- 5 pmol 13-2 aptamer in 5 µL H_2O
- 5 pmol BabySpinach in 5 µL H_2O
- approx. 5 pmol *E. coli* tRNA in 5 µL H_2O

The gel was run in TBE buffer at a constant voltage of 200 V for 20 min.

Afterwards, the gel was immersed in an aqueous staining solution containing 1 µM $DMHBO^+$, 125 mM KCl, 5 mM $MgCl_2$ and 40 mM HEPES pH 7.5 for 15 min and imaged on a ChemiDoc system (blue epi illumination, 605/50 nm emission filter).

Subsequently, the gel was restained by immersing it in an aqueous staining solution containing 1 µM DFHBI, 125 mM KCl, 5 mM $MgCl_2$ and 40 mM HEPES pH 7.5 for 15 min and imaged again (blue epi illumination, 605/50 nm emission filter or 530/30 nm emission filter).

Finally, the gel was restained by immersing it in 1x SYBR Green II in TBE buffer for 15 min and imaged again (blue epi illumination, 530/30 nm emission filter).

6.3. Deoxyribozyme kinetics

For the PAGE-based analysis of DNA-catalyzed RNA cleavage, the Atto 590-labeled Chili RNA ligation product (0.5 µM) was annealed with the 10-23 DNA enzyme (5 µM) in 7.5 µL buffered solution containing KCl (125 mM) and HEPES pH 7.5 (40 mM) by heating to 95 °C for 2 min, followed by incubation at ambient temperature for 20 min. The reaction was initiated by addition of $MgCl_2$ to a final concentration of 5 mM (2.5 µL of 20 mM $MgCl_2$). Aliquots (1 µL) were removed after 15 sec, 0.5, 1, 2, 5, 10, 20, 40, and 60 min, mixed with stop solution (4 µL, 80% formamide, 89 mM Tris-HCl, 89 mM boric acid, 50 mM EDTA, pH 8.3) and kept on ice. The samples were then analyzed on a 15% denaturing polyacrylamide gel (7 M urea, 0.4 × 200 × 200 mm; 32 wells, run in 1x TBE at 20 W for 45 min). The gel was imaged on a ChemiDoc system with green epi illumination to visualize the Atto 590-labeled RNA, then stained with 1 µM $DMHBO^+$ solution for 5 min and imaged by blue epi illumination to visualize the Chili RNA fragments.

SUPPORTING INFORMATION

Supporting Tables

Table S1: DNA and RNA Sequences.

Description	5'-Sequence-3'	nt
RNA:		
13-2 RNA aptamer	GGGCUAUUGCUGGAGGGGCGCCACAUGAAAGUGGUGGUUGGGUGCGGUCGGCGAUAGCUC	60
Chili RNA aptamer	GGCUAGCUGGAGGGGCGCCAGUUCGCUGGUGGUUGGGUGCGGUCGGCUAGCC	52
BabySpinach RNA aptamer	GGUGAAGGACGGGUCCAGUAGUUCGCUACUGUUGAGUAGAGUGUGAGCACC	51
Broccoli RNA aptamer	GAGACGGUCGGGUCCAGAUAUUCGUAUCUGUCGAGUAGAGUGUGGGCUC	49
RNA substrate for 10-23	GCACAUCUGUUAAACGAUAA–NH_2	20
DNA:		
Txn template for 13-2	GAGCTATCGCCGACCGCACCCAACCACCACTTTCATGTGGCGCCCCTCCAGCAATAGCCCTATAGTGAGTCGTATTACAG	80
Txn template for Chili	GGCTAGCCGACCGCACCCAACCACCAGCGAACTGGCGCCCCTCCAGCTAGCCTATAGTGAGTCGTATTACAG	72
Txn template for BabySpinach	GGTGCTCACACTCTACTCAACAGTAGCGAACTACTGGACCCGTCCTTCACCTATAGTGAGTCGTATTACAG	71
Txn template for Broccoli RNA	GAGCCCACACTCTACTCGACAGATACGAATATCTGGACCCGACCGTCTCTATAGTGAGTCGTATTACAG	69
T7 promoter	CTGTAATACGACTCACTATA	20
Splint for ligation	TTTAACAGATGTGCGGCTAGCCGA	24
10-23 DNA enzyme	ATCGTTTAAGGCTAGCTACAACGAAGATGTGC	32
Quadruplex DNA	TGGGTGGGTGGGTGGGT	17

Table S2: Photophysical data of the four HBI fluorophores in aqueous buffer as well as bound to the Chili aptamer.

Fluorophore	$\lambda_{Ex,max}$ (nm)		$\lambda_{Em,max}$ (nm)		Stokes shift (nm)		ϕ_{rel}[a]		ε (L mol^{-1} cm^{-1})	K_D (mol L^{-1})
	free[b]	bound[c]	free[b]	bound[c]	free	bound	free	bound	bound	
DMHBI	378/479	400	485/537	537	107/58	137	$6.57\pm0.05\times10^{-4}$	$7.6\pm0.1\times10^{-2}$	18000	$5.7\pm1.2\times10^{-7}$
DMHBI$^+$	379/493	413	486/540	542	107/47	129	$1.09\pm0.01\times10^{-3}$	$3.99\pm0.08\times10^{-1}$	21000	$6.3\pm0.6\times10^{-8}$
DMHBI-Imi	455/542	463	544/610	545, 594[d]	89/68	82, 131	$3.3\pm0.4\times10^{-3}$	$7.5\pm0.2\times10^{-2}$	20000	$7.1\pm0.2\times10^{-8}$
DMHBO$^+$	436/547	456	546/594	592	90/47	136	$1.02\pm0.09\times10^{-3}$	$9.4\pm0.4\times10^{-2}$	22000	$1.2\pm0.2\times10^{-8}$

[a] Relative fluorescence quantum yields were determined using Coumarin 153 as the standard (see Figures S8–S12). The excitation wavelength for each dye was set to $\lambda_{Ex,max}$ of the respective Chili complex. [b] The fluorophore concentration was 10 µM. The two wavelengths correspond to protonated and deprotonated phenolate, respectively. [c] The concentration of Chili and the fluorophore was 0.5 µM each. The buffer contained 125 mM KCl, 5 mM $MgCl_2$ and 40 mM HEPES at pH 7.5. [d] The Chili–DMHBI-Imi complex exhibits a broad, bimodal emission spectrum.

Table S3: Comparison of selected fluorogenic aptamers reported in the literature.

RNA	Ligand	$\lambda_{Ex,max}$ (nm)	$\lambda_{Em,max}$ (nm)	Stokes shift (nm)	ϕ	K_D (µM)	Mg^{2+} demand[a] (mM)	Reference (No. in main text)
Chili	DMHBI	400	537	137	0.08	0.57	~ 5	this work
	DMHBI$^+$	413	542	129	0.40	0.063	low	this work
	DMHBI-Imi	463	594	131	0.08	0.071	~ 5	this work
	DMHBO$^+$	456	592	136	0.10	0.012	low	this work
13-2min	DMHBI	398	529	131	0.06	0.46	–	9
Spinach	DFHBI	469	501	32	0.72	0.537	~ 10	9
Spinach2	DFHBI	447	501	54	0.72	0.530	–	SI[8]
	DFHBI-1T	482	505	23	0.94	0.560	–	
Broccoli	DFHBI-1T	472	507	35	0.94	0.36	0.2	10
Corn	DFHO	505	545	40	0.25	0.07	> 10	11
Red Broccoli	DFHO	518	582	64	0.34	0.206	~ 6	11
Mango	TO1	510	535	25	0.14	0.0032	–	8
	TO3	637	658	21	–	0.007	–	
Mango II	TO1	510	535	25	–	0.0007	~ 75	7
DIR2s	DIR-Pro	600	658	58	0.33	0.252–0.313	8	6
	OTB-SO3	380	421	41	0.51	0.662–0.739	~ 6	

[a] Concentration of Mg^{2+} reported to achieve high brightness of the fluoromodules. If not provided directly, the value was estimated from data presented in figures; – data not reported

SUPPORTING INFORMATION

Supporting Figures

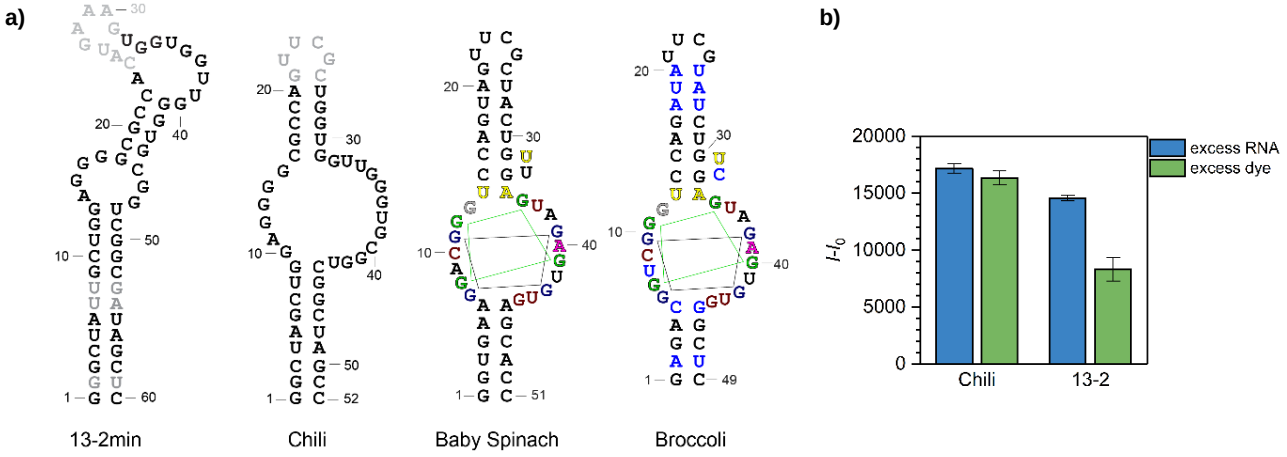

Figure S1: a) Secondary structure graphs of 13-2min (Paige et al, Science 2011) in comparison to Chili RNA (this work), as well as Baby Spinach (Warner et al., NSMB 2014) and Broccoli (Filonov et al., JACS 2014). The nucleotides replaced/removed from 13-2min to generate Chili are shown in grey The UUCG tetraloop was introduced to assist folding of the apical stem-loop, to prevent misfolding of the RNA and to favour formation of the ligand-binding competent structure. The basal stem was shortened to reduce the overall length of the RNA. Currently no structure of the 13-2 or Chili RNAs are known, and therefore a putative quadruplex in the core region can only be suggested. In contrast, the structure of the Spinach RNA is known, and the G quartets are indicated by dark blue and green letters (and connected by corresponding lines), and the key base triple stacking on top of DFHBI is indicated in yellow. By sequence comparison, the same structural elements can be identified in the Broccoli sequence, but not in the Chili RNA. The nucleotides that are different in Broccoli compared to Spinach are shown in bright blue. b) Fluorescence intensities of DMHBI with the Chili RNA or 13-2min aptamer. Integrated emission intensities after background correction for 10 µM of the RNA mixed with 0.1 µM of the dye (blue bars), and 0.1 µM of the RNA mixed with 10 µM of the dye (green bars). Error bars represent the standard deviation (n = 3). Measurement conditions and parameters for all spectra: 125 mM KCl, 5 mM $MgCl_2$, 40 mM HEPES pH 7.5; Ex bandwidth 2.5 nm, Em bandwidth 5 nm, PMT voltage 680 V. b).

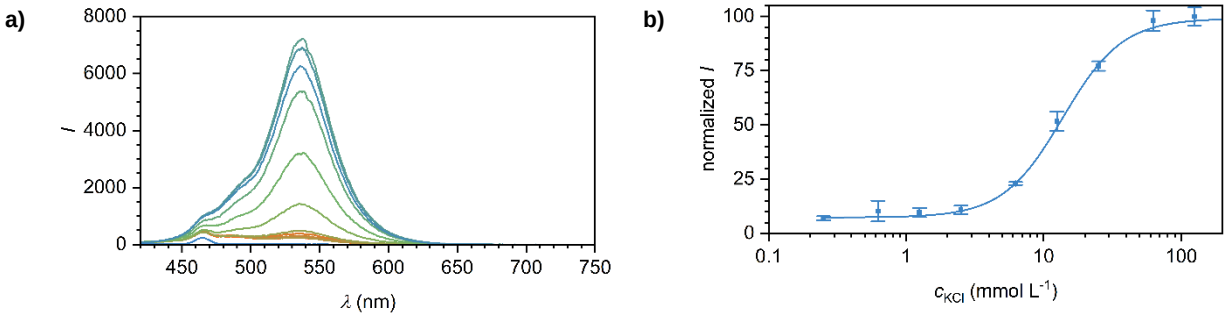

Figure S2: a) Fluorescence spectra and b) normalized integrated intensities for the titration of the Chili–DMHBI complex with KCl. The apparent dissociation constant K_d was obtained by fitting the data to the Hill equation (solid line) and was found to be 1.2±0.1×10^{-2} mol L^{-1} with a Hill coefficient of 2.5±0.4. Error bars represent the standard deviation (n = 3). Spectra are shown for a single run of triplicates. Measurement conditions and parameters: 0.5 µM RNA, 0.5 µM dye, 5 mM $MgCl_2$, 40 mM HEPES pH 7.5; Ex bandwidth 2.5 nm, Em bandwidth 10 nm, PMT voltage 740 V.

a) Chili RNA

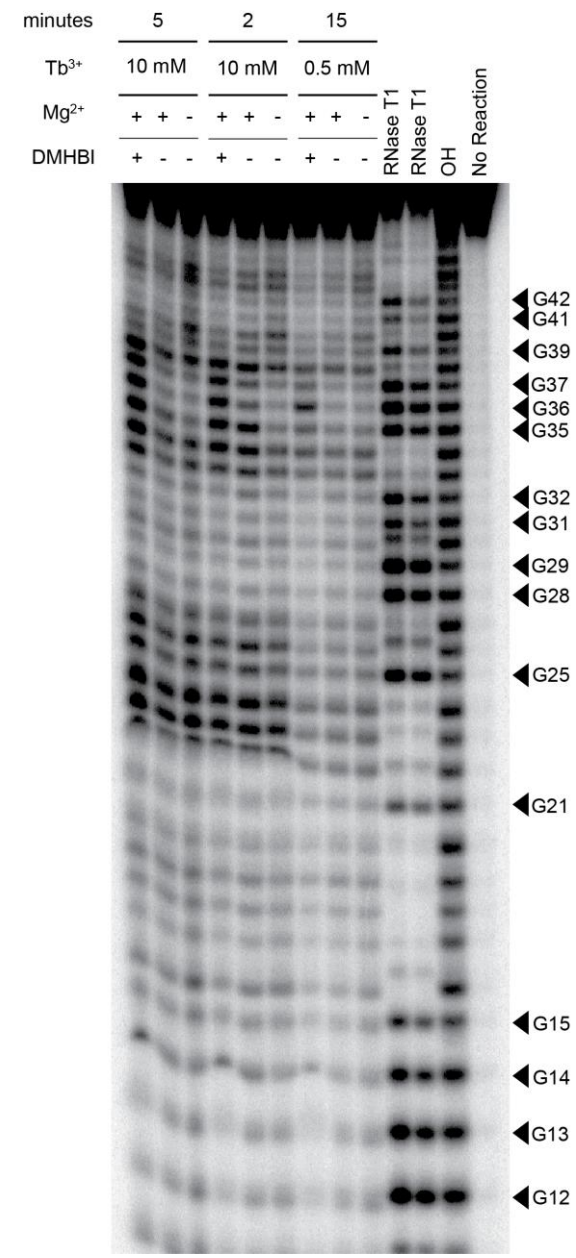

b) 13-2min

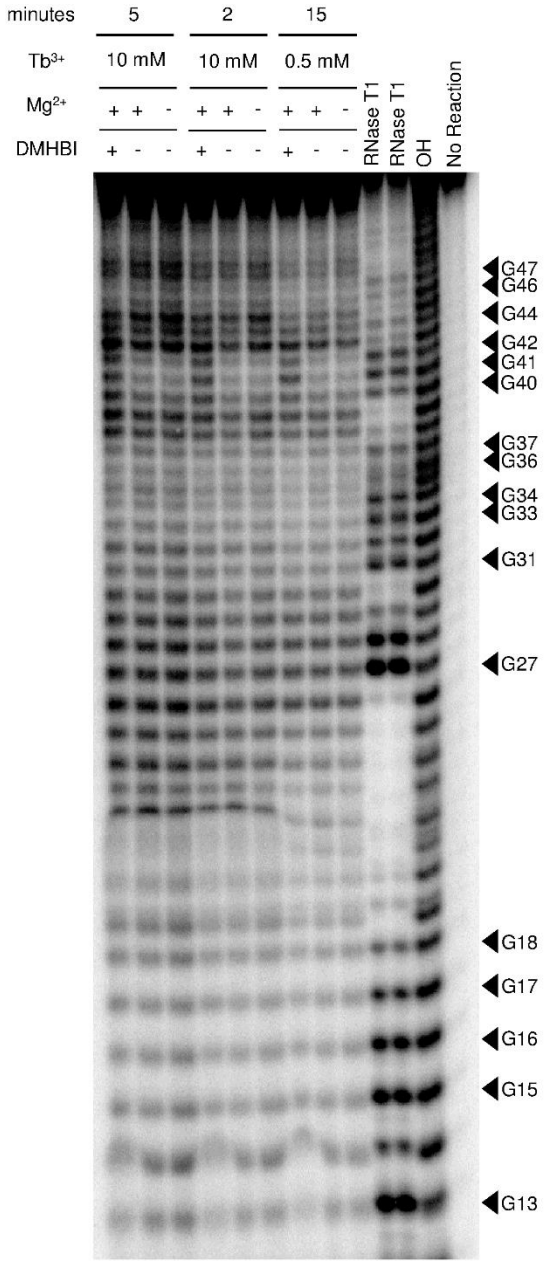

Figure S3: a) Enlarged gel image corresponding to Figure 1b showing Tb^{3+} probing under three different conditions. Digestion by RNase T1 was used to generate a reference ladder for guanosines and alkaline hydrolysis (lane labeled OH) was used to generate a single-nucleotide resolution ladder. The Chili RNA was folded in binding buffer (40 mM HEPES pH 7.5, 125 mM KCl), then water (-), $MgCl_2$ (5 mM final concentration), or $MgCl_2$ (5 mM) and DMHBI (30 µM) were added. Structure probing was performed at 37 °C; concentrations of $TbCl_3$ and incubation time as indicated in the Figure. b) The analogous experiment performed with 60-nt long 13-2min RNA.

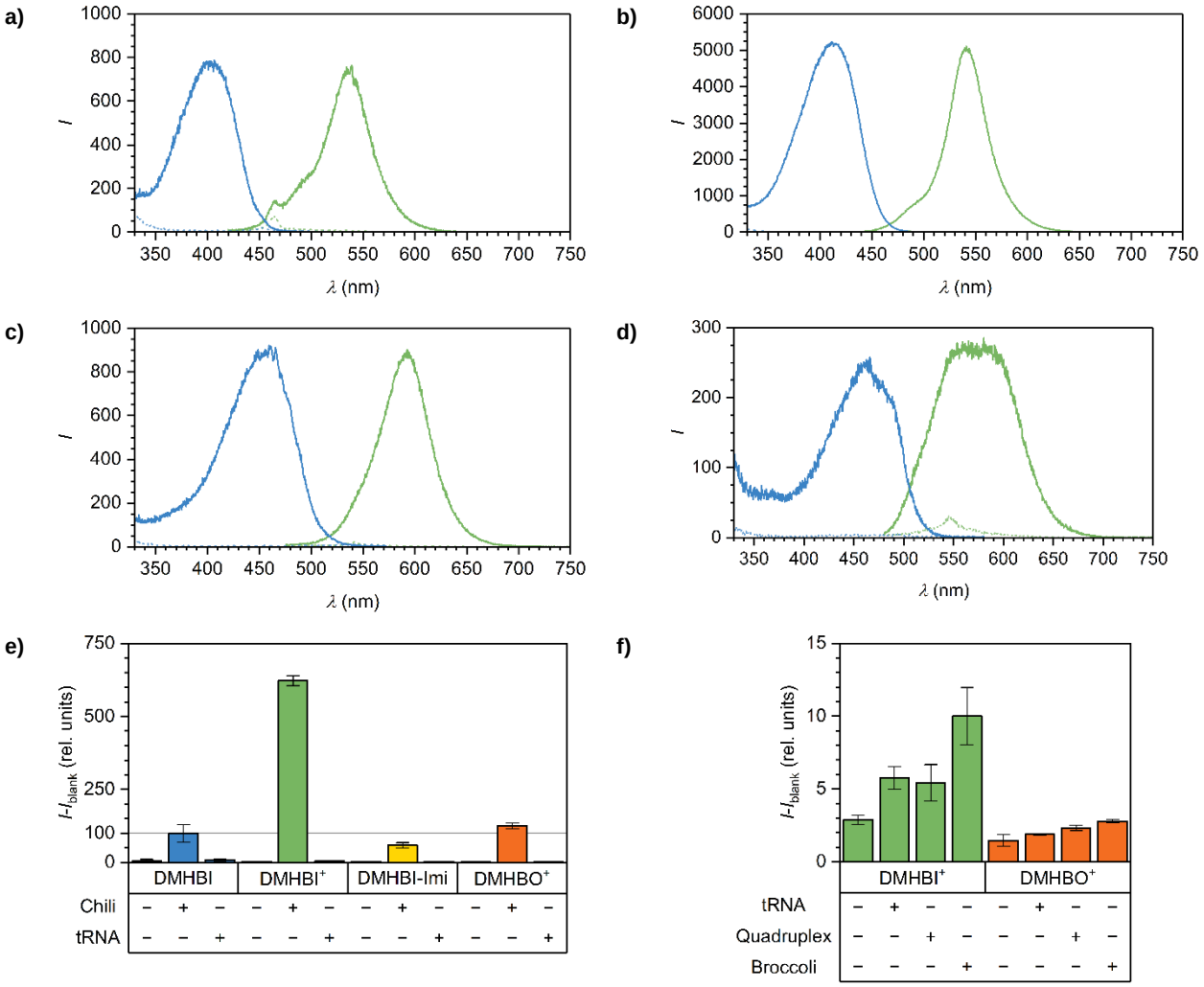

Figure S4: Fluorescence excitation (blue) and emission (green) spectra of a) DMHBI, b) DMHBI$^+$, c) DMHBO$^+$ and d) DMHBI-Imi with the Chili aptamer (solid lines) and in buffer alone (dashed lines). e) Integrated emission intensities of the dyes in buffer, their Chili complexes and the dyes in the presence of *E. coli* tRNA relative to the Chili–DMHBI complex. f) Integrated emission intensities of DMHBI$^+$ and DMHBO$^+$ in buffer and in the presence of a tenfold excess of the indicated RNA (tRNA, Broccoli RNA) or DNA (quadruplex). The y-axis scale is identical for panels e and f. Error bars represent the standard deviation (n = 3). Spectra in a)-d) are shown for a single run of triplicates. Measurement conditions and parameters for spectra in a)-d): 0.5 µM RNA, 0.5 µM dye, 125 mM KCl, 5 mM $MgCl_2$, 80 mM HEPES pH 7.5; Ex bandwidth 2.5 nm, Em bandwidth 5 nm, PMT voltage 680 V.

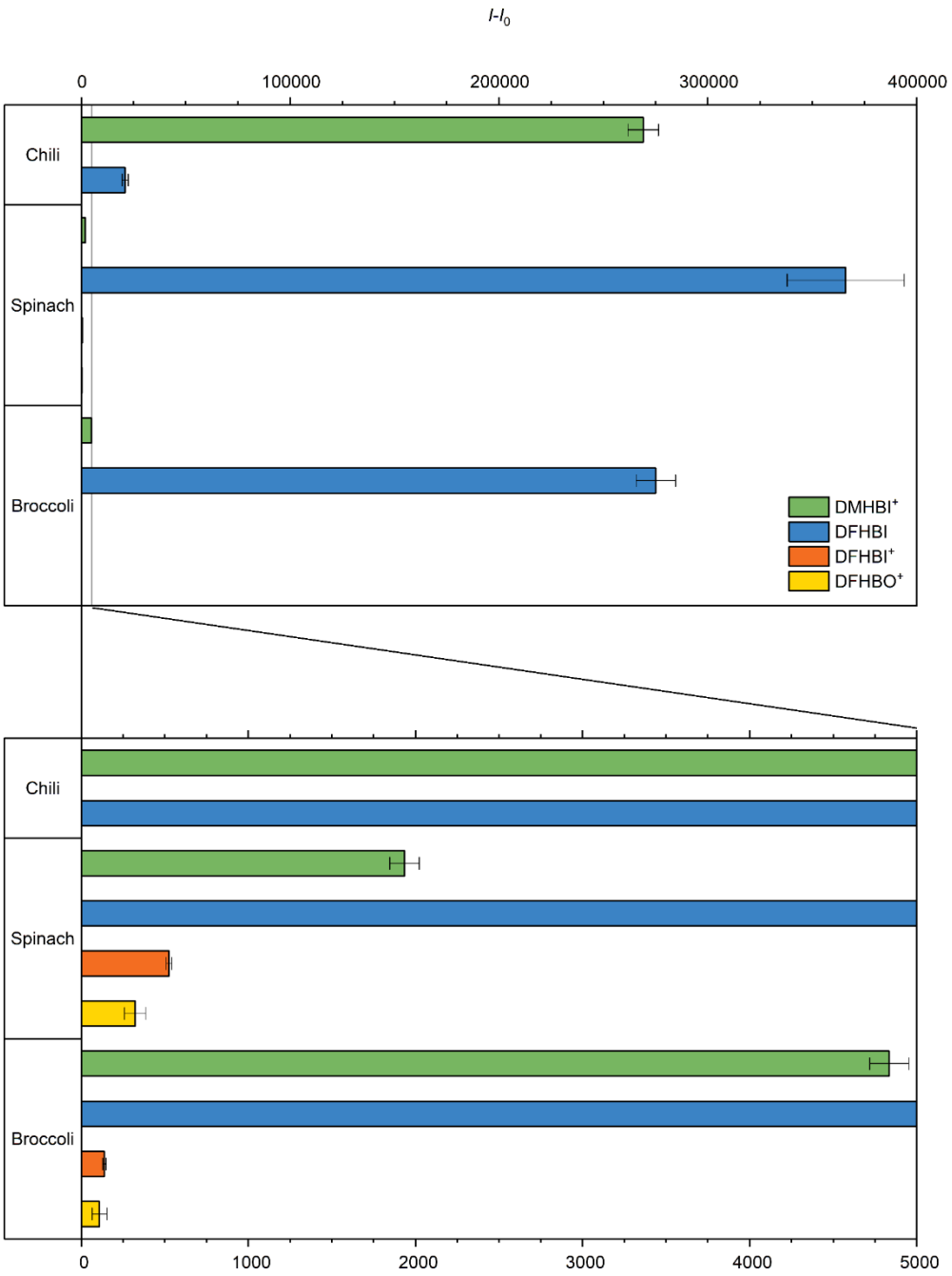

Figure S5: Integrated emission intensities of DMHBI$^+$, DFHBI, DFHBI$^+$ and DFHBO$^+$ in the presence of the Chili, Spinach or Broccoli aptamer. A magnification of the axis interval between 0 and 5000 intensity units is shown in the bottom panel. Error bars represent the standard deviation (n = 3). Measurement conditions and parameters: 0.5 µM RNA, 0.5 µM dye, 125 mM KCl, 5 mM $MgCl_2$, 80 mM HEPES pH 7.5; Ex bandwidth 2.5 nm, Em bandwidth 5 nm, PMT voltage 680 V. In the case of DFHBI$^+$ and DFHBO$^+$ with Broccoli, the fluorescence emission was barely above the background at any excitation wavelength.

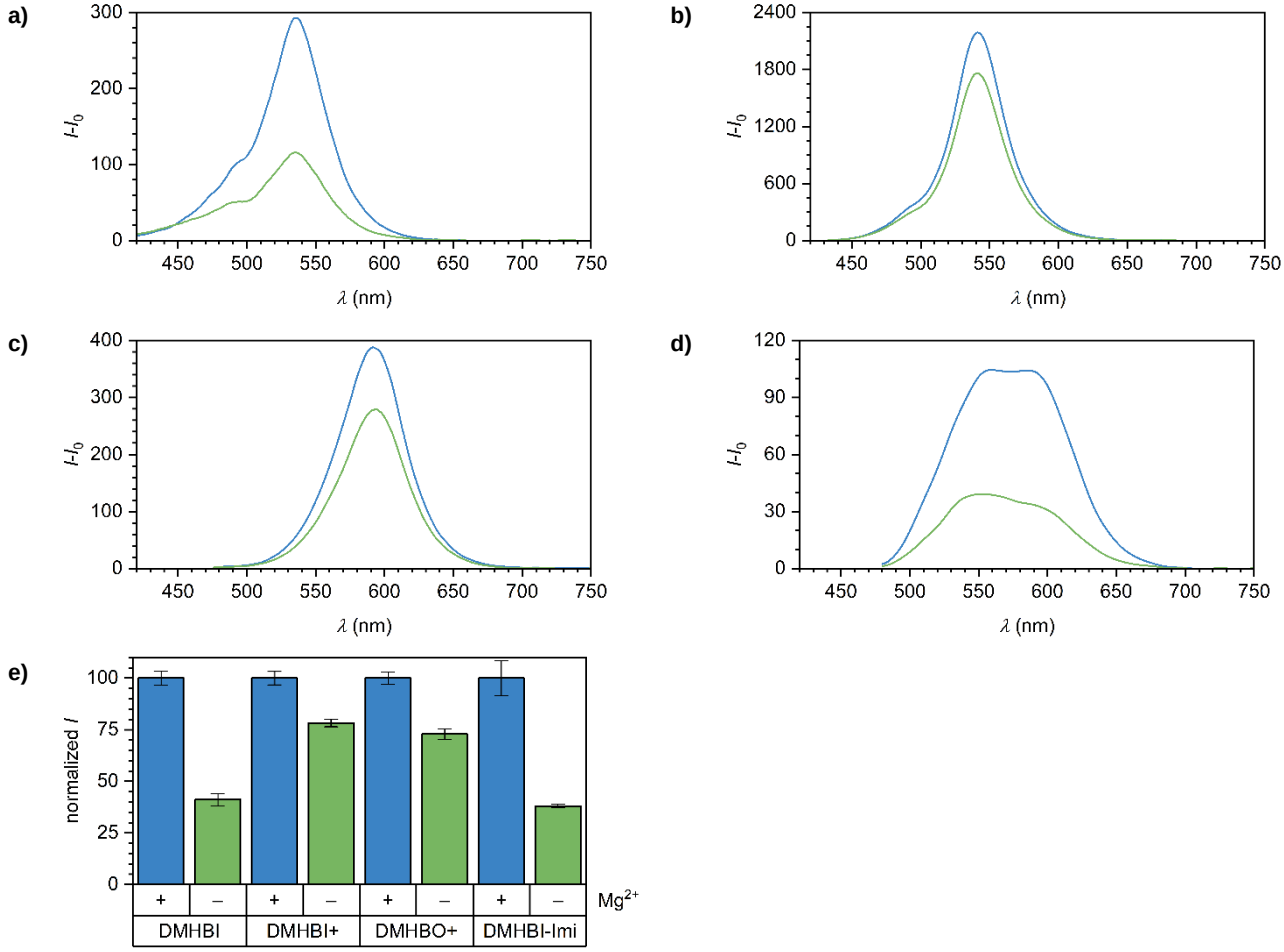

Figure S6: Fluorescence spectra of a) Chili–DMHBI, b) Chili–DMHBI$^+$, c) Chili–DMHBO$^+$ and d) Chili–DMHBI-Imi with 5 mM $MgCl_2$ (blue) or without added $MgCl_2$ (green). e) Integrated emission intensities of the Chili–dye complexes in the presence or absence of 5 mM Mg^{2+}. The intensities of the respective Mg^{2+}-containing samples were set to 100. Spectra are shown for a single run of triplicates. Measurement conditions and parameters for all spectra: 0.5 µM RNA, 0.5 µM dye, 125 mM KCl, 40 mM HEPES pH 7.5; Ex bandwidth 2.5 nm, Em bandwidth 5 nm, PMT voltage 680 V.

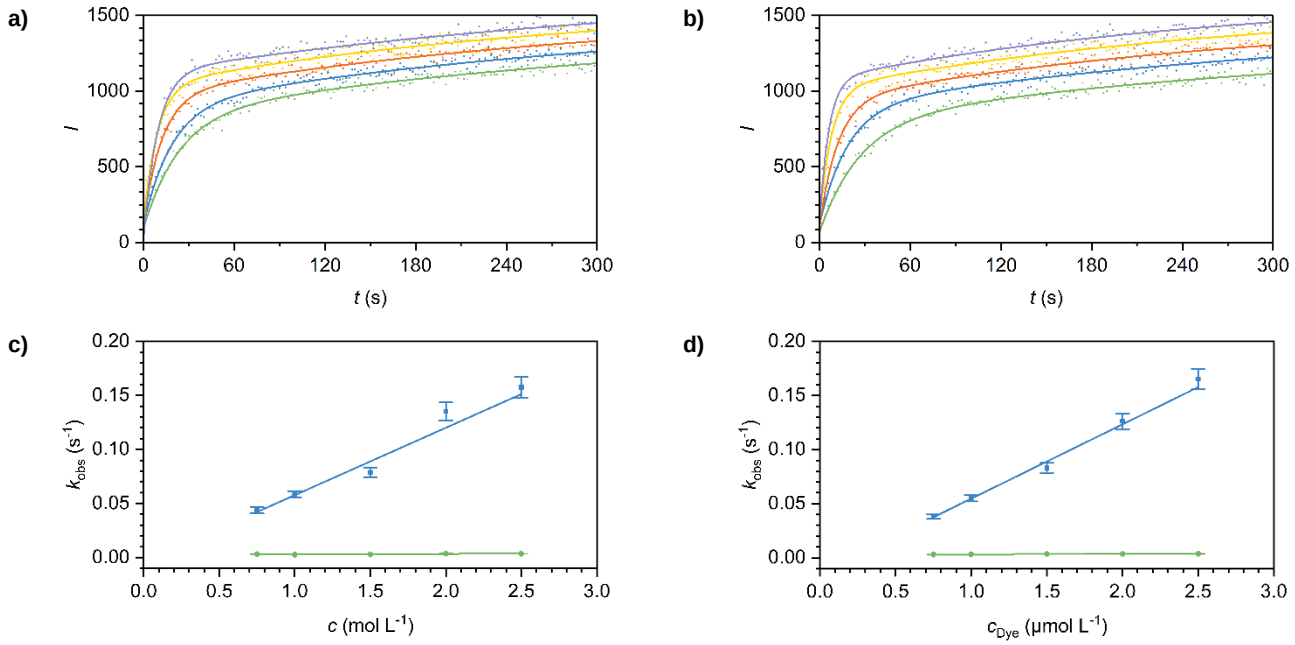

e)

c_{Dye} (µmol L^{-1})	k_{obs} fast (s^{-1})		k_{obs} slow (s^{-1})	
	before	after	before	after
0.75	0.044±0.003	0.038±0.002	0.0032±0.0003	0.0030±0.0003
1.00	0.058±0.003	0.055±0.003	0.0027±0.0003	0.0031±0.003
1.50	0.079±0.004	0.083±0.005	0.0028±0.0003	0.0035±0.0002
2.00	0.135±0.008	0.126±0.007	0.0037±0.0002	0.0034±0.0002
2.50	0.16±0.01	0.165±0.009	0.0035±0.0003	0.0037±0.0002
fit slope (L mol^{-1} s^{-1})	62342±7528	68774±3526	468±292	376±73

Figure S7: Fluorescence time courses for the binding of $DMHBO^+$ at five different concentrations to the Chili aptamer a) shortly after annealing of the RNA and b) after prolonged incubation. The pseudo-first order rate constants k_{obs} were obtained by fitting the data to a biexponential association model (solid lines). A plot of kobs against the dye concentration (blue: fast component, green: slow component) shows no significant difference c) before and (d) after prolonged incubation. Error bars represent standard errors of the non-linear regression. e) Fitted k_{obs} values from a and b and slopes of the linear fits shown in c and d. Shown is a single run of triplicates. Measurement conditions and parameters: 25 nM RNA, 125 mM KCl, 5 mM $MgCl_2$, 40 mM HEPES pH 7.5; Ex bandwidth 1 nm, Em bandwidth 20 nm, PMT voltage 780 V.

SUPPORTING INFORMATION

Quantum yield measurement

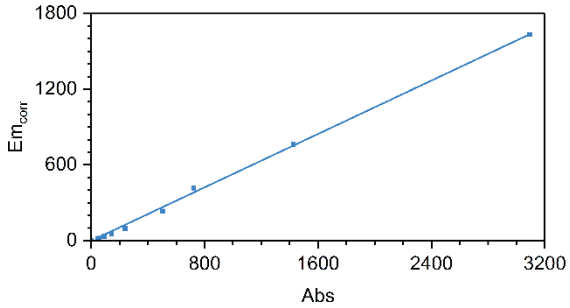

Figure S8: Plot of the integrated fluorescence intensity against the integrated absorption for Coumarin 153 in EtOH at nine different concentrations. An absolute quantum yield of 0.529±0.006 was obtained by fitting the data to a linear model. Measurement parameters for all spectra: Ex bandwidth 2.5 nm, Em bandwidth 2.5 nm, PMT voltage 450 V.

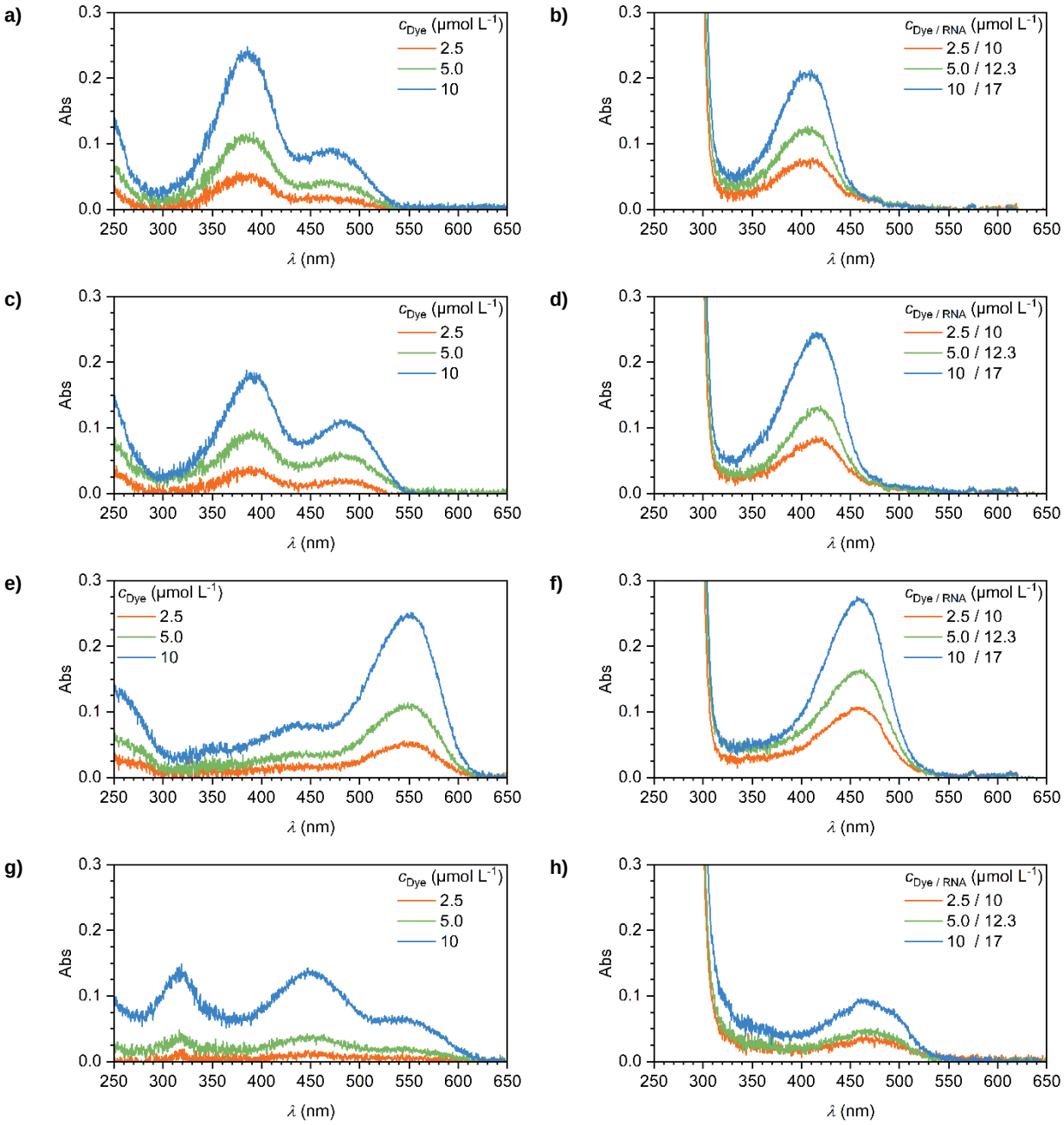

Figure S9: UV/Vis spectra of the dyes in buffer (left colulmn) and bound to the Chili aptamer (right column), respectively. a, b) DMHBI. c, d) DMHBI$^+$. e, f) DMHBO$^+$. g, h) DMHBI-Imi. Measurement conditions and parameters for all spectra: 125 mM KCl, 5 mM $MgCl_2$, 40 mM HEPES pH 7.5; UV/Vis bandwidth 1.0 nm.

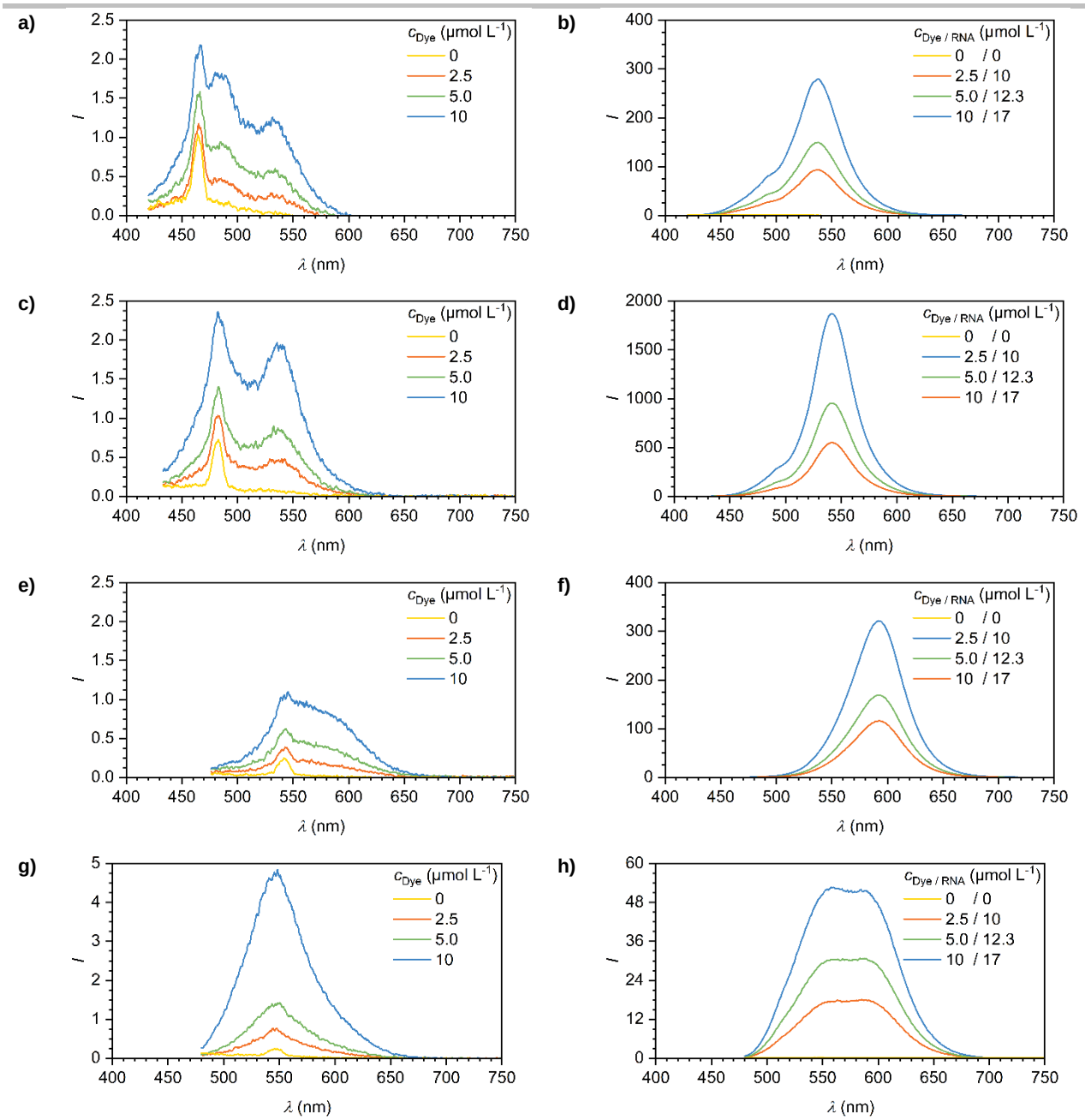

Figure S10: Fluorescence spectra of the dyes in buffer and bound to the Chili aptamer, respectively. a, b) DMHBI, λ_{Ex} = 400 nm. c, d) DMHBI$^+$, λ_{Ex} = 413 nm. e, f) DMHBO$^+$, λ_{Ex} = 456 nm. g, h) DMHBI-Imi, λ_{Ex} = 460 nm. Measurement conditions and parameters for all spectra: 125 mM KCl, 40 mM HEPES pH 7.5; Ex bandwidth 2.5 nm, Em bandwidth 2.5 nm, PMT voltage 475 V.

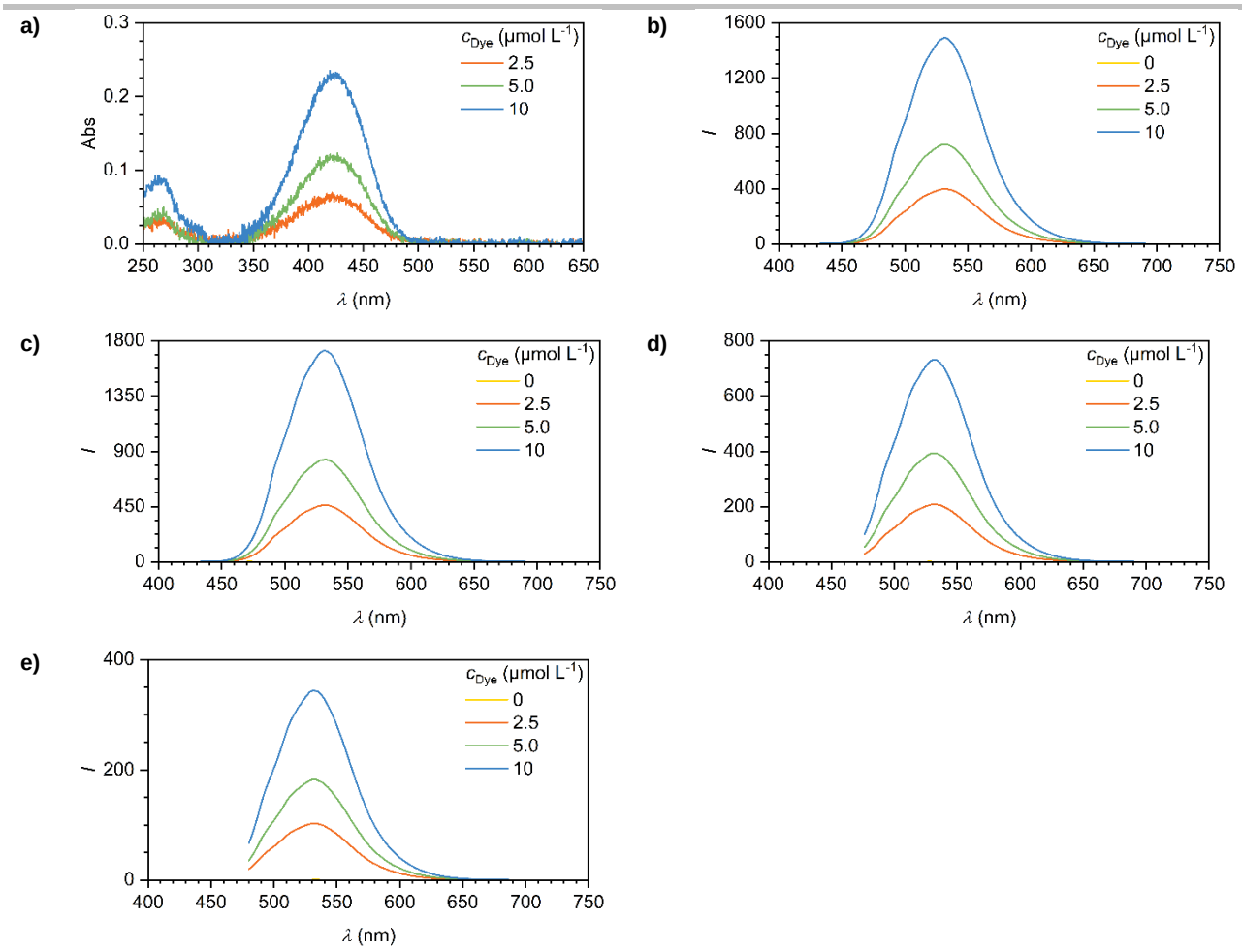

Figure S11: a) UV/Vis spectra of the quantum yield standard Coumarin 153 in EtOH. Fluorescence spectra of the same samples with b) λ_{Ex} = 400 nm, c) λ_{Ex} = 413 nm, d) λ_{Ex} = 456 nm, e) λ_{Ex} = 460 nm. Measurement parameters for the UV/Vis spectra: UV/Vis bandwidth 1.0 nm. Spectra are shown for a single run of triplicates. Measurement parameters for the fluorescence spectra: Ex bandwidth 2.5 nm, Em bandwidth 2.5 nm, PMT voltage 475 V.

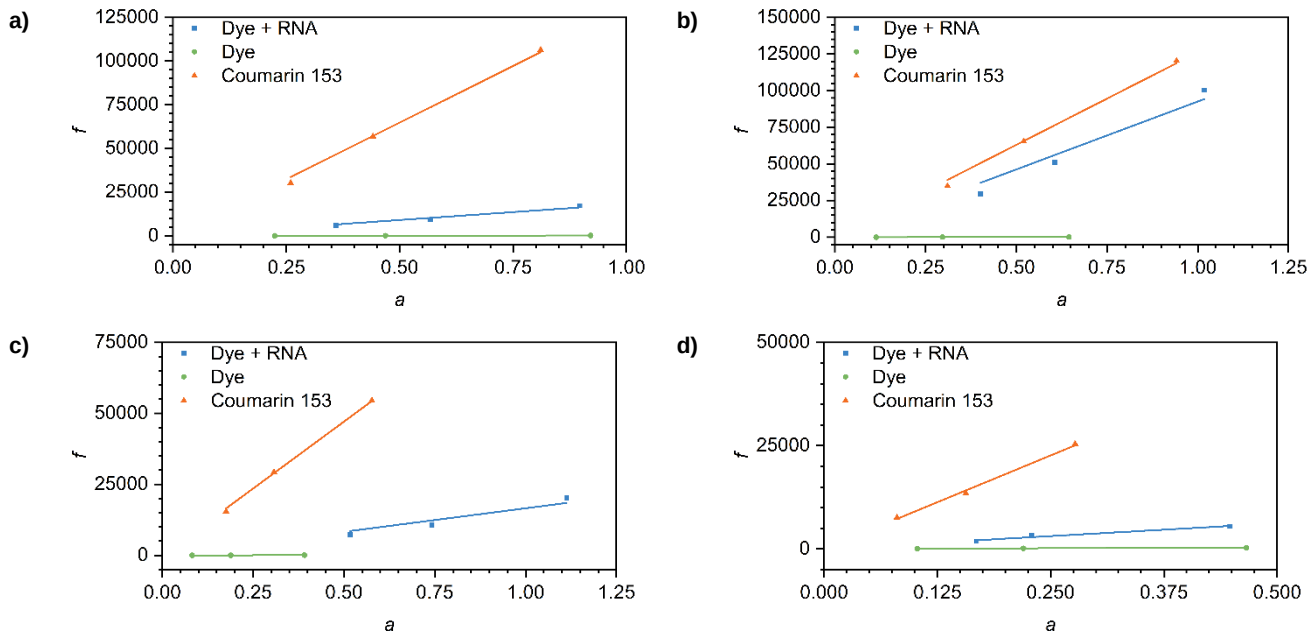

Figure S12: Plots of the integrated fluorescence intensity *f* against the absorption factor *a* for the dye-RNA complexes, the dyes in buffer and Coumarin 153. a) DMHBI. b) DMHBI$^+$. c) DMHBO$^+$. d) DMHBI-Imi. Linear fits were used to calculate the relative quantum yields. Data is shown for a single run of triplicates.

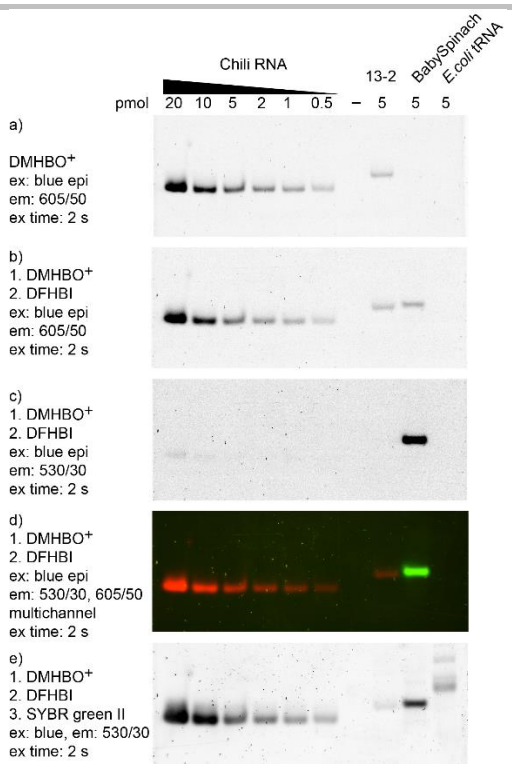

Figure S13: The indicated amounts of the Chili, 13-2, and BabySpinach aptamers as well as *E. coli* tRNA were loaded onto a 10% native polyacrylamide gel and run at a constant voltage of 200 V for 20 min in TBE buffer. The gel was subsequently stained with 1 µM $DMHBO^+$ in binding buffer, 1 µM DFHBI in binding buffer and 1x SYBR Green II in TBE buffer for 15 min each without intermediate washing steps. a) After staining with $DMHBO^+$ only, using blue epi illumination and a 605/50 nm emission filter. b) After subsequent staining with DFHBI, using blue epi illumination and a 605/50 nm emission filter, c) using blue epi illumination and a 530/30 nm emission filter or d) in false color using blue epi illumination, a 605/50 nm filter for the red channel and a 530/30 nm filter for the green channel. e) After subsequent staining with SYBR Green II, using blue epi illumination and a 530/30 nm emission filter. The binding buffer contained 125 mM KCl, 5 mM $MgCl_2$ and 40 mM HEPES pH 7.5.

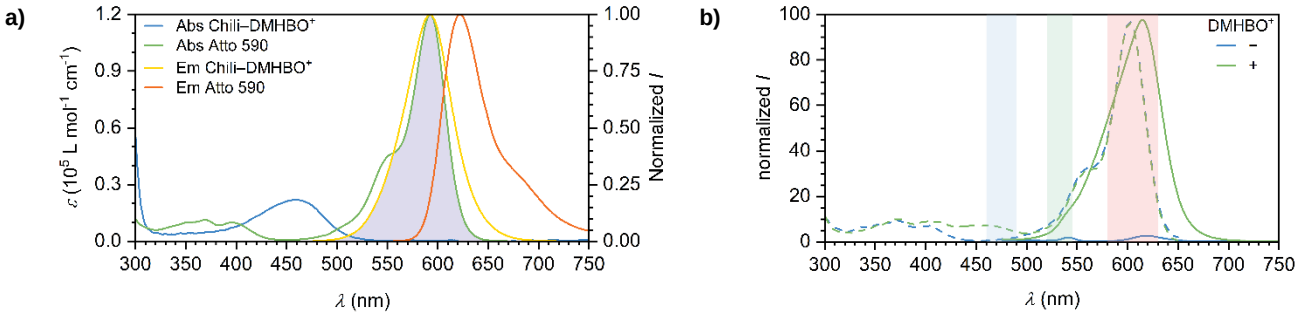

Figure S14: a) Absorption and emission spectra of the Chili–$DMHBO^+$ complex and Atto 590, respectively. The emission maxima are normalized to an intensity of 1. Data for Atto 590 was supplied by the manufacturer. b) Fluorescence excitation (dashed) and emission (solid) spectra of Atto 590-labeled Chilli in the absence (blue) or presence (green) of $DMHBO^+$. The emission spectra were obtained by excitation at 456 nm; the excitation spectra result from observing the emission at 670 nm. The shaded areas correspond to the excitation and emission windows used for the gel images shown in Fig. 4c of the main text.

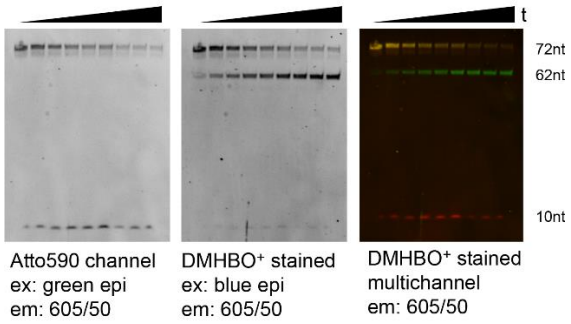

Figure S15: Full PAGE image of 10-23 deoxyribozyme kinetics according to Figure 4d, here shown with false color code: red = Atto 590, green = $DMHBO^+$, therefore double-labeled RNA (72 nt uncleaved starting material) appears yellow.

NMR spectra

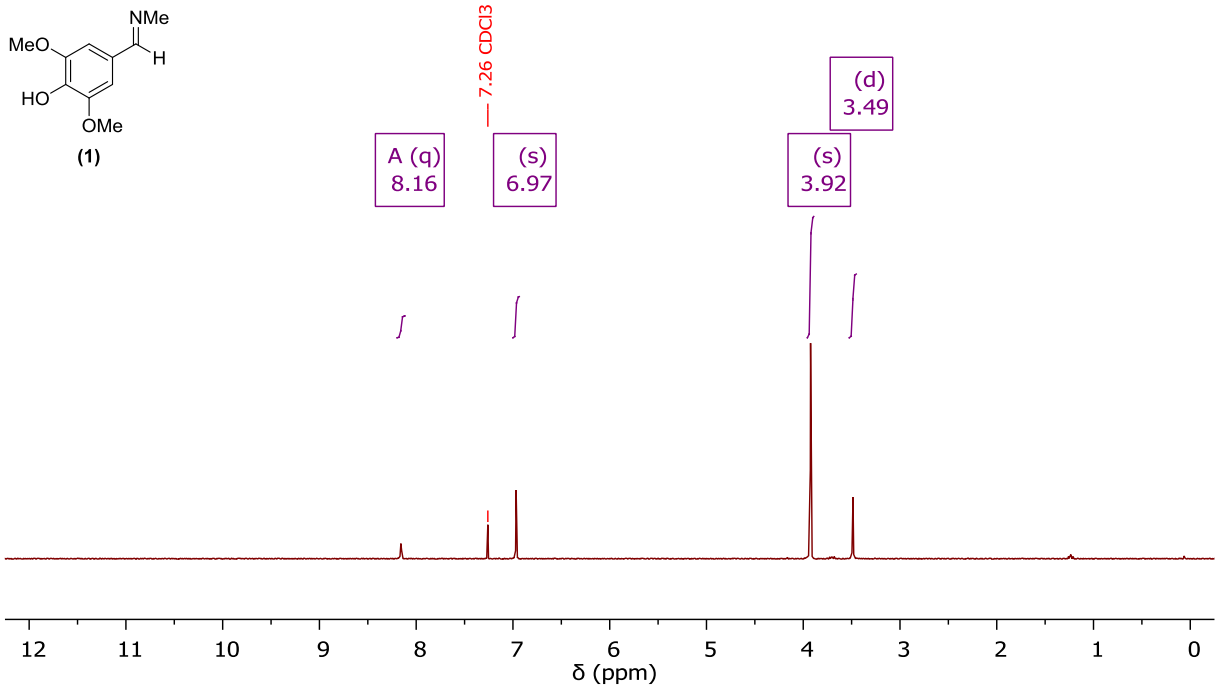

Figure S16: ^{1}H NMR spectrum of **1** in $CDCl_3$, 300 MHz.

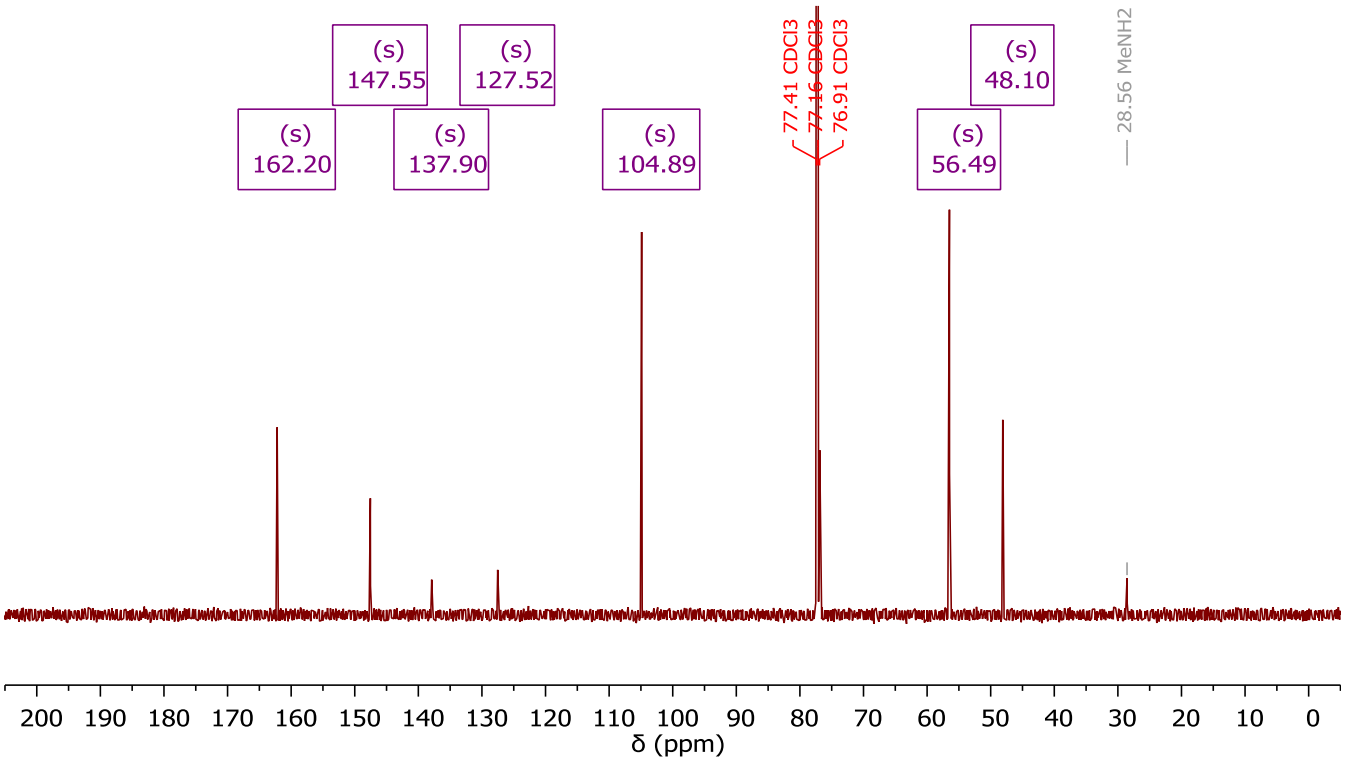

Figure S17: ^{13}C NMR spectrum of **1** in $CDCl_3$, 125 MHz.

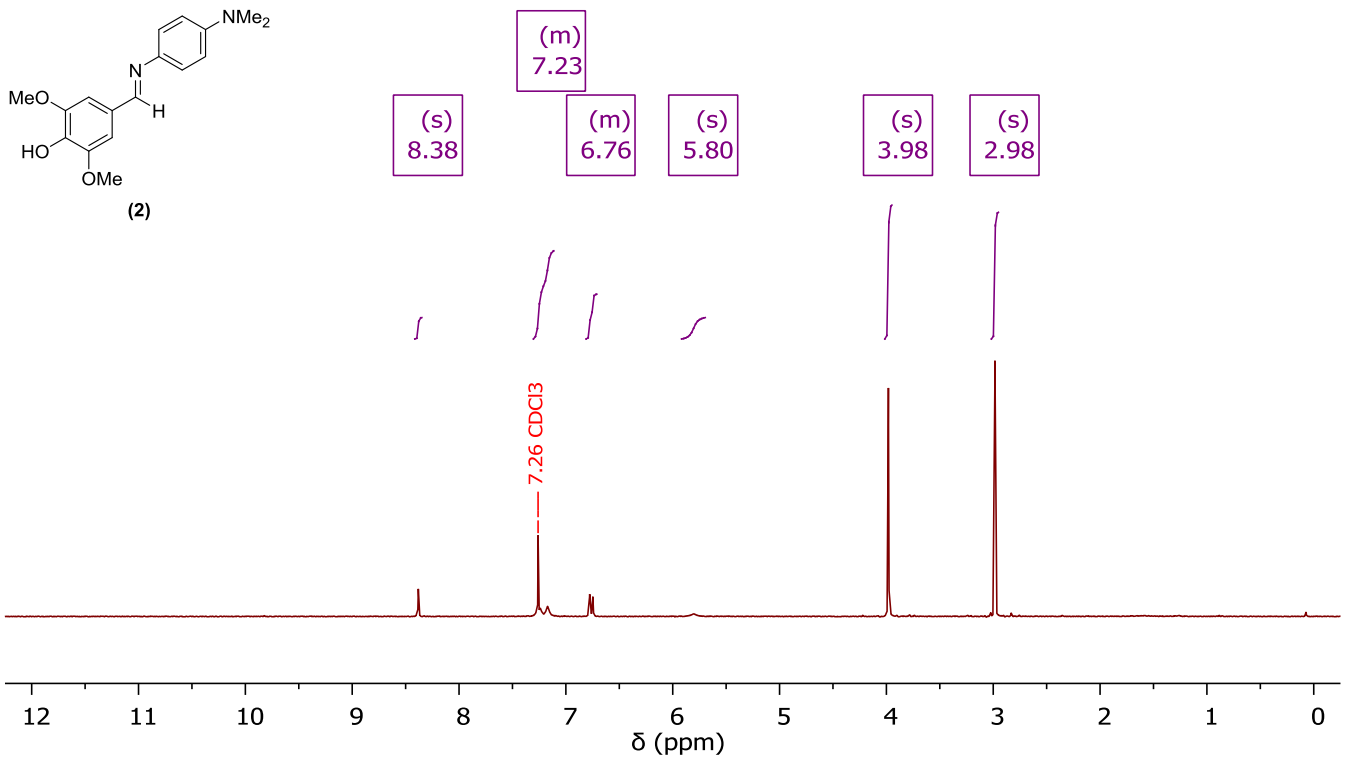

Figure S18: ^{1}H NMR spectrum of **2** in $CDCl_3$, 300 MHz.

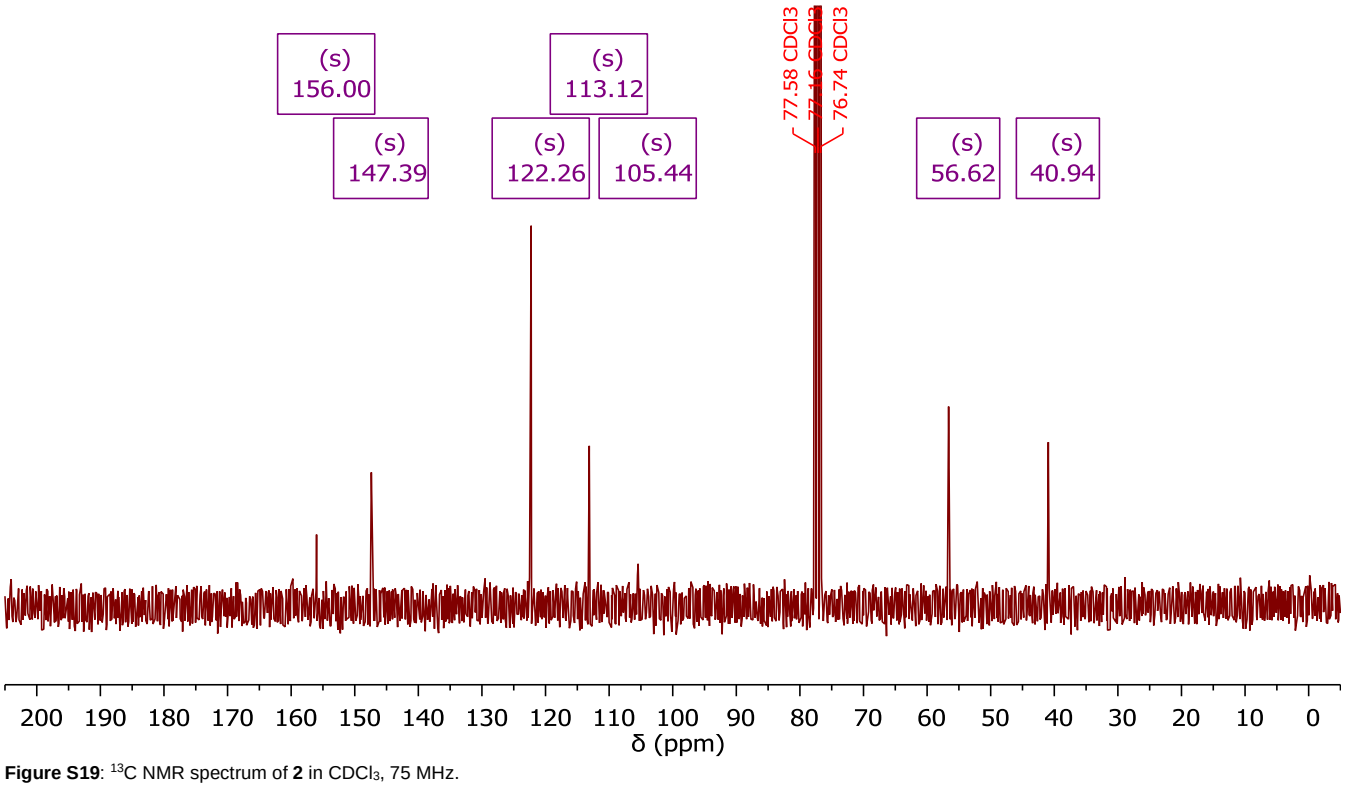

Figure S19: ^{13}C NMR spectrum of **2** in $CDCl_3$, 75 MHz.

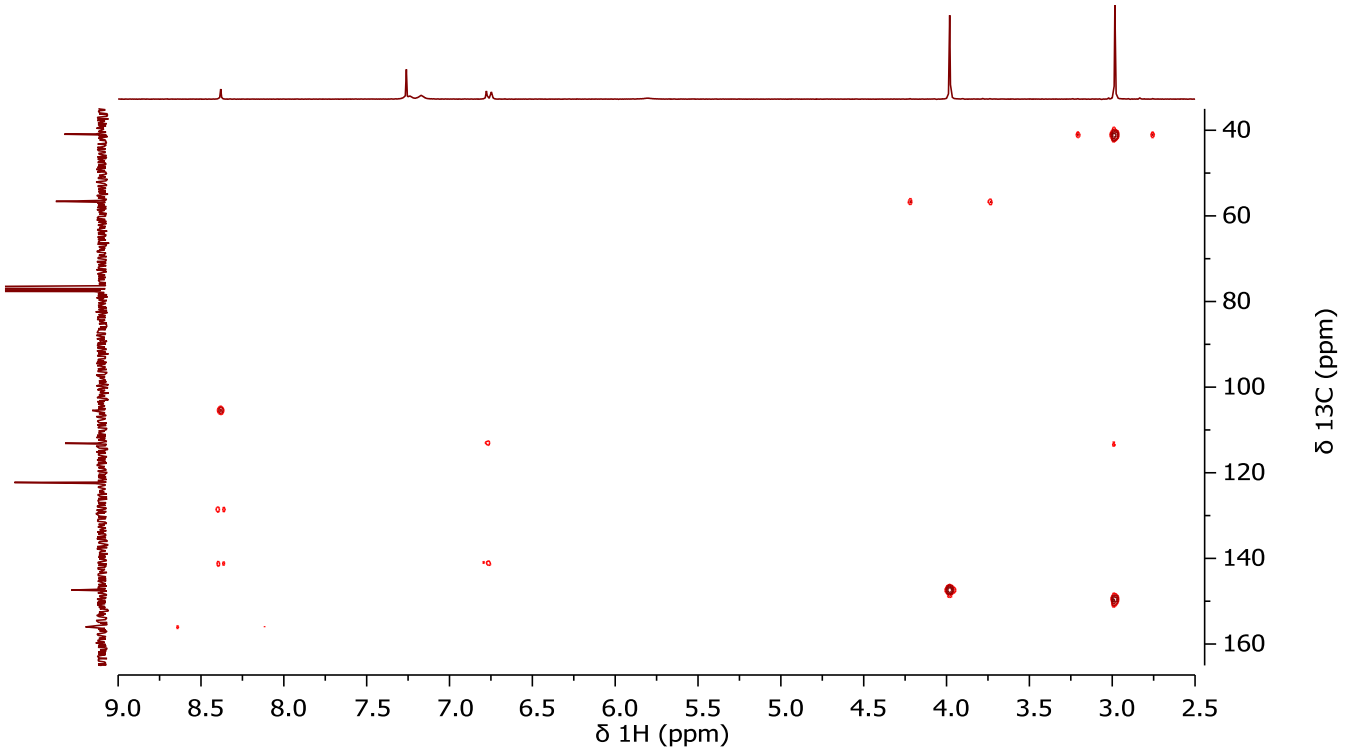

Figure S20: ^{1}H-^{13}C HMBC NMR spectrum of **2** in $CDCl_3$, 300/75 MHz.

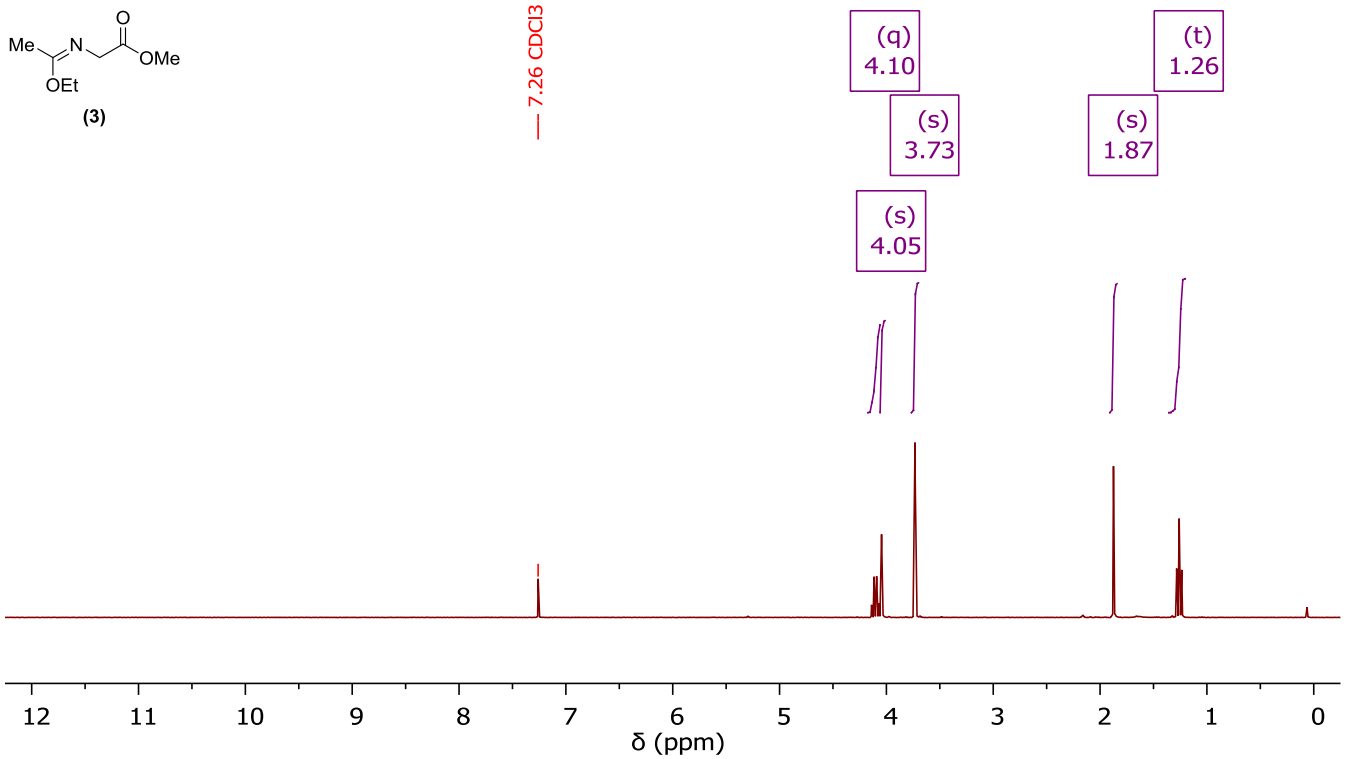

Figure S21: ^{1}H NMR spectrum of **3** in $CDCl_3$, 300 MHz.

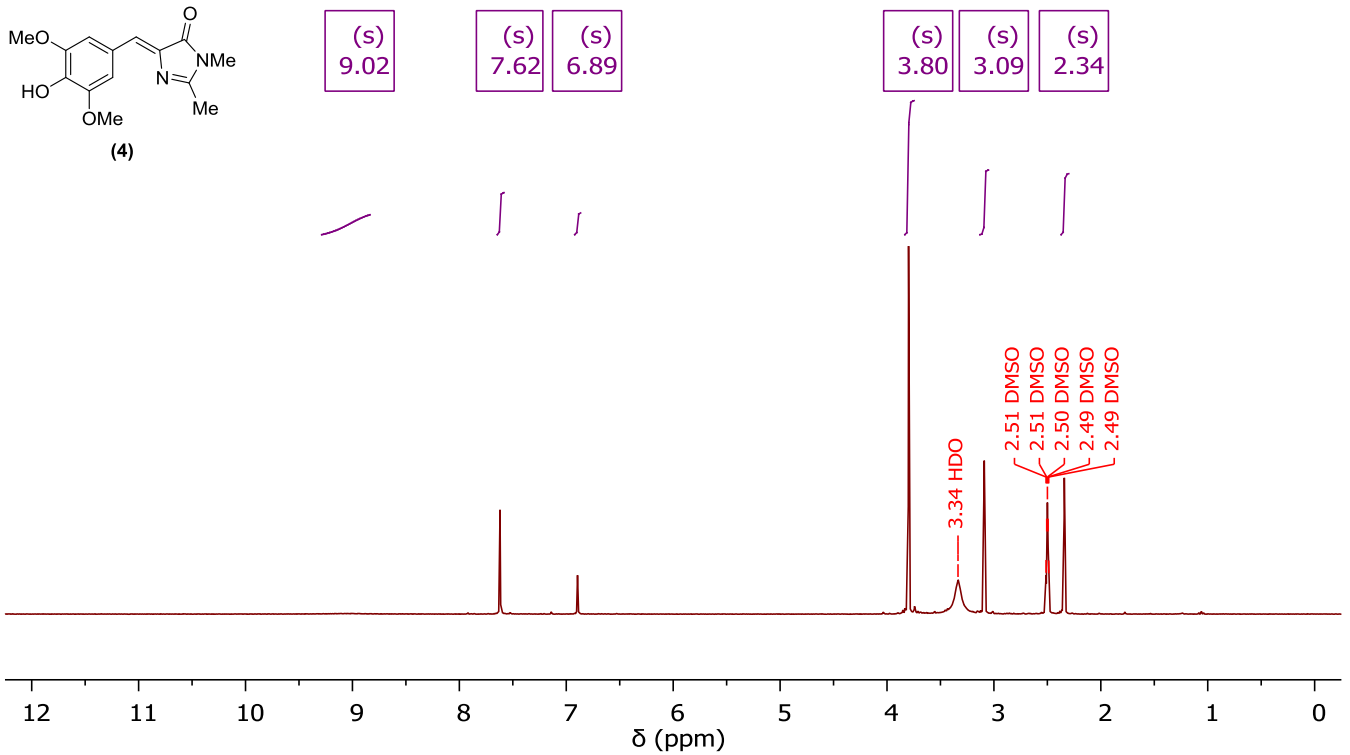

Figure S22: ^{1}H NMR spectrum of **4** in DMSO-d_6, 300 MHz.

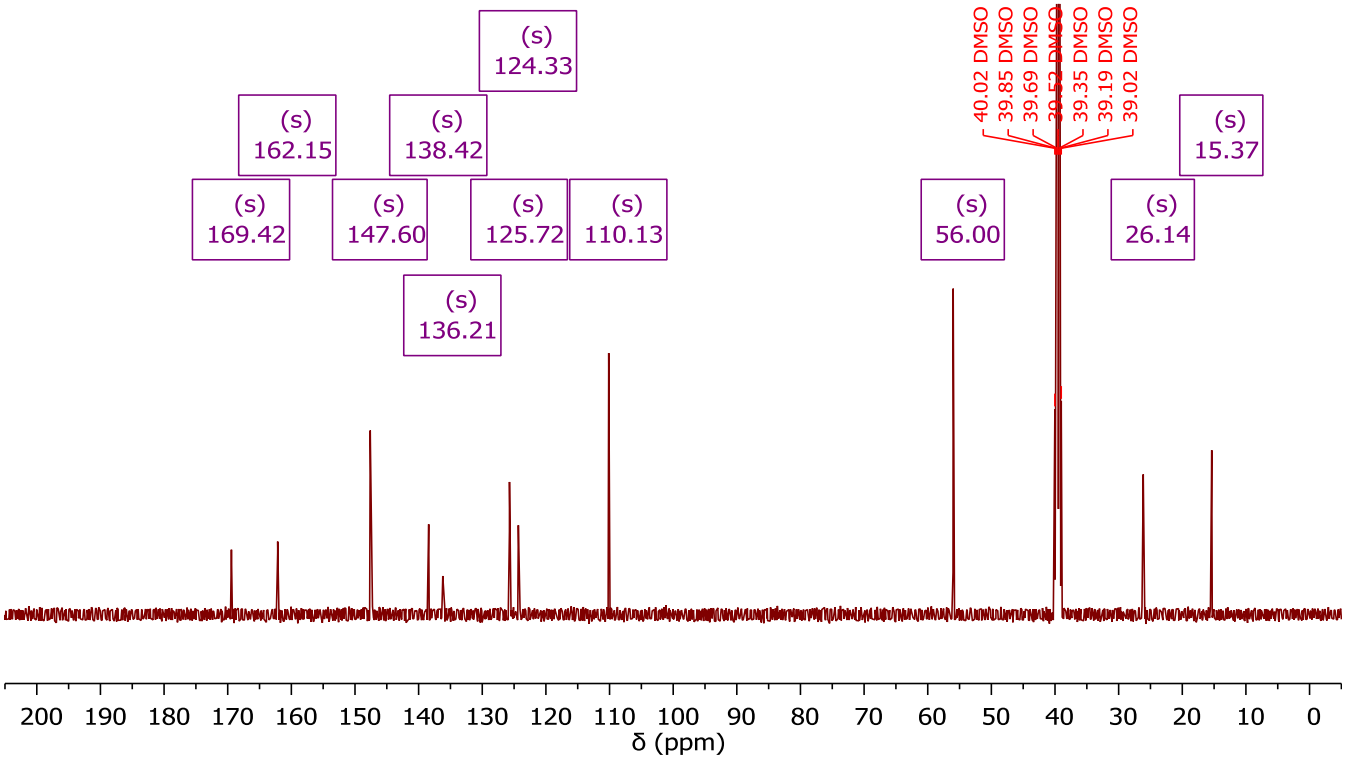

Figure S23: ^{13}C NMR spectrum of **4** in DMSO-d_6, 125 MHz.

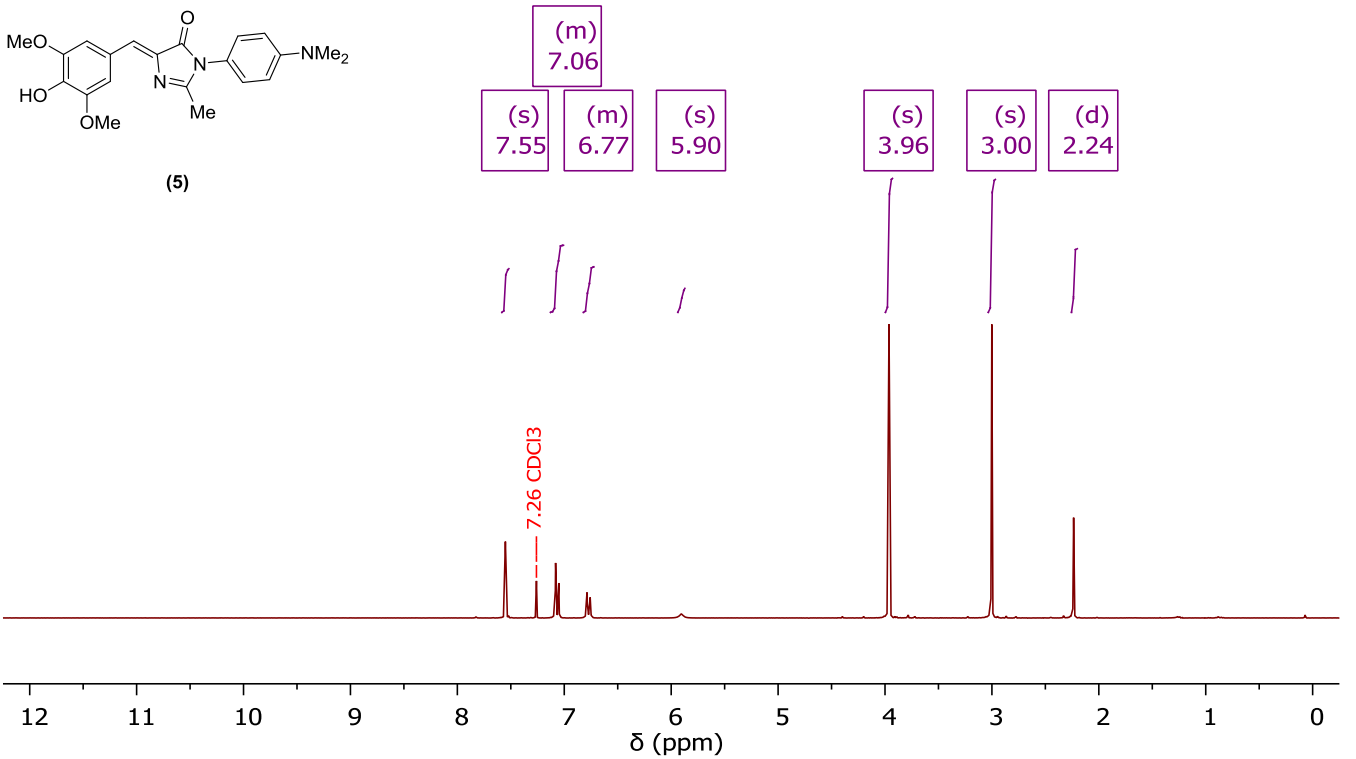

Figure S24: ^{1}H NMR spectrum of **5** in $CDCl_3$, 300 MHz.

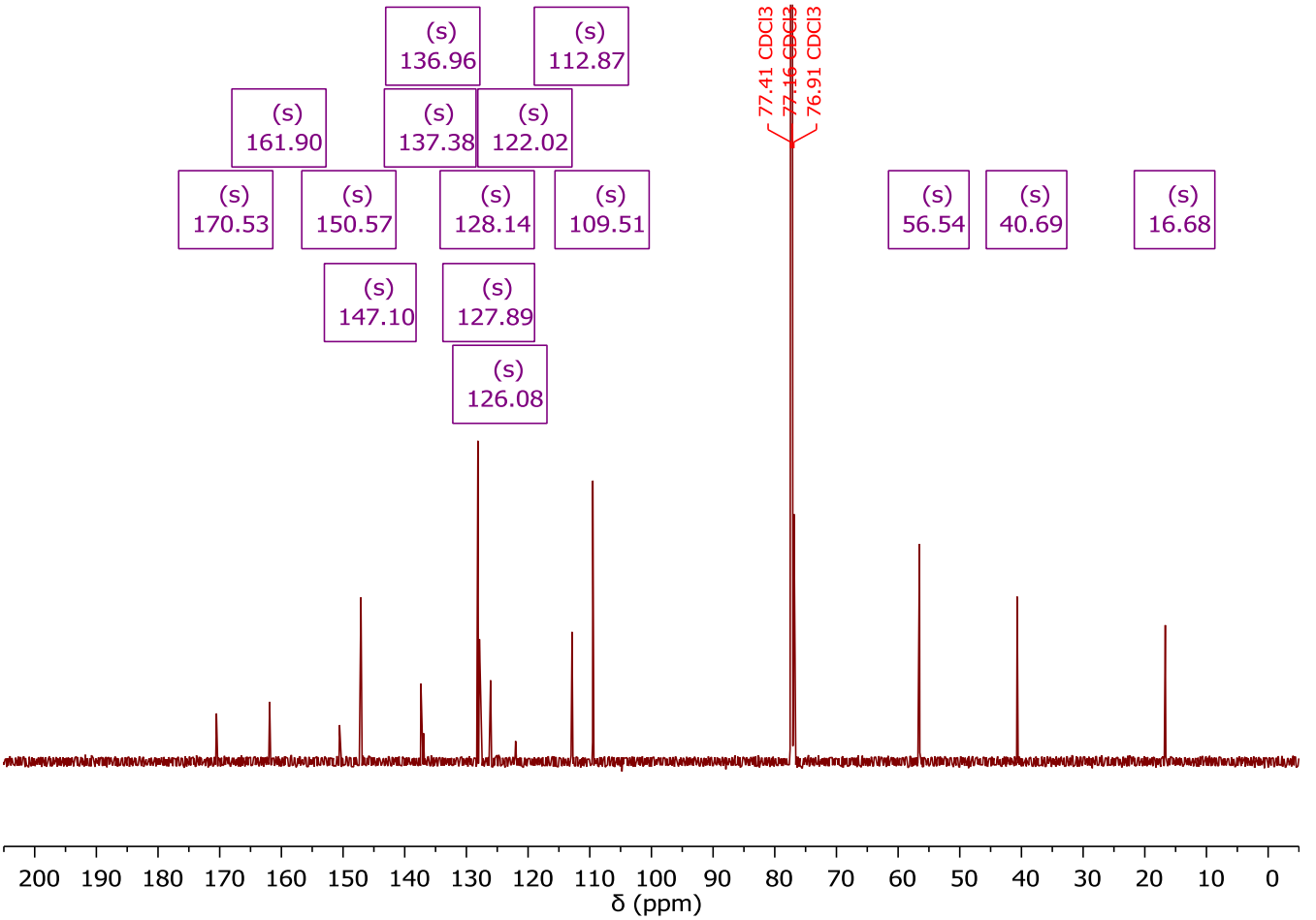

Figure S25: ^{13}C NMR spectrum of **5** in $CDCl_3$, 125 MHz.

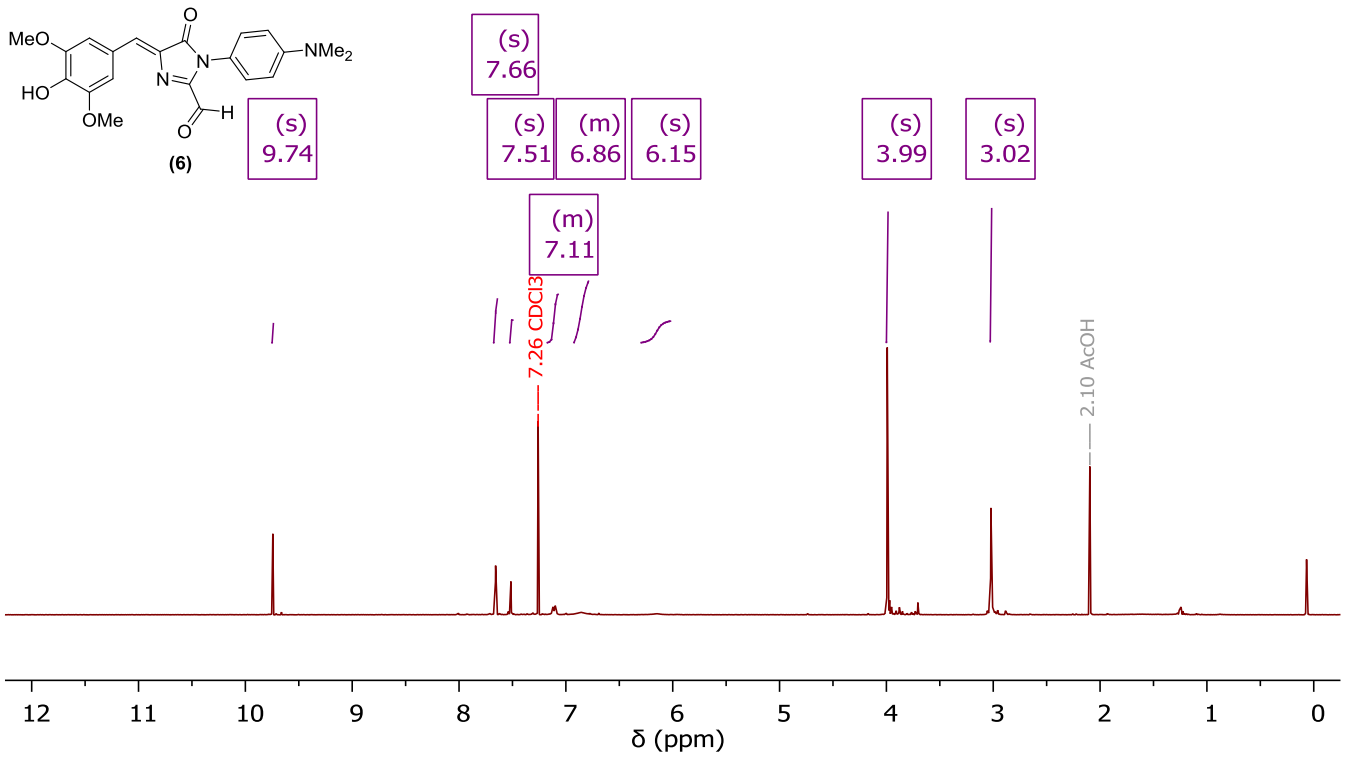

Figure S26: ^{1}H NMR spectrum of **6** in $CDCl_3$, 400 MHz.

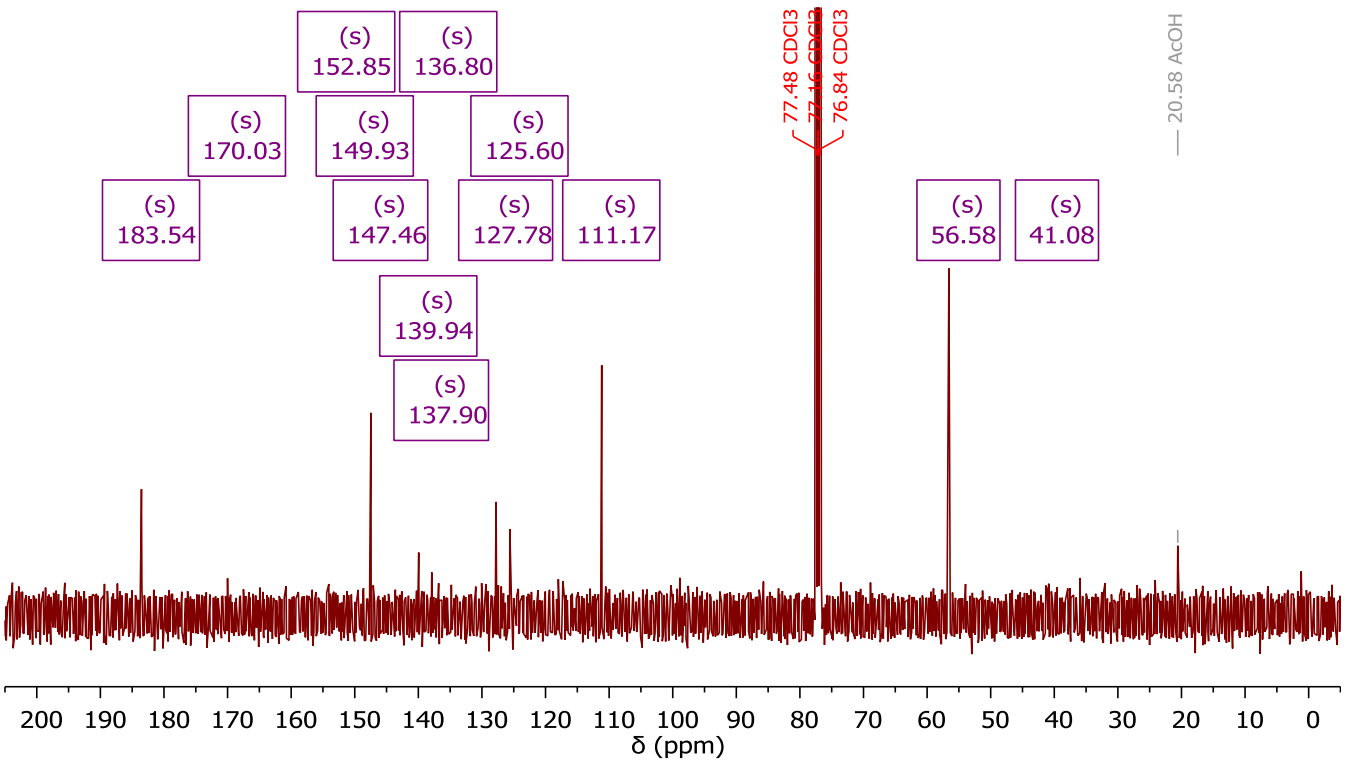

Figure S27: ^{13}C NMR spectrum of **6** in $CDCl_3$, 100 MHz.

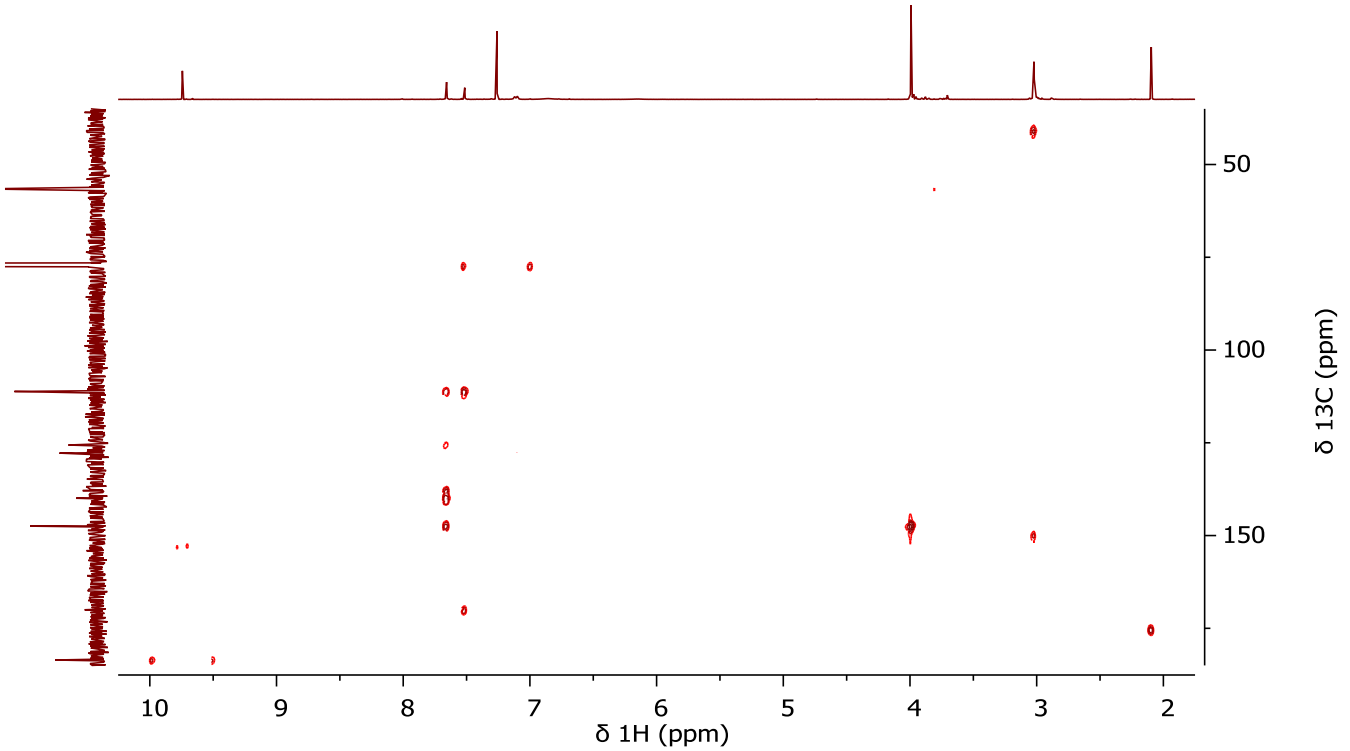

Figure S28: ^{1}H-^{13}C HMBC NMR spectrum of **6** in $CDCl_3$, 400/100 MHz.

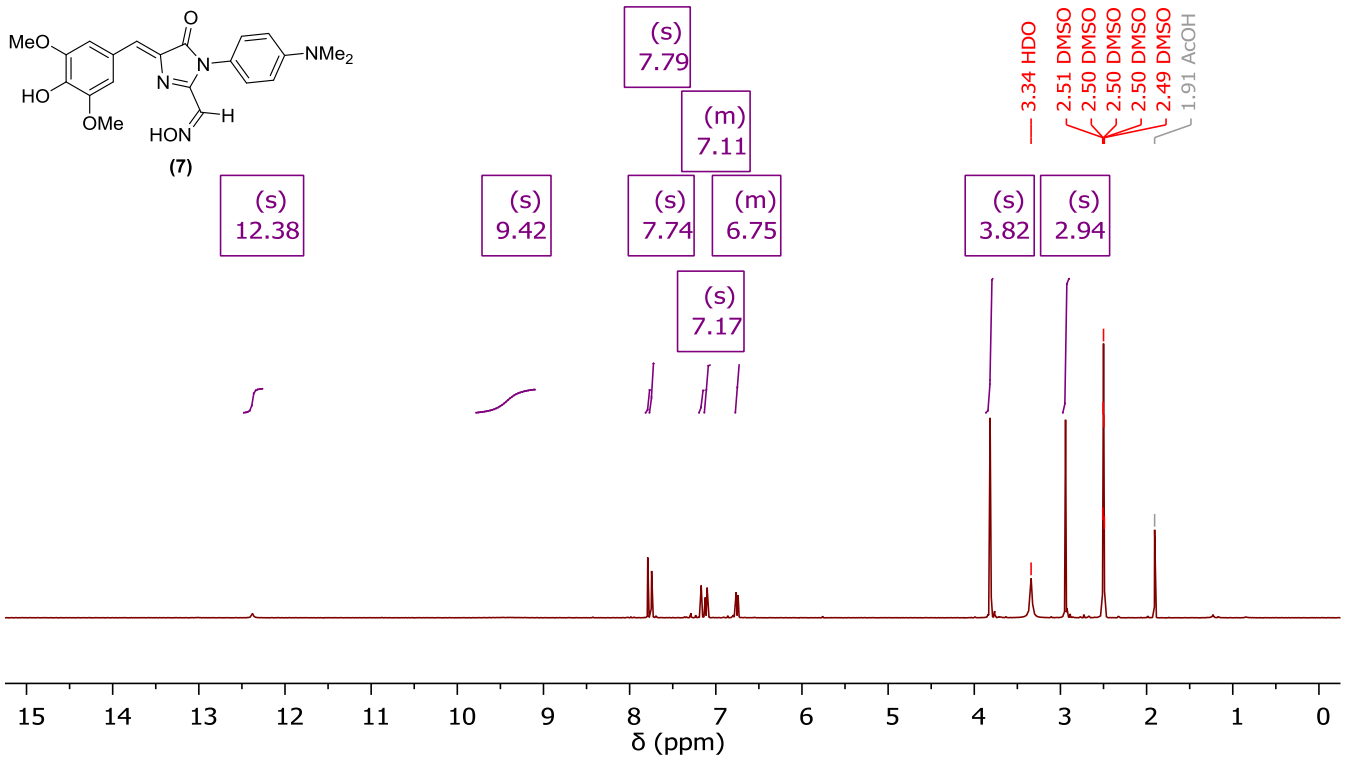

Figure S29: ^{1}H NMR spectrum of **7** in DMSO-d_6, 400 MHz.

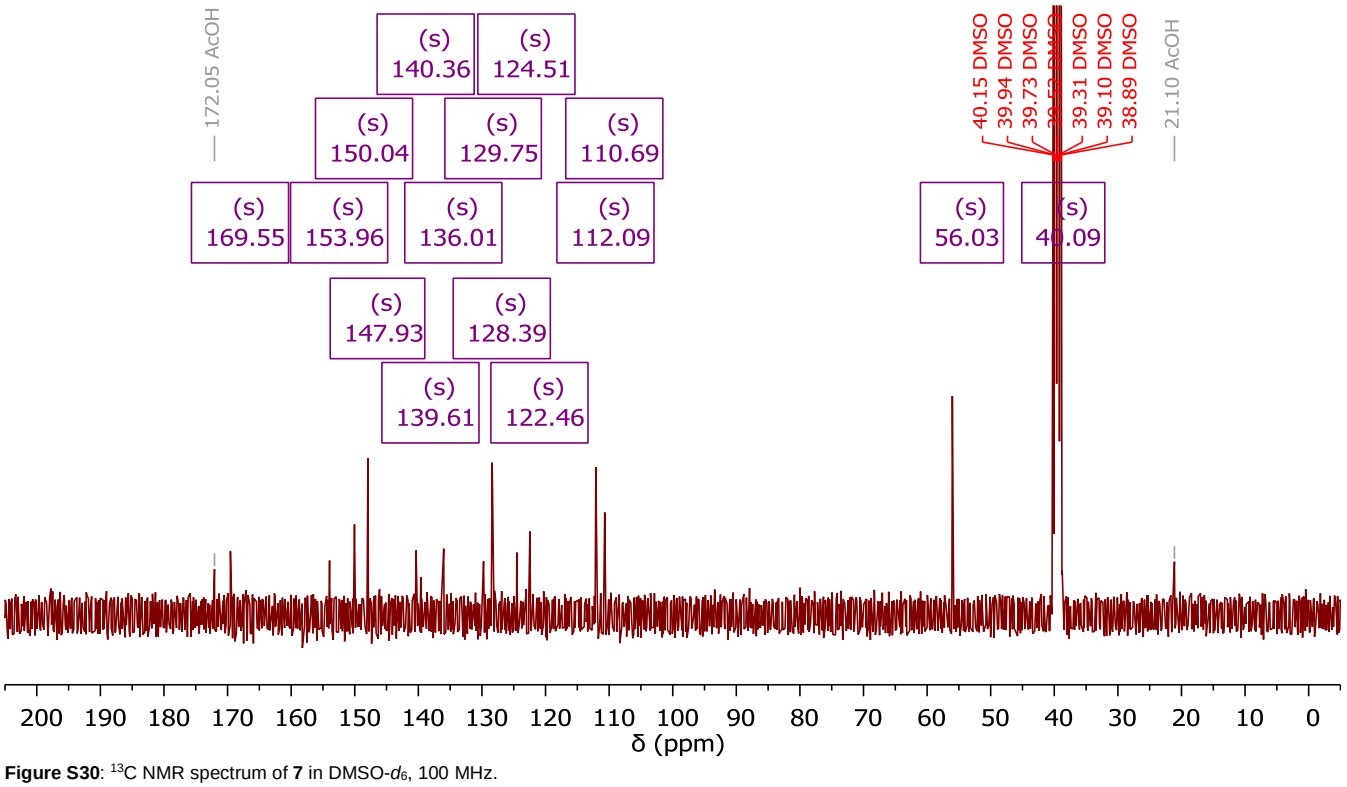

Figure S30: ^{13}C NMR spectrum of **7** in DMSO-d_6, 100 MHz.

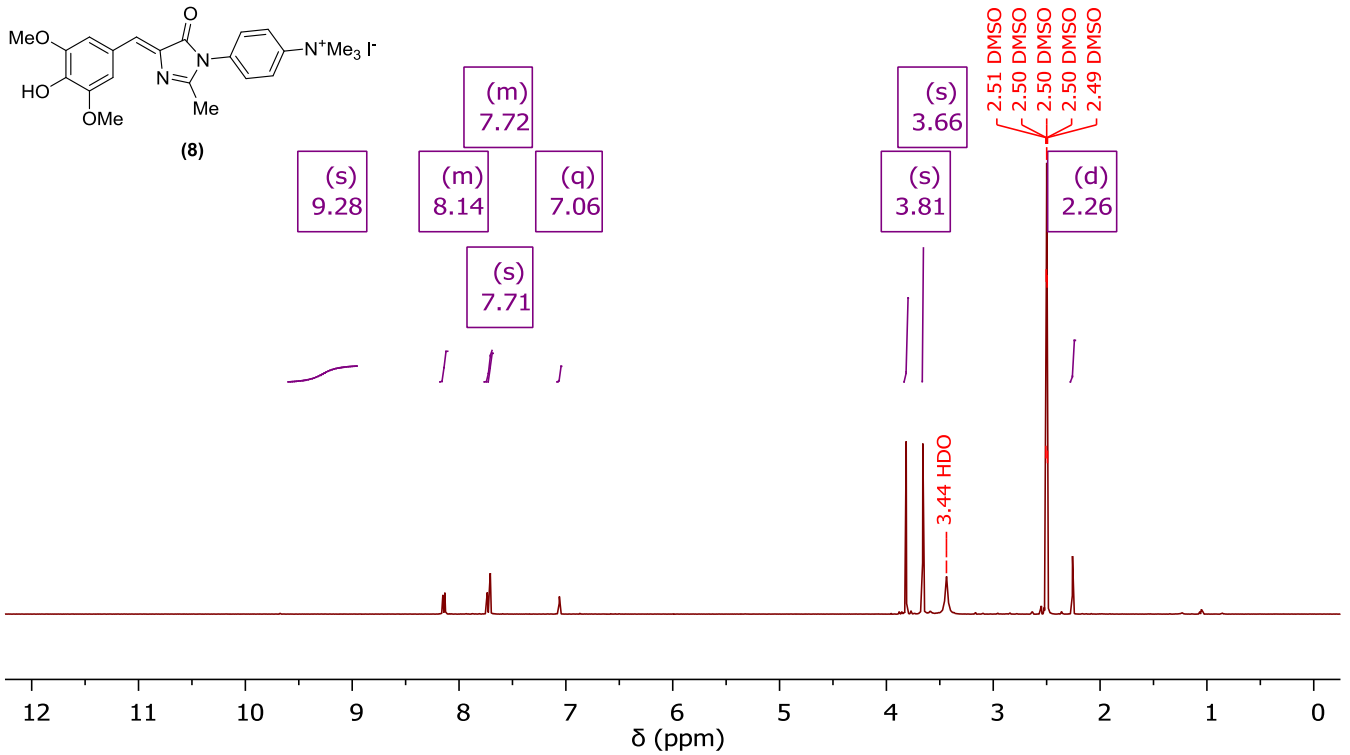

Figure S31: ^{1}H NMR spectrum of **8** in DMSO-d_6, 500 MHz.

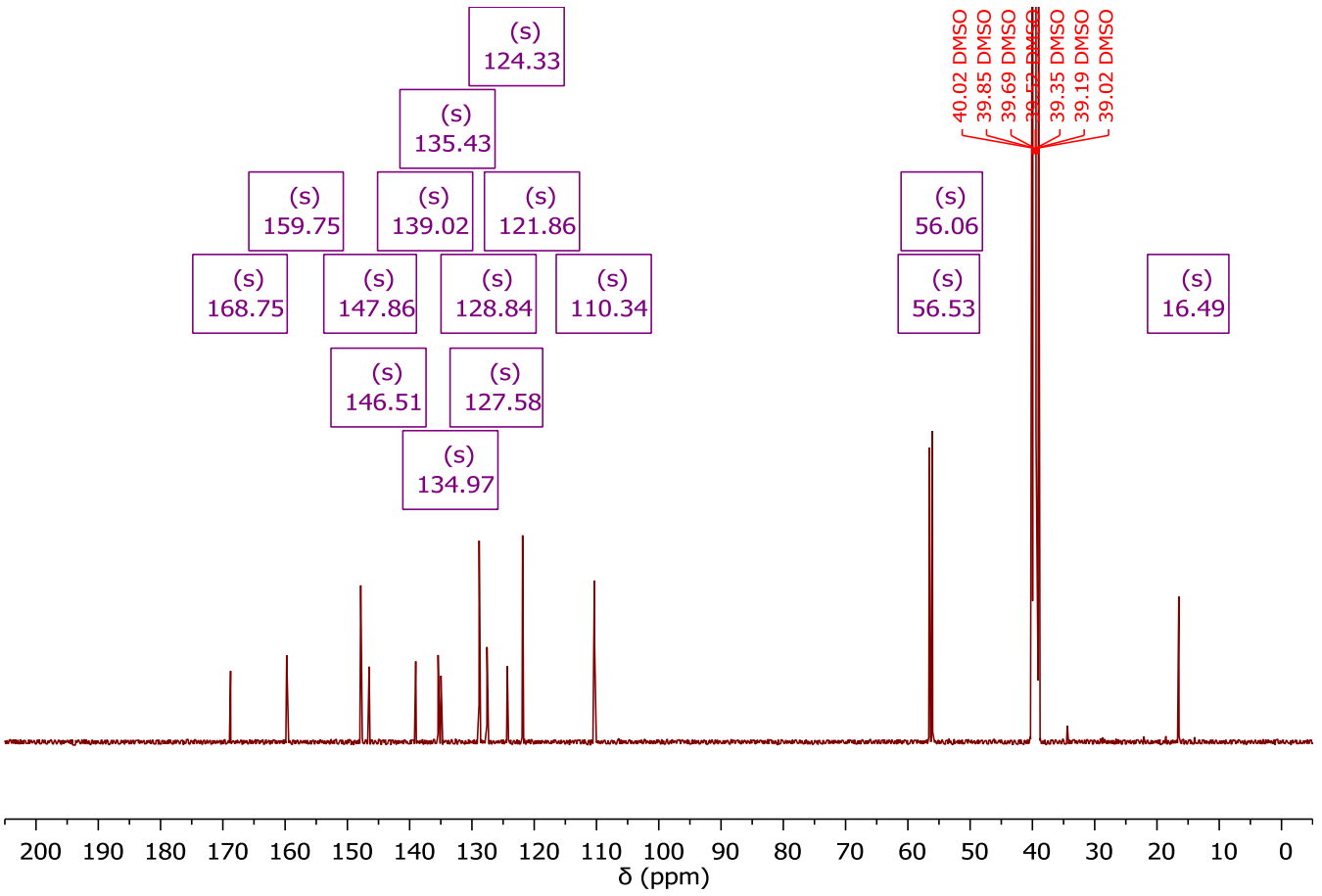

Figure S32: ^{13}C NMR spectrum of **8** in DMSO-d_6, 125 MHz.

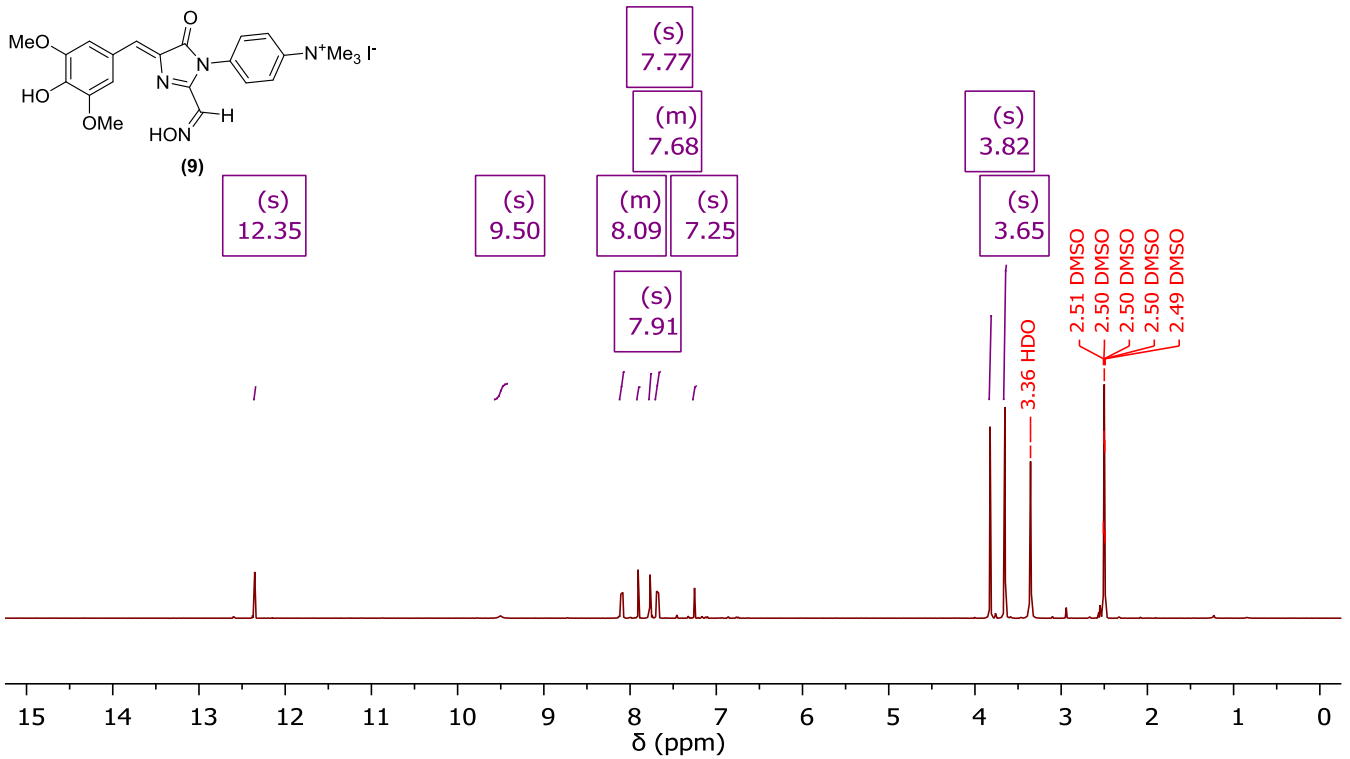

Figure S33: ^{1}H NMR spectrum of **9** in DMSO-d_6, 400 MHz.

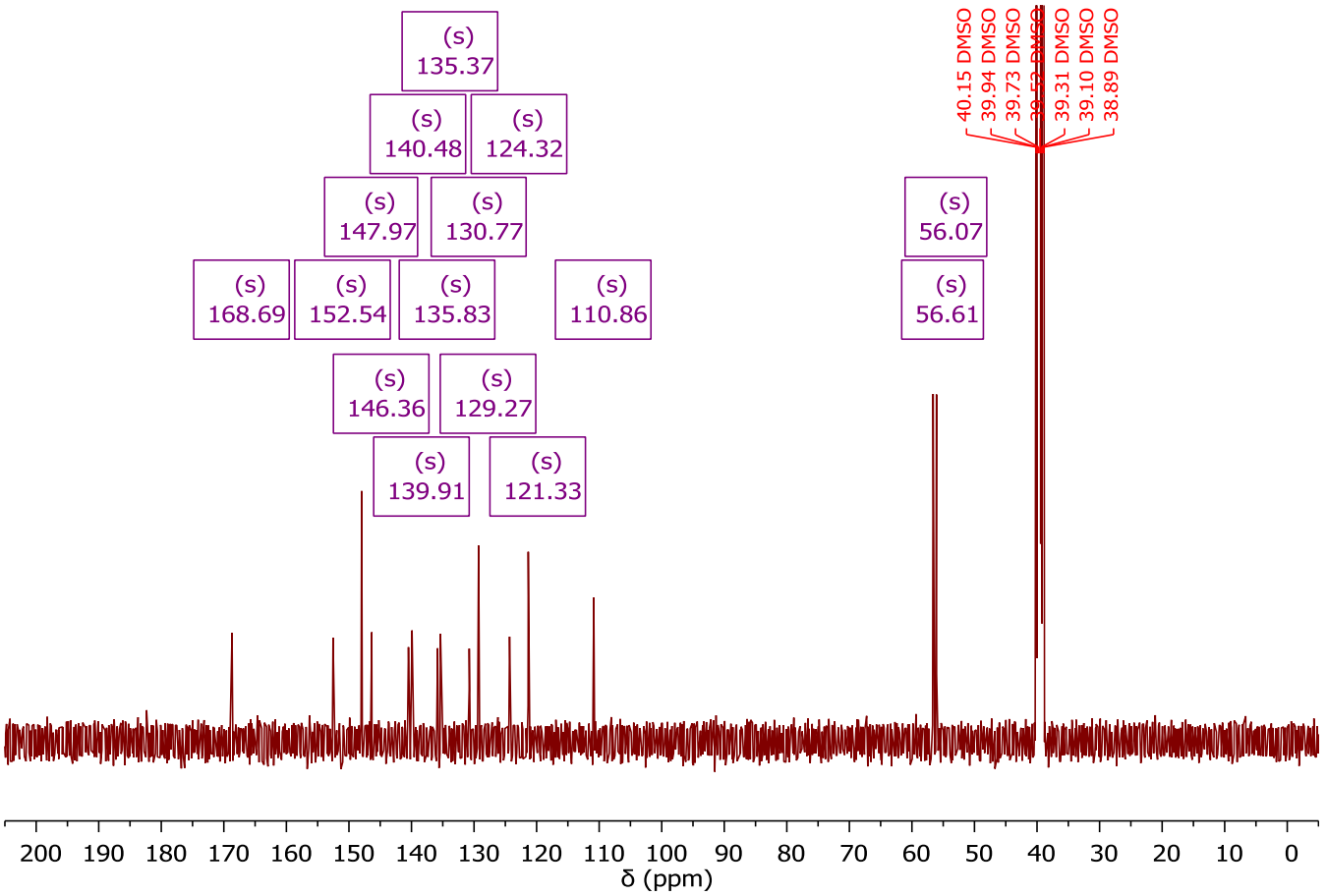

Figure S34: ^{13}C NMR spectrum of **9** in DMSO-d_6, 100 MHz.

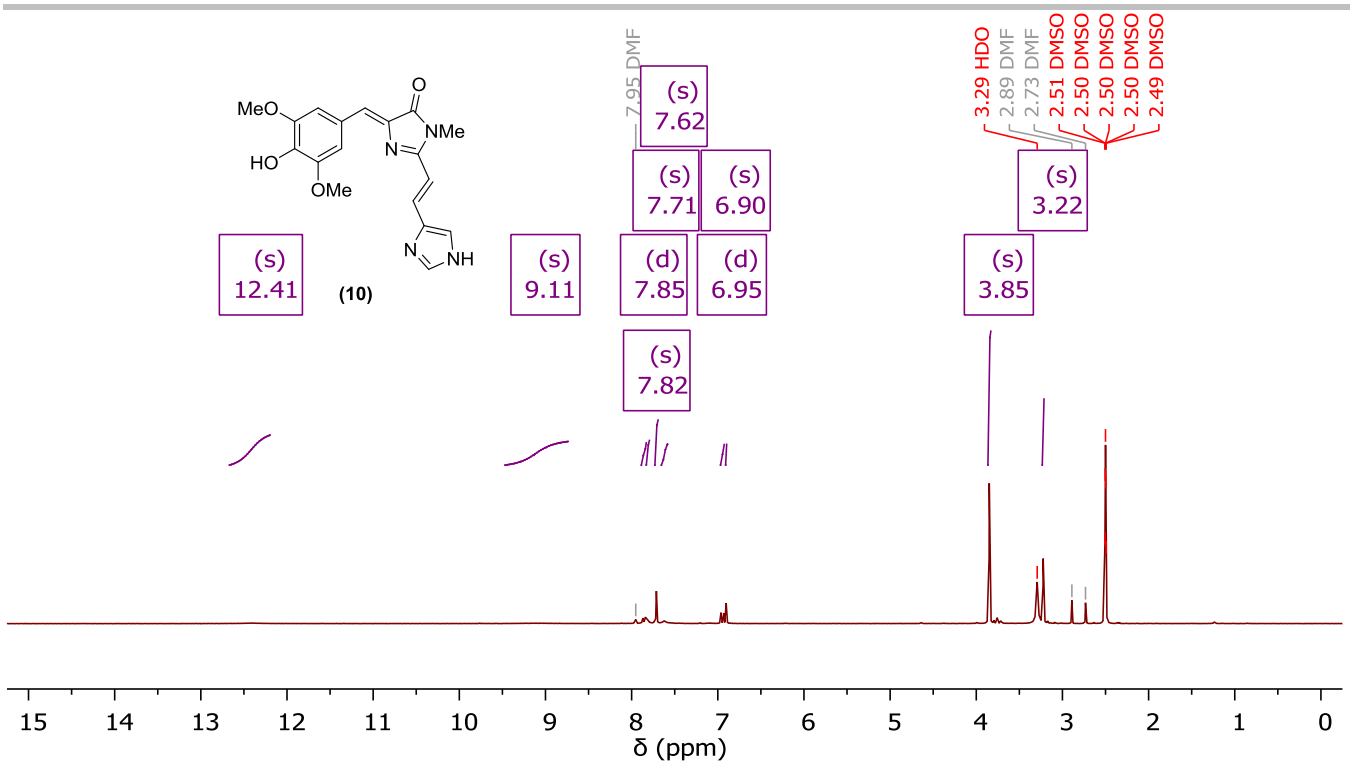

Figure S35: ^{1}H NMR spectrum of **10** in DMSO-d_6, 500 MHz.

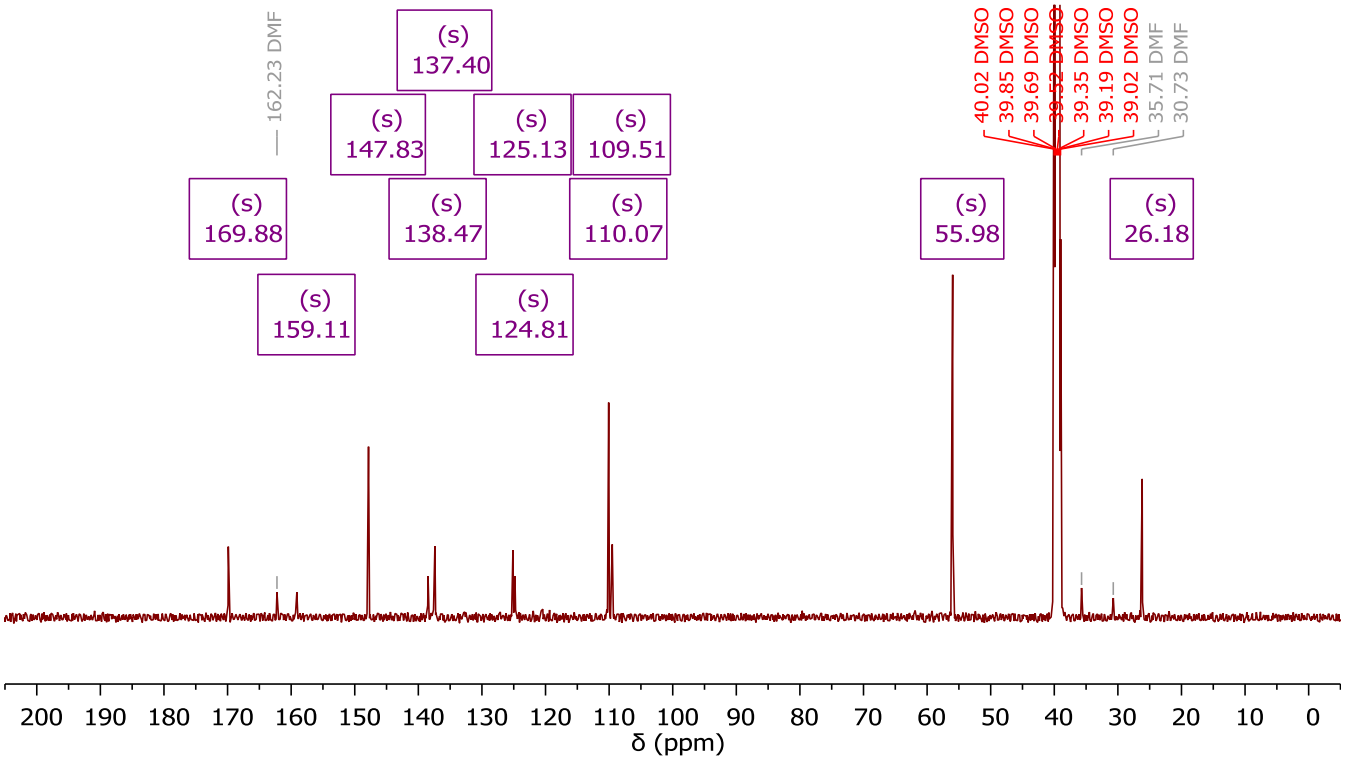

Figure S36: ^{13}C NMR spectrum of **10** in DMSO-d_6, 125 MHz.

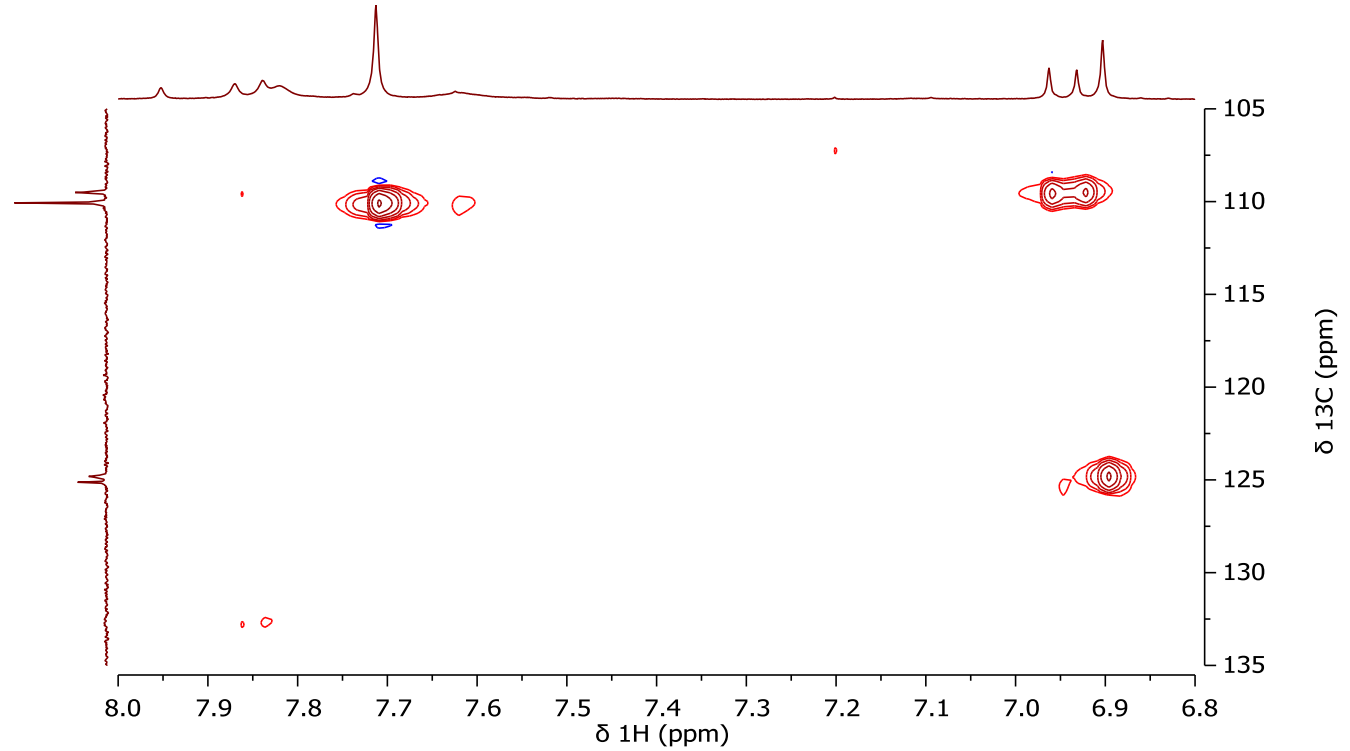

Figure S37: ^{1}H-^{13}C HSQC NMR spectrum (excerpt) of **10** in DMSO-d_6, 500/125 MHz.

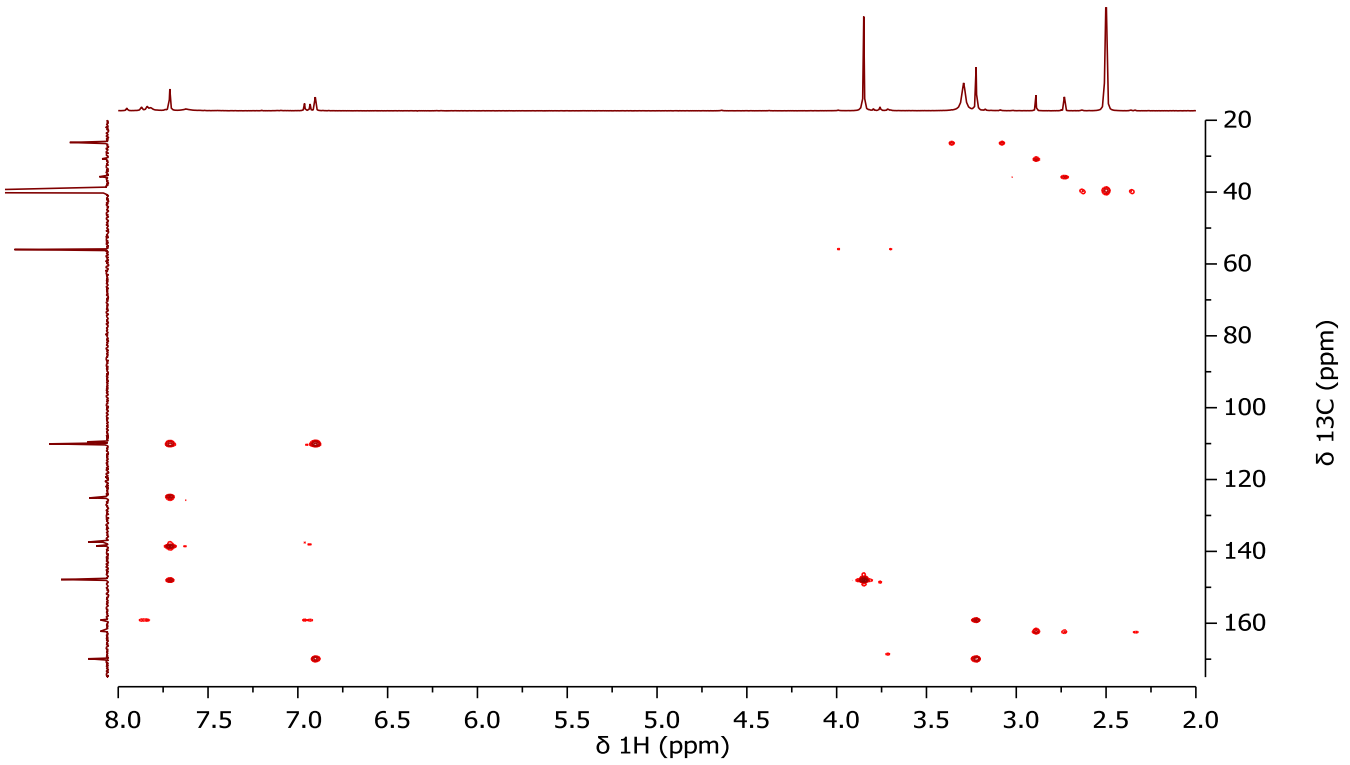

Figure S38: ^{1}H-^{13}C HMBC NMR spectrum of **10** in DMSO-d_6, 500/125 MHz.

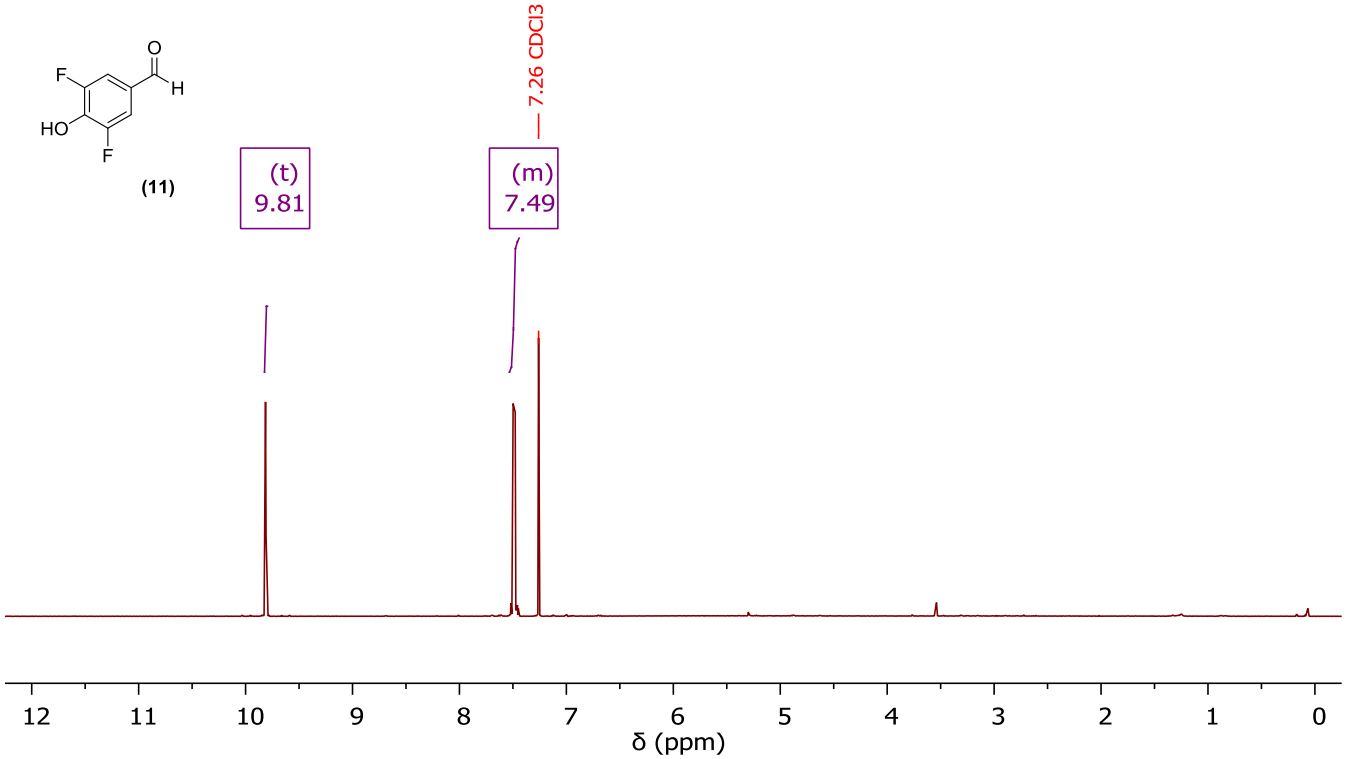

Figure S39: ^{1}H NMR spectrum of **11** in $CDCl_3$, 400 MHz.

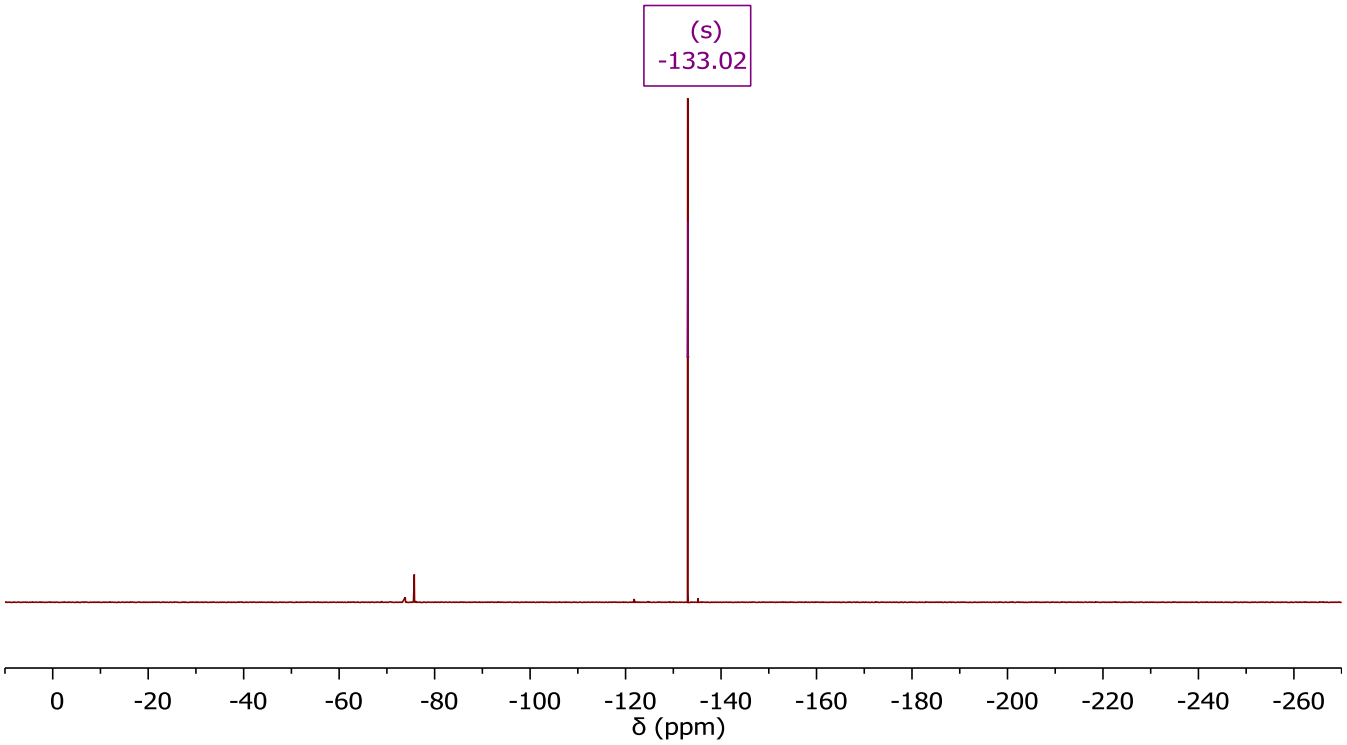

Figure S40: ^{19}F NMR spectrum of **11** in $CDCl_3$, 376 MHz.

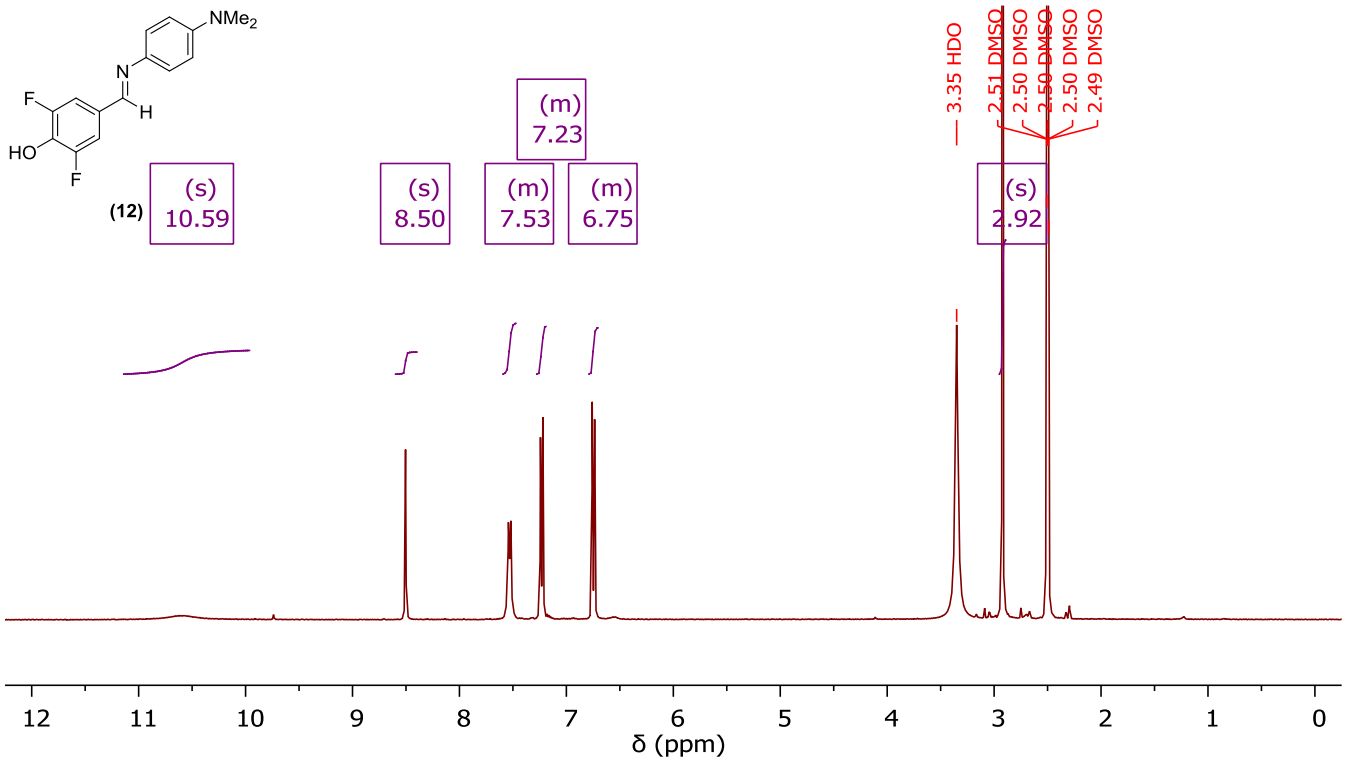

Figure S41: ^{1}H NMR spectrum of **12** in DMSO-d_6, 400 MHz.

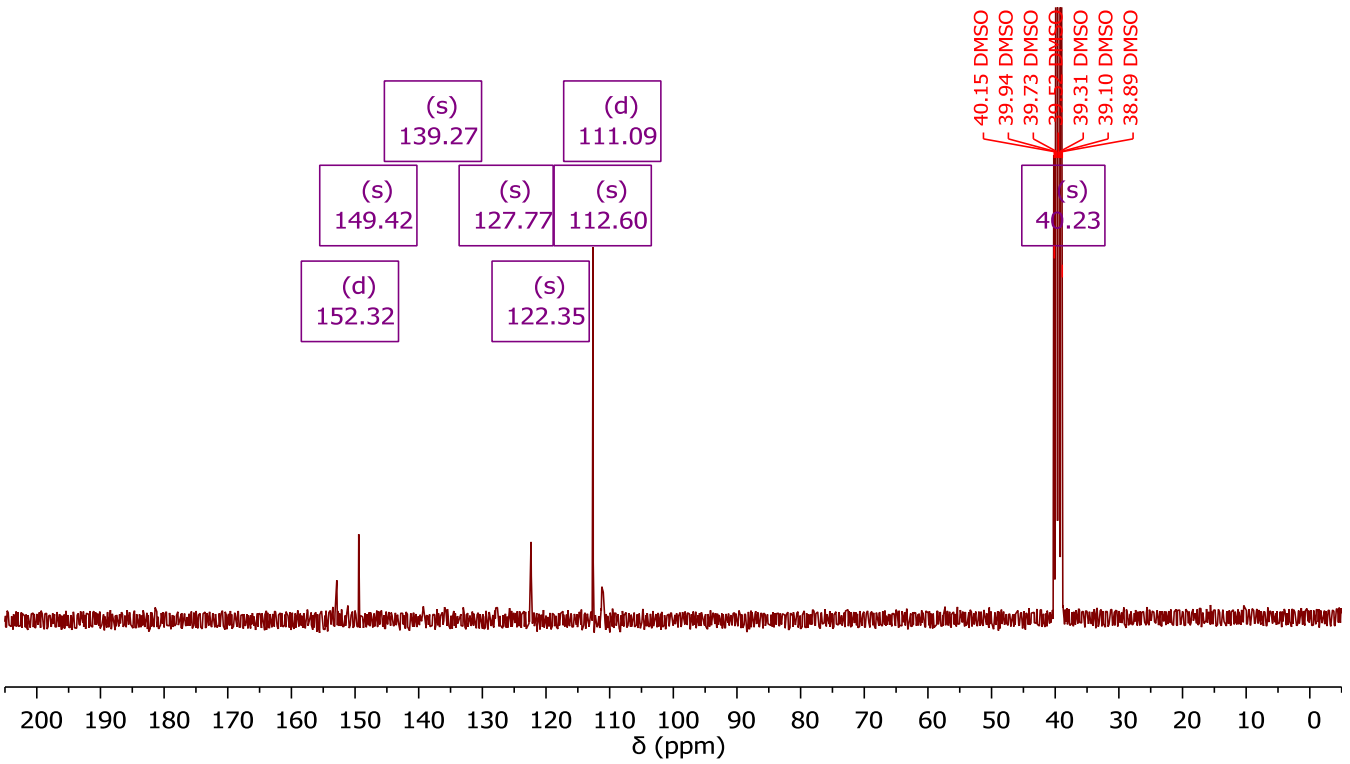

Figure S42: ^{13}C NMR spectrum of **12** in DMSO-d_6, 100 MHz.

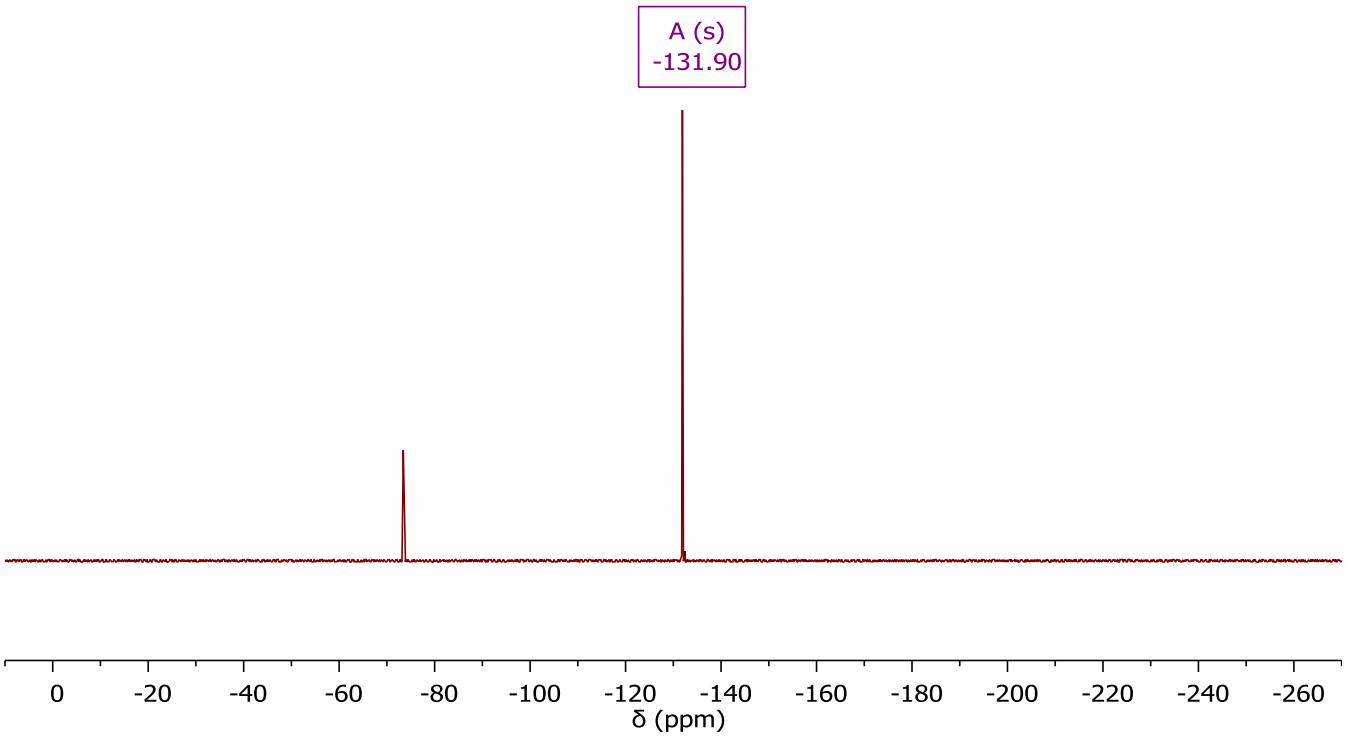

Figure S43: ^{19}F NMR spectrum of **12** in DMSO-d_6, 376 MHz.

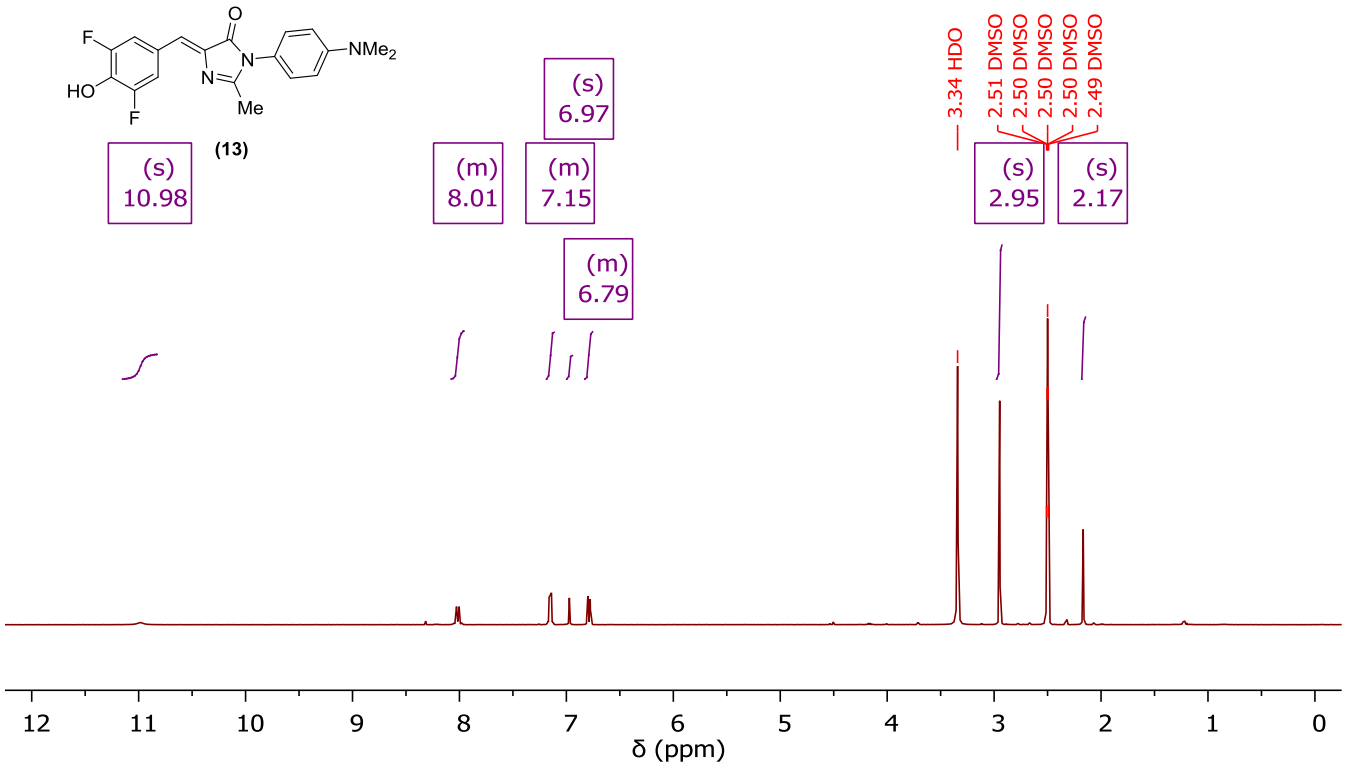

Figure S44: ^{1}H NMR spectrum of **13** in DMSO-d_6, 400 MHz.

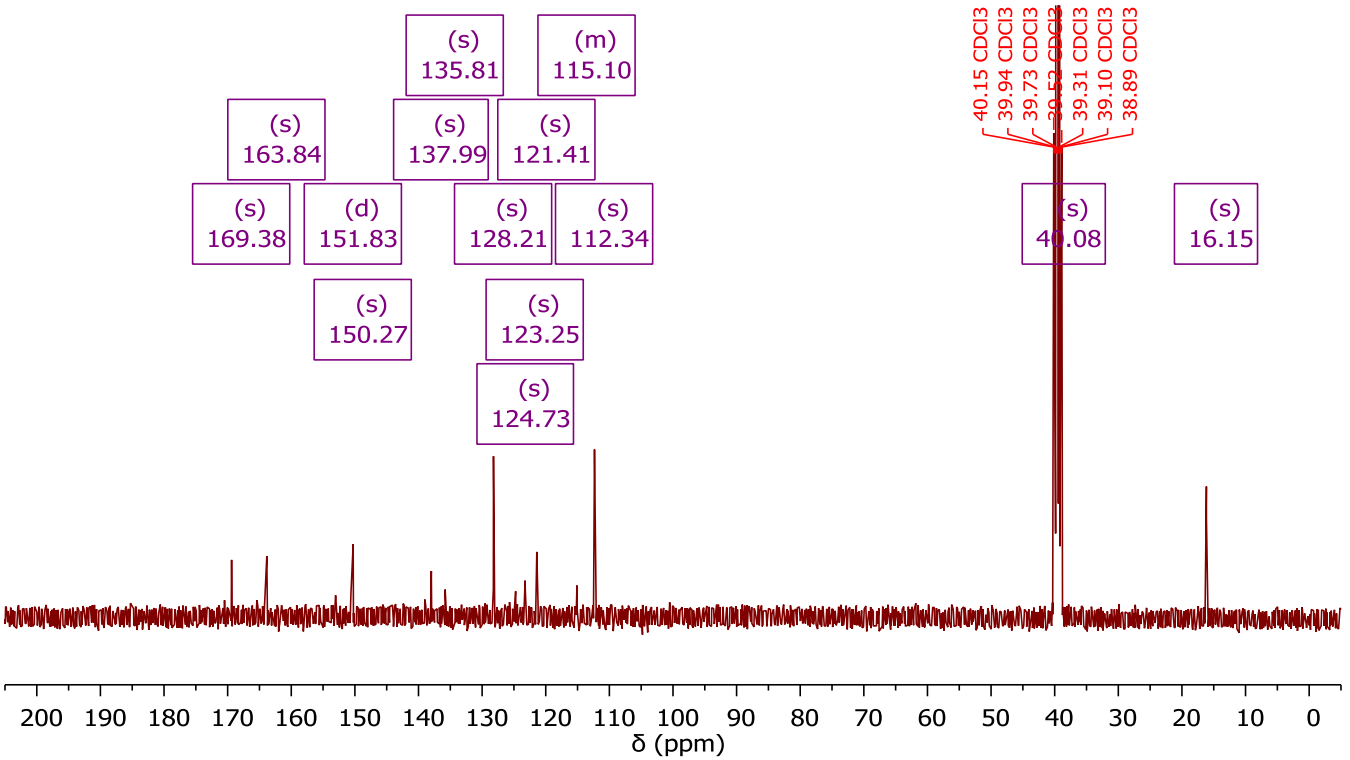

Figure S45: ^{13}C NMR spectrum of **13** in DMSO-d_6, 100 MHz.

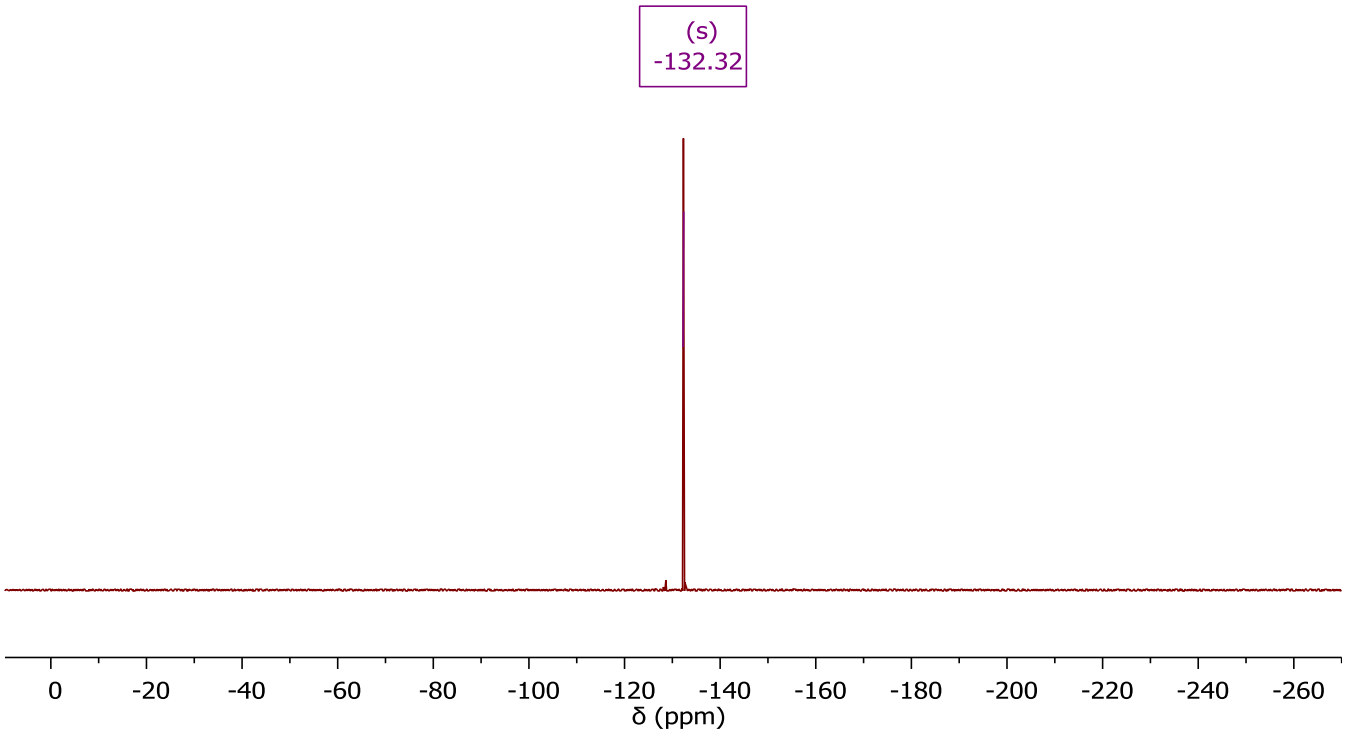

Figure S46: ^{19}F NMR spectrum of **13** in $CDCl_3$, 376 MHz.

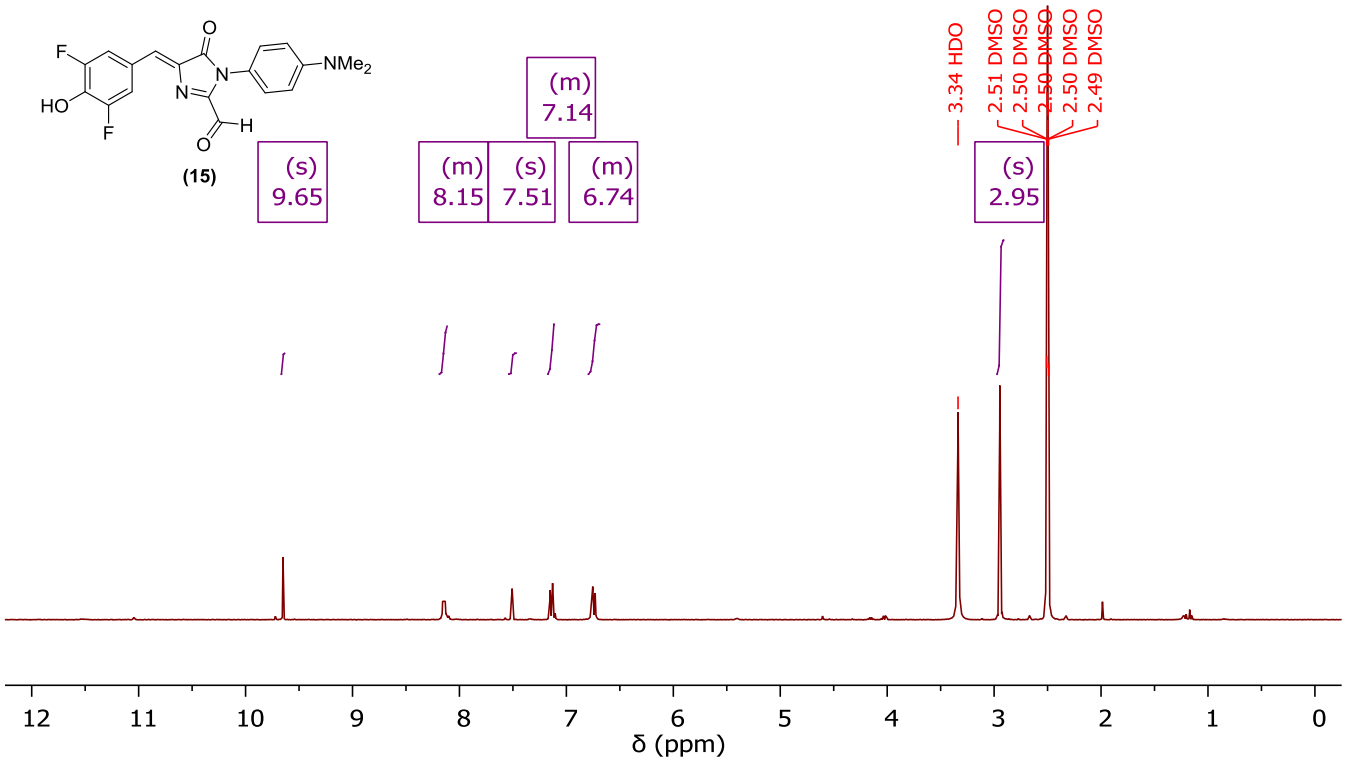

Figure S47: ^{1}H NMR spectrum of **15** in DMSO-d_6, 400 MHz.

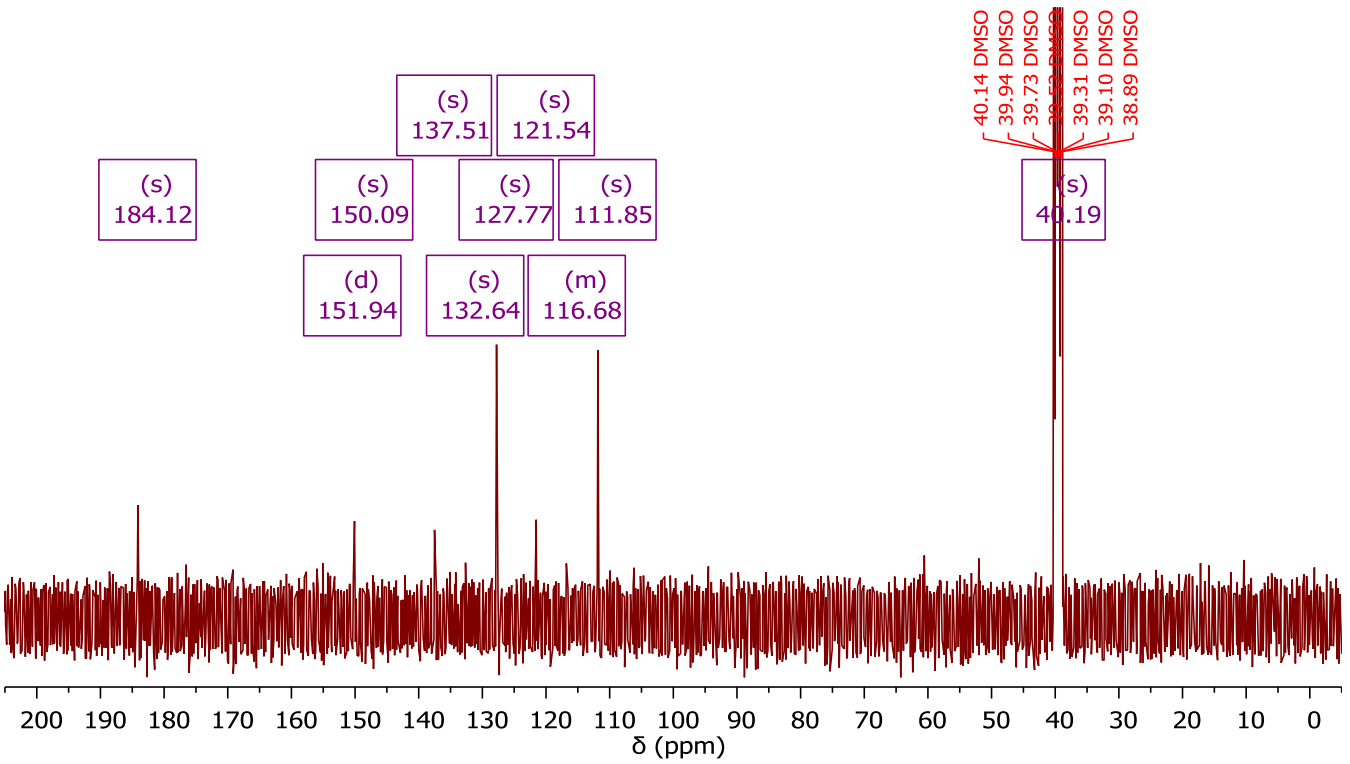

Figure S48: ^{13}C NMR spectrum of **15** in DMSO-d_6, 100 MHz.

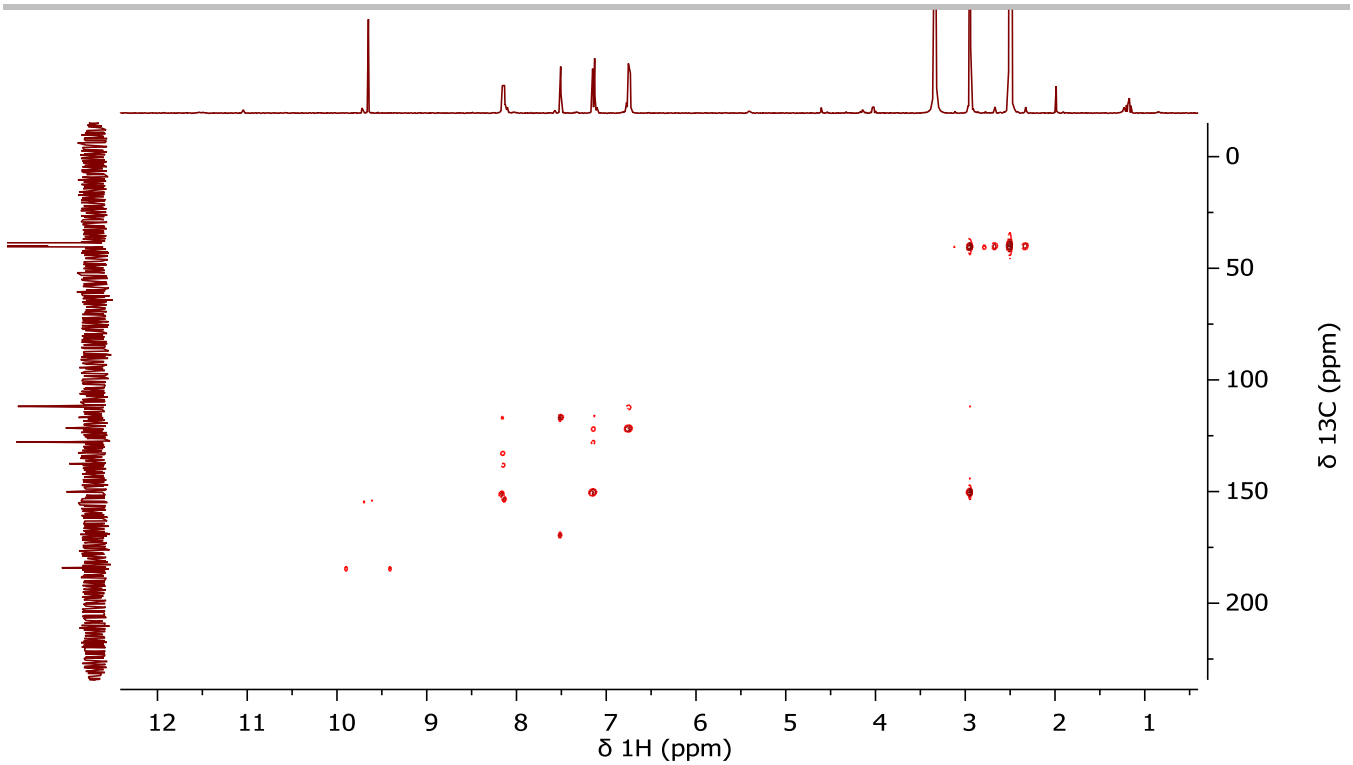

Figure S49: ^{1}H-^{13}C HMBC NMR spectrum of **15** in DMSO-d_6, 400/100 MHz.

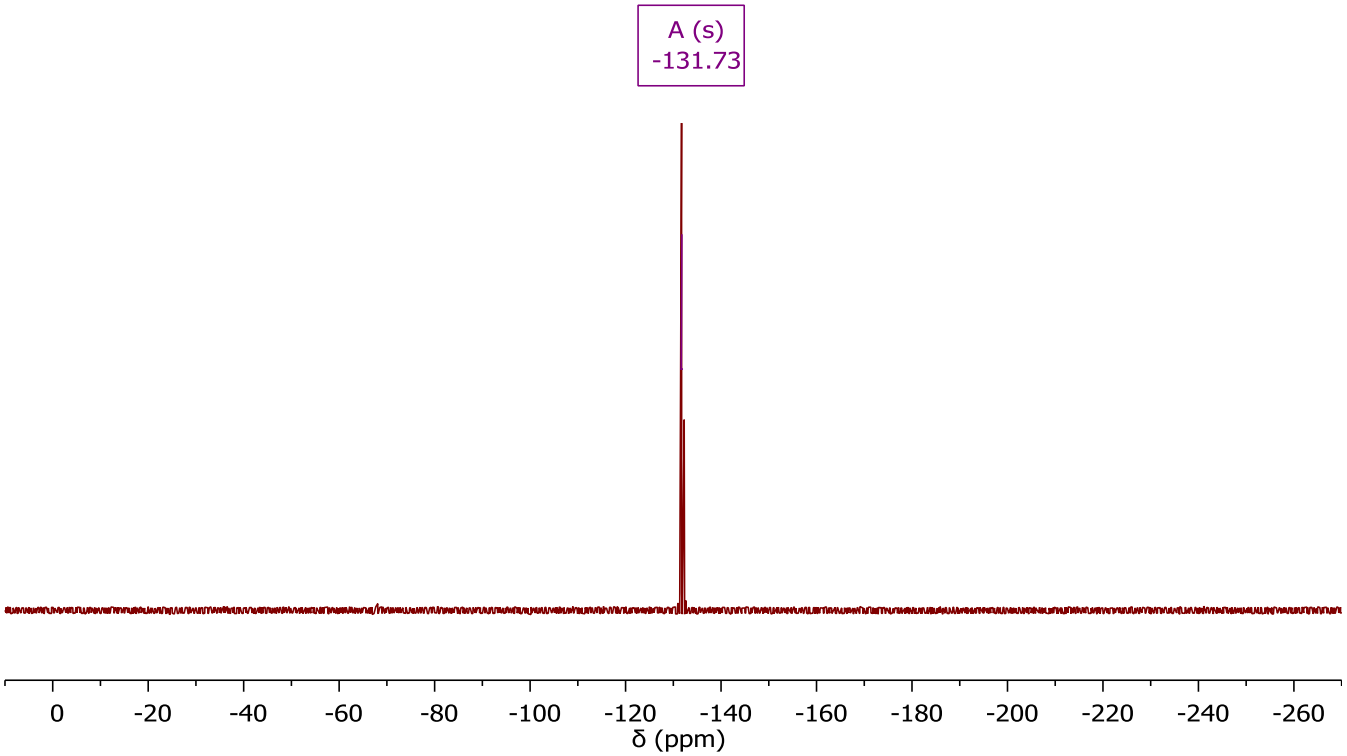

Figure S50: ^{19}F NMR spectrum of **15** in DMSO-d_6, 376 MHz.

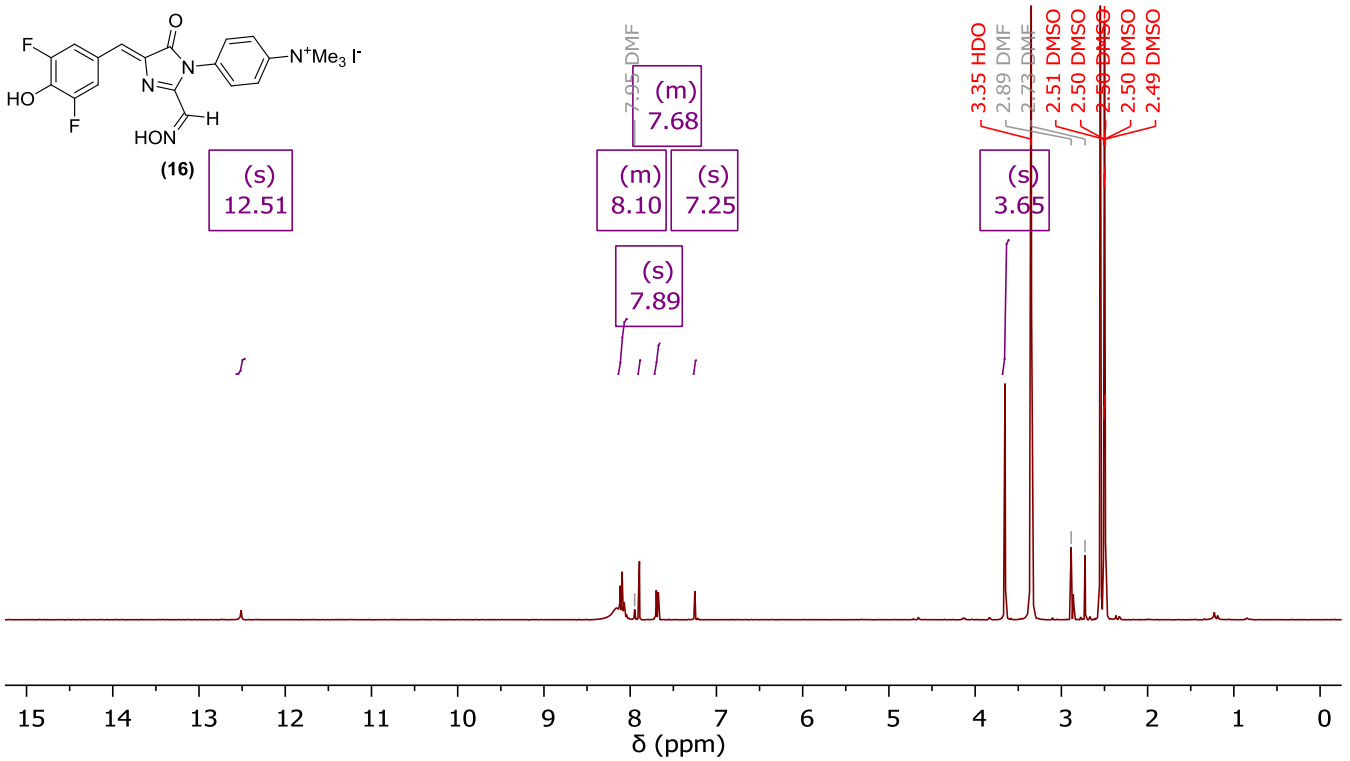

Figure S51: ^{1}H NMR spectrum of **16** in DMSO-d_6, 400 MHz.

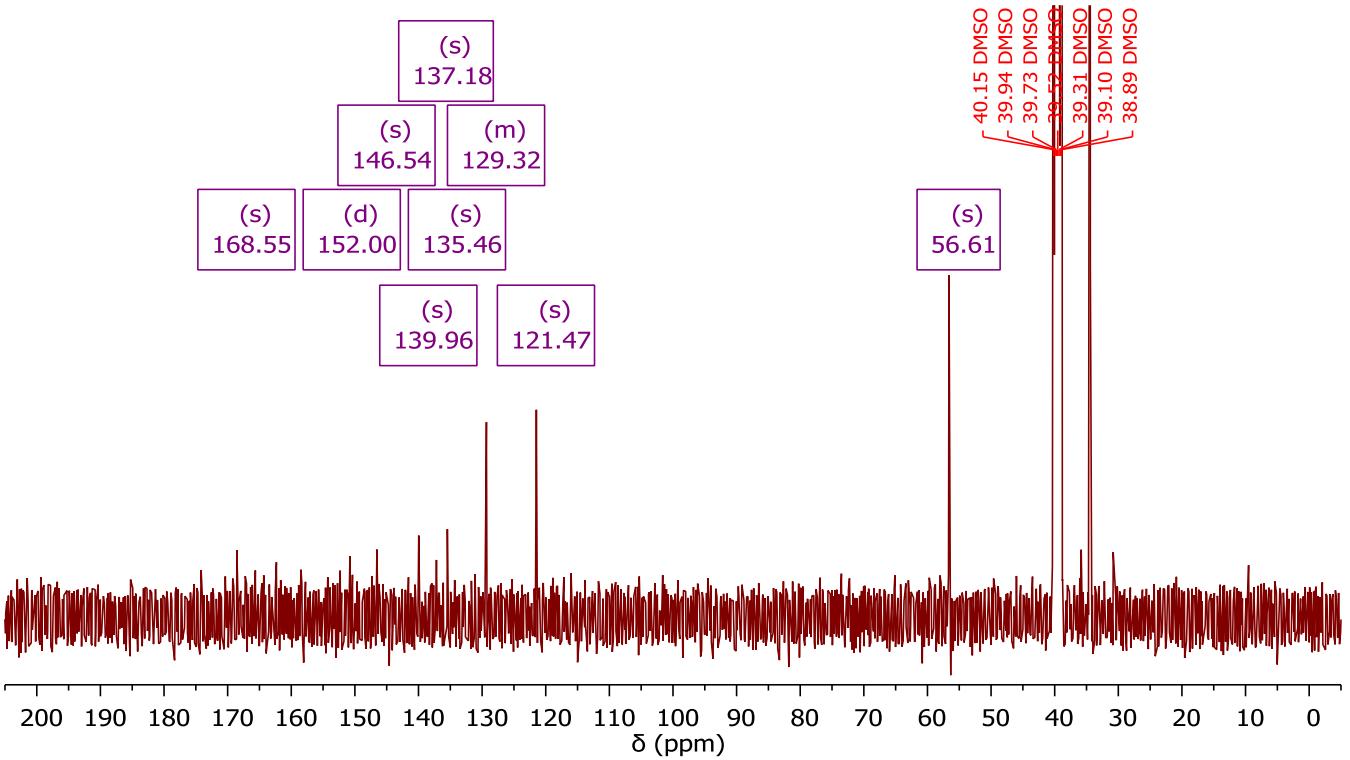

Figure S52: ^{13}C NMR spectrum of **16** in DMSO-d_6, 100 MHz.

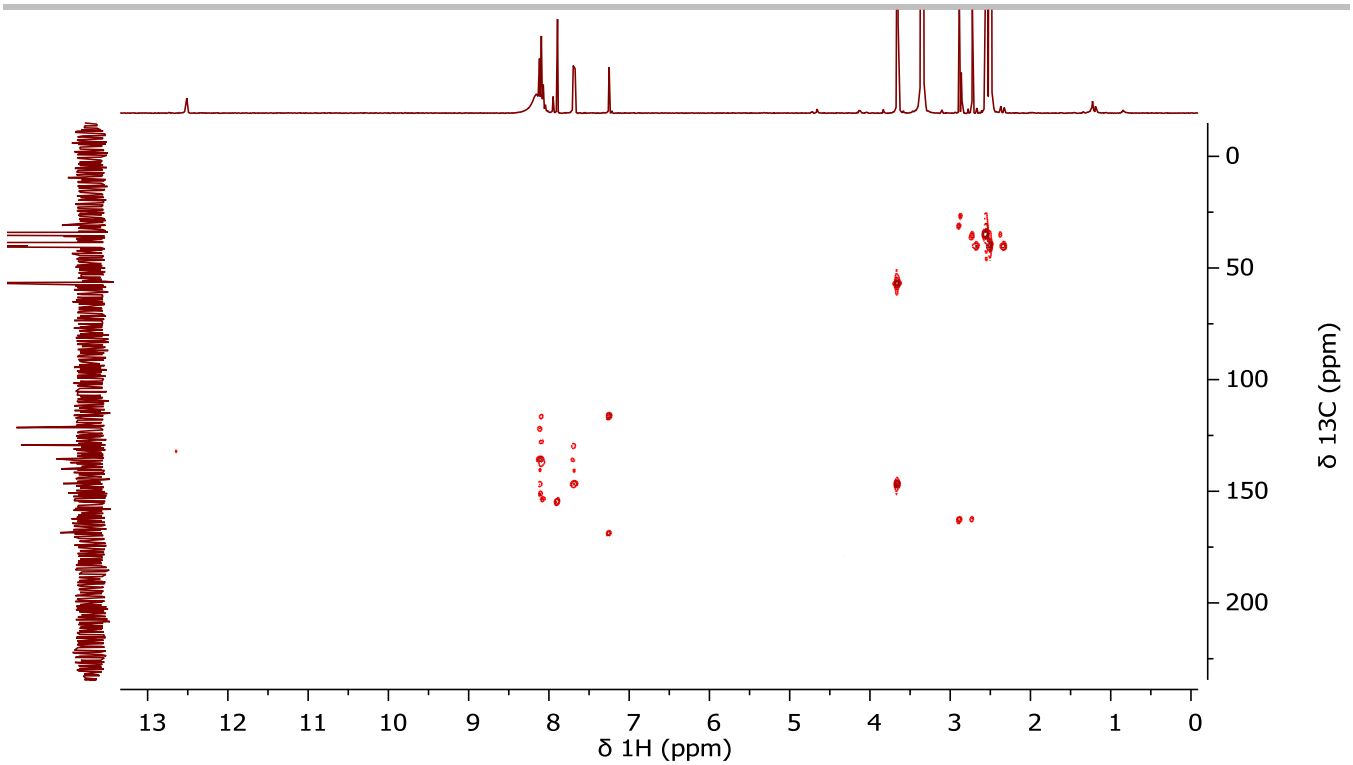

Figure S53: ^{1}H-^{13}C HMBC NMR spectrum of **16** in DMSO-d_6, 400/100 MHz.

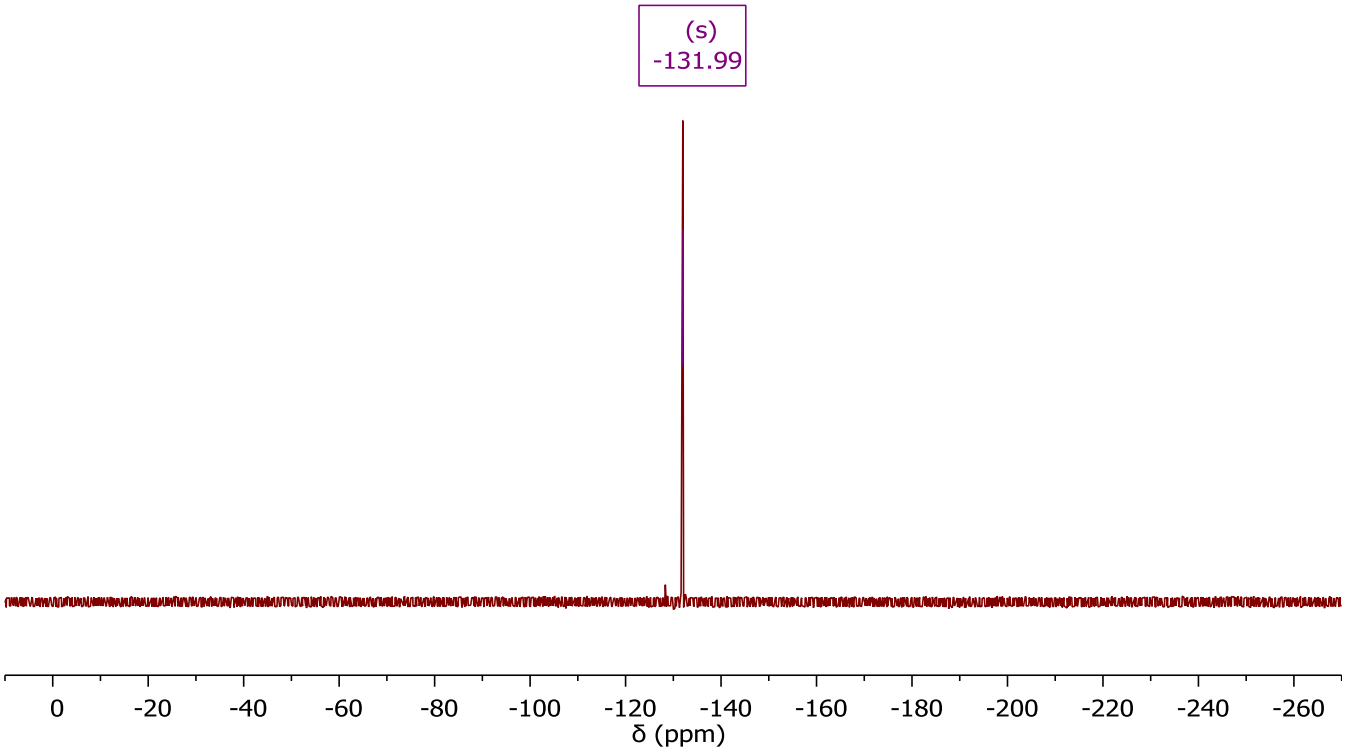

Figure S54: ^{19}F NMR spectrum of **16** in DMSO-d_6, 376 MHz.

SUPPORTING INFORMATION

References

[1] C. Höbartner, C. Kreutz, E. Flecker, E. Ottenschläger, W. Pils, K. Grubmayr, R. Micura, *Monatsh. Chem.* **2003**, *134*, 851.
[2] D. C. Rio, *Cold. Spring. Harb. Protoc.*, DOI: 10.1101/pdb.prot078527.
[3] a) G. R. Fulmer, A. J. M. Miller, N. H. Sherden, H. E. Gottlieb, A. Nudelman, B. M. Stoltz, J. E. Bercaw, K. I. Goldberg, *Organometallics* **2010**, *29*, 2176; b) R. K. Harris, E. D. Becker, S. M. Cabral de Menezes, R. Goodfellow, P. Granger, *Pure and Applied Chemistry* **2001**, *73*, 1795.
[4] W. B. Fellows, *Dissertation*, Georgia Institute of Technology, Atlanta, GA, **2014**.
[5] N. Ieda, H. Nakagawa, T. Horinouchi, T. Peng, D. Yang, H. Tsumoto, T. Suzuki, K. Fukuhara, N. Miyata, *Chem. Commun.* **2011**, *47*, 6449.
[6] H. T. S. Britton, R. A. Robinson, *J. Chem. Soc.* **1931**, 1456.
[7] C. Würth, M. Grabolle, J. Pauli, M. Spieles, U. Resch-Genger, *Nat. Protoc.* **2013**, *8*, 1535.
[8] R. L. Strack, M. D. Disney, S. R. Jaffrey, *Nat. Methods* **2013**, *10*, 1219.